USGS
science for a changing world

# Estimation of Unsaturated Zone Traveltimes for Rainier Mesa and Shoshone Mountain, Nevada Test Site, Nevada, Using a Source-Responsive Preferential-Flow Model

By Brian A. Ebel and John R. Nimmo




Prepared in cooperation with the U.S. Department of Energy, National Nuclear Security Administration, Nevada Site Office under Interagency Agreement DE-AI52-07NV28100.

Open-File Report 2009–1175

U.S. Department of the Interior

U.S. Geological Survey

U.S. Department of the Interior
KEN SALAZAR, Secretary

U.S. Geological Survey
Suzette M. Kimball, Acting Director

U.S. Geological Survey, Reston, Virginia 2009

For product and ordering information:
World Wide Web: http://www.usgs.gov/pubprod
Telephone: 1-888-ASK-USGS

For more information on the USGS—the Federal source for science about the Earth,
its natural and living resources, natural hazards, and the environment:
World Wide Web: http://www.usgs.gov
Telephone: 1-888-ASK-USGS

Suggested citation:
Ebel, B.A., and Nimmo, J.R., 2009, Estimation of unsaturated zone traveltimes for Rainier Mesa and Shoshone Mountain, Nevada Test Site, Nevada, using a source-responsive preferential-flow model: U.S. Geological Survey Open-File Report 2009–1175, 74 p.



Front cover (clockwise, from upper left): (1) View from the summit of Shoshone Mountain, Nevada, June 3, 2008. (2) U12e tunnel infiltration pond, June 3, 2008. (3) Infiltration-capacity estimation using a “bottomless bucket” on top of Rainier Mesa, Nevada, June 2, 2008. (4) Open fracture at Rainier Mesa, Nevada, June 2, 2008.

.

# Contents

## Figures

## Tables

## Conversion Factors

SI to Inch/Pound

| Multiply | By | To obtain |
|---|---|---|
| **Length** | | |
| centimeter (cm) | 0.3937 | inch (in.) |
| meter (m) | 3.281 | foot (ft) |
| kilometer (km) | 0.6214 | mile (mi) |
| **Area** | | |
| square meter ($m^2$) | 10.76 | square foot ($ft^2$) |
| square kilometer ($km^2$) | 0.3861 | square mile ($mi^2$) |
| **Volume** | | |
| liter (L) | 0.2642 | gallon (gal) |
| cubic meter ($m^3$) | 264.2 | gallon (gal) |
| liter (L) | 61.02 | cubic inch ($in^3$) |
| **Flow rate** | | |
| meter per second ($m\ s^{-1}$) | 3.281 | foot per second ($ft\ s^{-1}$) |
| meter per day ($m\ d^{-1}$) | 3.281 | foot per day ($ft\ d^{-1}$) |
| liter per second ($L\ s^{-1}$) | 15.85 | gallon per minute ($gal\ min^{-1}$) |
| **Radioactivity** | | |
| becquerel per liter ($Bq\ L^{-1}$) | 27.027 | picocurie per liter ($pCi\ L^{-1}$) |
| **Hydraulic conductivity** | | |
| meter per day ($m\ d^{-1}$) | 3.281 | foot per day ($ft\ d^{-1}$) |

Temperature in degrees Celsius (°C) may be converted to degrees Fahrenheit (°F) as follows:
°F=(1.8×°C)+32
Vertical coordinate information is referenced to the insert datum name (and abbreviation) here, for instance, “North American Vertical Datum of 1988 (NAVD 88)”
Horizontal coordinate information is referenced to the insert datum name (and abbreviation) here, for instance, “North American Datum of 1983 (NAD 83)”
Altitude and elevation, as used in this report, refers to distance above the vertical datum.
Concentrations of chemical constituents in water are given either in milligrams per liter ($mg\ L^{-1}$) or micrograms per liter
($\mu g\ L^{-1}$).
Altitude, as used in this report, refers to distance above the vertical datum.

# Estimation of Unsaturated Zone Traveltimes for Rainier Mesa and Shoshone Mountain, Nevada Test Site, Nevada, Using a Source-Responsive Preferential-Flow Model

By Brian A. Ebel and John R. Nimmo

## Abstract

Traveltimes for contaminant transport by water from a point in the unsaturated zone to the saturated zone are a concern at Rainier Mesa and Shoshone Mountain in the Nevada Test Site, Nevada. Where nuclear tests were conducted in the unsaturated zone, contaminants must traverse hundreds of meters of variably saturated rock before they enter the saturated zone in the carbonate rock, where the regional groundwater system has the potential to carry them substantial distances to a location of concern. The unsaturated-zone portion of the contaminant transport path may cause a significant delay, in addition to the time required to travel within the saturated zone, and thus may be important in the overall evaluation of the potential hazard from contamination.

Downward contaminant transport through the unsaturated zone occurs through various processes and pathways; this can lead to a broad distribution of contaminant traveltimes, including exceedingly slow and unexpectedly fast extremes. Though the bulk of mobile contaminant arrives between the time-scale end members, the fastest contaminant transport speed, in other words the speed determined by the combination of possible processes and pathways that would bring a measureable quantity of contaminant to the aquifer in the shortest time, carries particular regulatory significance because of its relevance in formulating the most conservative hazard-prevention scenarios.

Unsaturated-zone flow is usually modeled as a diffusive process responding to gravity and pressure gradients as mediated by the unsaturated hydraulic properties of the materials traversed. The mathematical formulation of the diffuse-flow concept is known as Richards' equation, which when coupled to a solute transport equation, such as the advection-dispersion equation, provides a framework to simulate contaminant migration in the unsaturated zone. In recent decades awareness has increased that much fluid flow and contaminant transport within the unsaturated zone takes place as preferential flow, faster than would be predicted by the coupled Richards' and advection-dispersion equations with hydraulic properties estimated by traditional means. At present the hydrologic community has not achieved consensus as to whether a modification of Richards' equation, or a fundamentally different formulation, would best quantify preferential flow.

Where the fastest contaminant transport speed is what needs to be estimated, there is the possibility of simplification of the evaluation process. One way of doing so is by a two-step process in which the first step is to evaluate whether significant preferential flow and solute transport is possible for the media and conditions of concern. The second step is to carry out (a) a basic Richards' and advection-dispersion equation analysis if it is concluded that preferential flow is not possible or (b) an analysis that considers only the fastest possible preferential-flow

processes, if preferential flow is possible. For the preferential-flow situation, a recently published model describable as a Source-Responsive Preferential-Flow (SRPF) model is an easily applied option. This report documents the application of this two-step process to flow through the thick unsaturated zones of Rainier Mesa and Shoshone Mountain in the Nevada Test Site.

Application of the SRPF model involves distinguishing between continuous and intermittent water supply to preferential flow paths. At Rainier Mesa and Shoshone Mountain this issue is complicated by the fact that contaminant travel begins at a location deep in the subsurface, where there may be perched water that may or may not act like a continuous supply, depending on such features as the connectedness of fractures and the nature of impeding layers. We have treated this situation by hypothesizing both continuous and intermittent scenarios for contaminant transport to the carbonate aquifer and reporting estimation of the fastest speed for both of these end members.

For Rainier Mesa our analysis suggests that preferential flow is possible through the entire unsaturated zone, which implies that the SRPF model can be applied to estimate the fastest radionuclide traveltimes down to the carbonate aquifer. SRFP model estimates for fastest travel times at Rainier Mesa are tens to hundreds of years for intermittently supplied preferential paths, as may be likely for contamination from those working points and tunnel inverts where there is no continuous discharge of water in bulk. The estimates at Rainier Mesa are approximately one month for continuously supplied preferential paths, as may be likely for contamination from working points and tunnel inverts with continuous discharge, tunnel effluent ponds, or sealed tunnel inverts. The SRPF model traveltimes at Shoshone Mountain for intermittently supplied preferential paths, considered likely for all working points and tunnel inverts at that site, are hundreds of years. The presence of a thick layer of siliceous rock under Shoshone Mountain may interrupt all preferential flow paths before they reach the carbonate aquifer, in which case it would increase estimated traveltimes to more than a thousand years. Even the fastest of these SRPF contaminant transport times may not imply serious potential for radionuclide contamination of the regional flow system beneath Rainier Mesa. This is because of the potential hydraulic disconnect between the saturated zone in the upper carbonate aquifer and the lower carbonate aquifer that forms the regional groundwater flow system. The application of the SRPF model to Rainier Mesa and Shoshone Mountain emphasizes the importance of radionuclide sources that are located in the vicinity of both continuously supplied water and preferential flow paths.

# Introduction

## Motivation

Underground nuclear tests in the unsaturated zone at the Nevada Test Site (NTS) produce radionuclides that have the potential to contaminate water in the saturated zone. In arid to semi-arid regions, radionuclides often must be conveyed through a thick section of unsaturated rock before reaching the saturated zone where radionuclides may be transported to more accessible environments. The transit time through the unsaturated zone is a concern of policy makers and is critical to making accurate predictions of future radionuclide distributions. The potential transport of radionuclides through the unsaturated zone at the NTS is of interest to the U.S. Department of Energy and certain regulatory agencies at the State and Federal level (Fenelon and others, 2008).

## Unsaturated Flow and Preferential Flow

Flow through the unsaturated zone is most often conceptualized using continuum mechanics, applying to the porous medium defined constitutive relationships between matric potential and soil-water content in combination with a function describing unsaturated hydraulic conductivity. The Darcy-Buckingham flux law combined with an expression for conservation of mass results in a partial differential equation, which when solved in terms of matric potential is referred to as Richards' equation. While the Richards' equation approach has been used successfully in some cases of matrix-dominated unsaturated flow, the importance of flow that bypasses portions of the porous medium, termed *preferential flow*, is increasingly well recognized in the hydrologic community (Gerke, 2006). Preferential flow is commonly classified as macropore flow, which consists of flow through well defined pathways such as root channels and fractures, or flow through a fraction of the matrix (Jarvis, 1998). The preferential flow through the matrix is considered as either unstable or focused unsaturated flow. Fingering is an example of unstable, unsaturated matrix flow (Baker and Hillel, 1990; Glass and others, 1989a; Glass and others, 1988; Selker and others, 1992a;1992b); funnel flow is an example of focused, unsaturated matrix flow (Kung, 1990a;1990b;1993; Miyakazi, 1993). Fingering refers to unstable flow through isolated finger-like volumes of the matrix that bypasses much of the porous medium. The term *unstable* denotes that flow is nonuniformly distributed in space; *stable* flow is continuously distributed throughout the matrix (Hillel and Baker, 1988). Funnel flow occurs when textural and permeability contrasts focus unsaturated flow into zones that are more permeable, either intrinsically or as a result of higher soil-water content, thus bypassing less permeable porous media.

Although unsaturated flow can occur both through preferential paths and diffusely through the collective pore space of the matrix, the fastest flow will likely occur by preferential flow. The fastest flow occurring in a hydrologic system can have considerable practical importance, in the context of minimum travel times, if this fast flow transports contaminants in the subsurface. Preferential solute transport has been observed in soils (Ghodrati and Jury, 1990) and unsaturated fractured rocks (Evans and Nicholson, 1987; Wang, 1991), even when the porous medium was seemingly homogenous and lacked well defined preferential paths (Glass and others, 1989c). Preferential solute transport has been shown to be significant for all preferential modes: macropore (Gjettermann and others, 2004), finger (Glass and others, 1988; Hendrickx and others, 1993), and funnel (Kung, 1993) flow.

## Evaluation of Unsaturated Flow Processes and Model Selection

In applications where only the fastest contaminant transport speed needs to be estimated, there is the possibility of major simplification of the flow and solute transport simulation process. For media and conditions where preferential flow can be ruled out, then Richards' equation coupled to the advection-dispersion equation with appropriate assignments of hydraulic property and solute transport parameter values may be suitable. Otherwise, if preferential flow is a significant possibility, it may be assumed that preferential flow processes will control the fastest travel time, and the portion of the analysis based on diffusive flow mechanisms is unnecessary. If estimates of transported quantities or average contaminant traveltimes are needed, such a simplified evaluation is not appropriate, but for minimum possible traveltimes, a simpler two-step process is reasonable. The steps are: (1) evaluate whether significant preferential flow is possible for the media and conditions of concern and (2) carry out the appropriate choice of (a) a basic Richards' and advection-dispersion equation analysis or (b) an

analysis that considers only the fastest possible preferential-flow processes. For the preferential-flow situation, a recently published model describable as a Source-Responsive Preferential-Flow (SRPF) model is an easily applied option. This report documents the application of this two-step process to flow through the thick unsaturated zones of Rainier Mesa and Shoshone Mountain.

## Source-Responsive Preferential-Flow Model

Intuitively, a mathematical model used to fully represent preferential solute transport in the unsaturated zone must be complicated, but analysis of tracer tests indicates that a surprisingly simple mathematical model can provide an estimate of the fastest solute traveltimes where flow is predominately preferential (Nimmo, 2007). The model simplification employed by Nimmo (2007) requires a departure from traditional unsaturated simulation approaches that represent preferential flow within a Darcy-Buckingham conceptual framework where the porous media characteristics dominate the physics of flow. The alternative paradigm used in the traveltime model by Nimmo (2007) is that the temporal nature of the water source supplying preferential paths (that is, continuous or intermittent supply) is the primary control on preferential flow traveltimes rather than soil-hydraulic properties. The model makes a strong distinction between cases where this water supply is continuous, such as surface water that persists in a ponded state, and intermittent cases, such as natural rainfall. A simple formula is applied for continuous cases, and a modified version of that formula to intermittent cases. This view is supported by collective evaluation of numerous case studies by Nimmo (2007) in which fastest traveltimes correlate strongly with the nature of the water supply but not with the particular earth materials involved. The Nimmo (2007) model is described here as a *Source-Responsive Preferential-Flow* (SRPF) model to emphasize the sensitivity to the temporal nature of water supply that drives flow along preferential paths.

Numerous studies have shown that the development of preferential flow depends strongly on the rate of water supply to preferential paths. For example, higher rates of applied water flux at the surface increased the prevalence of preferential flow in studies by Gjettermann and others (1997) and Kasteel (1997); ponded water at the surface increased preferential flow, relative to nonponded water application, in the work by Hamdi and others (1994). Finger flow initiation was found to be less prevalent at high infiltration rates, including ponded surface water (Glass and others, 1989b; Rice and others, 1991), and minimal at low infiltration rates (Hendrickx and Yao, 1996), with finger flow occurring most frequently at moderate infiltration rates (Selker and others, 1992b; Yao and Hendrickx, 1996). Whereas most models of preferential flow and solute transport distinguish between the multiple physical mechanisms of preferential flow, the SRPF model does not.

## Model Abstraction

In cases where unsaturated-zone preferential flow is believed to be a significant contaminant transport process, the evaluation of unsaturated-zone contaminant transport may be best treated with a comparison of multiple models, using a protocol such as model abstraction. The translation of the complex set of physical and chemical processes that make up a conceptual model into progressively simpler mathematical models that still represent the relevant flow processes is the crux of model abstraction (Frantz, 1995; Pachepsky and others, 2006). The application of the SRPF model, in a situation where a traditional coupled Richards' and advection-dispersion equation method would typically be used, can be described as model

abstraction. The advantages of using model abstraction to objectively employ the simplest model capable of answering the questions posed include (Pachepsky and others, 2006):

- Reduced data-collection requirements
- Less computational effort
- Easier explanation of model processes to decisionmakers and the public
- More direct quantification of uncertainty
- Simpler interfacing with other models (for example, hydrologic, geologic, and ecologic)
- Model complexity that is appropriate to a limited availability of data for evaluation

All of these benefits reduce the time required both to complete the simulations and transfer the simulation knowledge to managers making decisions, thus reducing overall modeling cost. Obviously, model abstraction runs the risk that the model has been oversimplified and essential physical or chemical processes have been omitted, introducing uncertainty through model structural error (Pachepsky and others, 2006). The progression of model abstraction should then be viewed as an opportunity to consider several models of varying complexity at the same site answering the same scientific question (Davis and Bigelow, 2003; Fishwick, 1995; Pachepsky and others, 2006). Model abstraction thus allows learning from models of a range of complexity, some more useful for scientific investigations and others that facilitate evaluating strategic decisions; the simpler model is not intended to replace, but rather to augment, the more complex models (Pruess and others, 1999). A fundamental disparity may exist between progressively simplifying a complex model (for example, combining hydrogeologic layers or upscaling grid size) versus shifting the conceptual paradigm of the models' underlying physical principles; perhaps the most benefit from model abstraction can be gained by comparing models that are widely disparate in terms of complexity and physics.

### Objectives of This Study

The principal objectives of this document and associated work are to:

- Develop a conceptual model of unsaturated flow from the land surface to the saturated zone in the carbonate rock at Rainier Mesa and Shoshone Mountain at the NTS.
- Evaluate the potential for preferential flow to transport radionuclides from possible sources to the saturated zone in the carbonate rock.
- Apply the SRPF model to estimate unsaturated-zone traveltimes for conservatively transported radionuclides to the saturated zone for plausible continuous and intermittent sources of water supply to preferential flow paths.

## Rainier Mesa and Shoshone Mountain

### Site Overview

Figure 1 shows the location of the NTS in Nye County, Nevada, approximately 140 km northwest of Las Vegas. The NTS is bordered by the Nellis Air Force Range and the Tonopah

Test Range and includes about 14,200 $km^2$ of unpopulated area (Department of Energy, 1997). This large unpopulated expanse made the NTS a viable location for atmospheric nuclear testing. After the atmospheric nuclear test ban, the arid to semiarid climate, deep regional saturated zone, and large surrounding unpopulated area made the site favorable for underground nuclear testing. A total of 928 nuclear tests were conducted at the NTS, 828 of which were underground (Department of Energy, 2000). This investigation focuses on the Rainier Mesa and Shoshone Mountain Areas shown in fig. 1. The Shoshone Mountain area is located approximately 20 km south of Rainier Mesa (fig. 1).

## Testing History

Rainier Mesa hosted 61 underground tests between 1957 and 1992; Shoshone Mountain hosted six underground tests between 1957 and 1992 (Department of Energy, 2000). With the exception of two tests conducted in vertical boreholes (see fig. 2) on Rainier Mesa, all the underground nuclear tests at the Rainier Mesa–Shoshone Mountain Corrective Action Unit (CAU) occurred within tunnels (see fig. 3) (National Security Technologies, 2007). A major reason for conducting tests in tunnels above the saturated zone was to facilitate examination of direct radiation blast exposure on military and communication equipment (Smith and others, 2003). The Rainier Mesa tests were detonated 365 to 715 m above the saturated zone in the carbonate rock (Bechtel Nevada, 2006; Stoller-Navarro Joint Venture, 2006a) and introduced radionuclides into the unsaturated and perched saturated zones. The underground testing locations typically are hundreds of meters below the ground surface, making in-place remediation difficult.

## Rainier Mesa and Shoshone Mountain Tunnels

Nearly all of the underground nuclear tests at the Rainier Mesa–Shoshone Mountain CAU were conducted in a series of tunnels (also referred to as drifts) excavated into the subsurface (shown in fig. 3). The characteristics of the Rainier Mesa and Shoshone Mountain tunnels are summarized in table 1. In this report, the term *tunnel* or *tunnels* is used to denote both individual tunnels and complexes comprising many connected tunnels. Underground tests at Rainier Mesa were also conducted in two boreholes (U-12q and U-12r). Construction of the six major (U12b, U12g, U12e, U12n, U12t, and U12p) and five minor (U12c, U12d, U12f, U12j, and U12k) tunnels used for nuclear testing occurred from the 1950s into the 1990s. Shoshone Mountain underground tests occurred in the U16a tunnel between the 1960s and early 1970s (National Security Technologies, 2007). The tunnels were driven primarily into zeolitic tuff, although a few tunnels (for example, U12p) were emplaced in vitric tuff (Ege and Cunningham, 1976; Emerick and Dickey, 1962; Hoover and Magner, 1990; Sawyer and others, 1994). A main tunnel provided access, and the nuclear detonations were conducted in side tunnels off the main tunnel. The locations of the nuclear tests are referred to as working points. The U12d tunnel has the highest elevation working point (2,050 m) and the U12e tunnel has the lowest elevation working point (1,880 m) (Townsend and others, 2007) for the tests conducted in the tunnels. The U-12q and U-12r tests emplaced in vertical boreholes have lower elevation working points of 1,711 m and 1,771 m, respectively (Townsend and others, 2007). All of the working points at Rainier Mesa and Shoshone Mountain are above the saturated zone in the underlying carbonate rock, but many of the Rainier Mesa tests were conducted in a zone of perched saturation within the zeolitic tuff. A downward slope from the working points to the tunnel portal facilitates drainage of water out of the tunnel portal onto the land surface. Some of the tunnels have prior or current discharge exiting the portal and flowing into unlined tunnel effluent ponds. The U12t and

U12n tunnels have been sealed near the tunnel portal. The location of the tunnel effluent ponds relative to the tunnel portals are shown in figures 4, 5, and 6 for the U12e, U12n, and U12t tunnels, respectively.

## Radionuclides of Concern

One of the principal radionuclides of concern at Rainier Mesa and Shoshone Mountain is tritium ($^{3}H$), which is highly soluble and conservative when incorporated into water molecules (Department of Energy, 1997). Other radionuclides of concern in the unsaturated and perched saturated zones at Rainier Mesa and Shoshone Mountain include long-lived radionuclides (for example, $^{36}Cl$, $^{99}Tc$, $^{106}Ru$, $^{129}I$, $^{85}Kr$) that have been found in groundwater at the NTS (Smith, 1998). The distribution of radionuclides generated from an underground nuclear detonation is complex and depends primarily on the temperature and pressure conditions during and after the explosion (Borg and others, 1976). The radionuclides introduced into the subsurface commonly include residual fission fuel, fission products, and tritium. Together, the mass of these radionuclides make up the radiologic source term, described by Bowen and others (2001) and Smith and others (2003) for the Rainier Mesa–Shoshone Mountain area. The inclusion criteria for radionuclides in the inventory presented by Bowen and others (2001) is that dissolved concentrations in the saturated zone (decay corrected to 100 years in the future) exceed 10 percent of the U.S Environmental Protection Agency maximum permissible concentrations for drinking water. Radionuclides with half lives less than ten years typically are excluded by this criterion (Bowen and others, 2001; Smith and others, 2003).

Underground tests detonated at Rainier Mesa and Shoshone Mountain had relatively low yields making up only 0.67 percent of the total NTS radiologic source term (Smith and others, 2003). By comparison, nearby Pahute Mesa contains more than 60 percent and Yucca Flat about 38 percent of the total radiologic source term at the NTS (Bowen and others, 2001). Uncertainty in the radiologic source term varies by type of radionuclide (that is, fission products versus undetonated fissile material) from about 10 to 300 percent, with the largest uncertainty corresponding to the amounts of tritium (Smith and others, 2003).

Radionuclide distributions depend on the phenomenology of underground nuclear detonation, the summary of which below is based on detailed descriptions from Borg and others (1976), U.S. Congress (1989), Bowen and others (2001), and Guell and Hunt (2003). Upon detonation, the geologic material surrounding the device is vaporized, forming a cavity. Geologic materials surrounding the cavity can be compressed, fractured, melted, or a combination thereof. Molten rock from the cavity walls collects at the bottom of the cavity, forming a pool of melt glass. Approximately 700 metric tons of melt glass is produced for each kiloton of test yield (Olsen, 1993). The melt glass can provide a long-term radionuclide source to groundwater, depending on the ambient temperature, pH, and fluid chemistry (Bourcier, 1993; Mazer, 1987). It is common for the region above the cavity to partially collapse, forming a disturbed zone called a rubble chimney that can extend upward to the land surface. The radionuclides with lower boiling points (for example, tritium, $^{36}Cl$, $^{129}I$) tend to condense on the walls of the cavity and rubble chimney. The radial extent of radionuclide deposition is variable, depending on the geology, degree of water saturation, and other factors. Hoffman and others (1977) conceptualized the zone of radionuclide deposition as a spherical volume centered on the blast cavity with a radius of about twice the cavity radius. Guell (1997) and Hoffman and others (1977) noted that certain radionuclides (for example, $^{85}Kr$, $^{90}Kr$, $^{137}Xe$) can be distributed in a gaseous phase for a distance greater than twice the cavity radius.

While the radiologic source term is important to radionuclide transport, only a small fraction of the radionuclides are readily mobile, with the remainder bound in melted rock and metal residues in the melt glass. The mobile portion, in an aqueous solution, is called the hydrologic source term. The release of radionuclides from the melt glass into aqueous solution and interactions between radionuclides and rock along flow paths are highly complex. Important processes include (i) kinetically controlled glass dissolution and radionuclide precipitation and (ii) equilibrium-controlled aqueous speciation, surface complexation, and ion exchange (Pawloski and others, 2001). Chemical speciation is a dominant control on mobility, with highly mobile neutral and anionic species contrasting with sorbing cations. However, some cations sorb onto colloids (organic matter or inorganic material from the host rock), facilitating advective transport (Finnegan and Thompson, 2001; Kersting and others, 1998). Ramsay (1988) described how uncharged colloid particles can be transported without retardation and how colloids with the same polarity as the porous medium are repelled by the medium walls, resulting in enhanced colloid transport. The aqueous transport of cations as colloids in groundwater has been demonstrated at the NTS (for example, Kersting and others, 1999).

## Effects of Underground Nuclear Testing on Hydraulic Properties

The underground detonation of nuclear tests can change subsurface hydraulic properties, alter surface topography, and induce temperature and pressure gradients that drive groundwater flow. Changes in fault geometry and position and generation of fractures as a result of underground nuclear tests have been observed at the NTS (Ege and others, written commun., 1980; Thompson and Misz, 1959). The immediate test-cavity vicinity may have decreased permeability and porosity (Tompson and others, 2006) owing to the melt-glass deposition. Regions beyond the melt-glass zone will have increased fracture porosity and permeability (Tompson and others, 2006). Test-generated rock fractures typically extend out from the detonation cavity for a distance of three times the test-cavity radius (Bowen and others, 2001). In the U12n tunnel, Ege and others, written commun. (1980) noted that fractures and small bedding-plane displacements extended nearly 240 m from a working point. If the test cavity collapses and a rubble chimney is formed, the permeability increases (Borg and others, 1976; Hansen and others, 1981; Rozsa and others, 1975; Snoeberger and others, 1973; Wadman and Richards, 1961). Ege and others, written commun. (1980) showed that the fracturing and permeability changes from nuclear testing can extend to the surface of Rainier Mesa at the U12n tunnel, but the effects of testing at other tunnels are not as well characterized.

The underground nuclear detonations also generate heat and pressure gradients that can drive subsurface flow. Russell (1987) noted large increases in U12n tunnel flow and a shift in deuterium concentrations immediately following a nearby nuclear test in 1986. He postulated that the detonation caused the release of interstitial waters into the fracture system, which then discharged into the tunnel. Underground nuclear tests have also been shown to vaporize or drive out water in the immediate vicinity of the test (Thordarson, 1987) while raising the elevations of portions of the saturated zone further away from the test cavity and rubble chimney (Thordarson, 1987). The effects of underground tests on groundwater levels may take months to years to re-equilibrate (Thordarson, 1987). The heat generated by an underground nuclear test has been shown to create buoyancy-driven flow, which can affect radionuclide transport at the NTS (Maxwell and others, 2000, Glascoe and others, 2000, and Pawloski and others, 2000).

## Physiographic Setting

The NTS consists of approximately 3,560 $km^2$ of Basin and Range topography of north-southtrending mountains separated by alluvial valleys (Bowen and others, 2001). Within the NTS, elevations range from 910 m in the southern and eastern sections to over 2,300 m at Rainier Mesa (Department of Energy, 1997).

### Rainier Mesa Physiographic Setting

Rainier Mesa ranges in elevation from 2,243 to 2,340 m and is capped by a densely welded volcanic tuff that forms a relatively flat upland. The highest elevation at the NTS, 2,340 m, is located at Rainier Mesa. Aqueduct Mesa adjoins Rainier Mesa to the north and has less regular topography and slightly lower elevations (but still generally above 1,920 m).

### Shoshone Mountain Physiographic Setting

Shoshone Mountain, approximately 20 km south of Rainier Mesa (National Security Technologies, 2007), ranges in elevation from 1,707 to 2,073 m. While the central portion of Shoshone Mountain is mesa-like, the remainder of the topography is primarily ridges, peaks, and steep canyons. Tippipah Point, which is part of Shoshone Mountain, has an elevation of 2,015 m and is located at the north end of Shoshone Mountain (National Security Technologies, 2007).

## Geology

The geologic history of the NTS is summarized briefly here based on Frizzell and Shulters (1990) and Laczniak and others (1996). The NTS geology consists of Paleozoic and older sedimentary rocks (600-280 Ma), Cretaceous granitic intrusions (100 Ma), Miocene volcanics (16-8 Ma), and postvolcanic gravel and sand alluvial and colluvial deposits (Laczniak and others, 1996). Thrust faulting likely occurred 150-100 Ma, followed by extensional faulting beginning in the early Tertiary and continuing during and after the deposition of the Miocene volcanics (Armstrong, 1968; Cole and others, 1993; Hodges and Walker, 1992).

### Rainier Mesa Lithology and Hydraulic Properties

A simplified lithologic model of Rainier Mesa, based on the ER-12-4 borehole, is shown in figure 7. The corresponding stratigraphic units from National Security Technologies (2007) are shown for each lithology in figure 7. The knowledge of the subsurface lithology at Rainier Mesa is derived from boreholes [see fig. 2 and Fenelon and others (2008)] and from extensive tunnel construction information (fig. 3). The nonperched saturated zone beneath Rainier Mesa is in a Paleozoic carbonate aquifer, which can be divided into an upper and lower carbonate aquifer that are structurally and hydrologically separated (Fenelon and others, 2008). A thin layer of argillic palecolluvium overlies the upper carbonate aquifer (Thordarson, 1965). Zeolitic tuff overlies the argillic paleocolluvium. Although some debate exists as to the exact mechanism responsible for zeolitization of the tuff (Moncure and others, 1981), the general consensus (Bowers and Burns, 1990; Hay and Sheppard, 1977; Hoover, 1968; Vaniman and others, 2001) is that percolating water (recharge) altered the volcanic rocks to form zeolites. A perched or semiperched zone of saturation occurs within the zeolitic tuff at Rainier Mesa and possibly at portions of Shoshone Mountain. Vitric tuff overlies the zeolitic tuff. Densely welded and fractured tuff overlies the vitric tuff. A depositional syncline that has dips of 2-12° in the limbs greatly affects the thickness of the units making up the tuff across Rainier Mesa (Hoover and

Magner, 1990; Thordarson, 1965). The tuff was deposited from calderas west, south, and southwest of Rainier Mesa (Russell, 1987). Cooling joints, fractures, and steeply dipping normal faults that trend north-south are typical in the volcanic rocks of Rainier Mesa (Hansen and others, 1963). In this report, the term fracture will be used to denote both fractures and faults. Most nuclear tests at Rainier Mesa were detonated within the zeolitic tuff, with the exception of a few tests that were detonated in vitric tuff.

Hydraulic properties of the lithologic units at Rainier Mesa are summarized in table 2. The shallowest portion of the regional saturated zone at Rainier Mesa is located within dolomites and limestone that make up the upper carbonate aquifer (Fenelon and others, 2008). Pumping tests in deep wells demonstrate that the carbonate rock is far more hydraulically conductive than the overlying zeolitic tuff (Thordarson, 1965), despite the low saturated hydraulic conductivity of the carbonate-rock matrix given in table 2. Thordarson (1965) attributed the higher conductivity to a connected fracture network. Drill-core analyses indicate that some carbonate fractures exhibit enlargement by dissolution, although not to the point of forming karst (Thordarson, 1965). The zeolitic tuff has low matrix permeability (table 2). Although numerous fractures occur in the zeolitic tuff, these preferential flow paths irregularly drain the tuff to create a hummocky perched saturated zone, in which elevations vary by 100 m. The mean elevation of the perched saturated zone is about 1,820 m (Thordarson, 1965). The perched saturated zone has likely declined in the last 50 years as a result of drainage by mining activities and nuclear testing (Russell, 1987). Observed matrix saturations in the zeolitic tuff in the U12e tunnels are nearly 100 percent (Byers, 1962). These saturated conditions are corroborated by the electrical log analyses by Keller (1960; 1962). Although the matrix is nearly saturated, tunnel walls excavated in the zeolitic tuffs often are dry, indicating either that the matrix is tension saturated or that any water on the tunnel walls is quickly evaporated (Thordarson, 1965).

Inspection of table 2 indicates that the vitric tuff has the largest matrix permeability of any of the lithologies for which permeameter tests were conducted at Rainier Mesa. While no fracture permeability data are available for the vitric tuff, the friable nature of the tuff suggests that fractures are not readily preserved. The few fractures observed in the vitric tuff are filled with a clayey fault-gouge material (Laraway and Houser, 1962). The vitric tuff is considered to be the only lithology at Rainier Mesa that transmits water primarily by matrix flow (Thordarson, 1965). The welded tuff has relatively low matrix permeability (table 2) but is permeable because of well-connected fracture networks (Poole and Rooler, 1959). Thordarson (1965) noted that aquifer tests within the welded tuff units at Pahute Mesa to the northwest of Rainier Mesa and at Jackass Flats in the southwestern section of the NTS indicated that the fractures could transmit large quantities of water.

### Shoshone Mountain Lithology and Hydraulic Properties

Figure 8 shows a simplified lithologic model of Shoshone Mountain based on the ER-16-1 borehole. The corresponding stratigraphic units from National Security Technologies (2007) are shown for each lithology in figure 8. The siliceous rock acts as a confining unit and comprises mostly shale (Stoller-Navarro Joint Venture, 2006b). Several hundred meters of zeolitic tuff lie above the paleocolluvium. Approximately 100 m of vitric tuff overlie the zeolitic tuff, followed by a relatively thin welded tuff unit. Unlike Rainier Mesa, no perched water was observed during tunnel construction (National Nuclear Security Administration, 2004), which may be the result of lower recharge fluxes relative to Rainier Mesa (Russell and Minor, 2002).

### Climate and Vegetation

#### Rainier Mesa Climate and Vegetation

Precipitation at Rainier Mesa is principally derived from cool-season, mid-tropospheric cyclones (rain or snow) and summertime convective thunderstorms associated with the southwestern monsoon (National Oceanic and Atmospheric Administration, 2006). The average annual precipitation on the top of Rainier Mesa is 319 mm, based on a record from 1960-2007, with snow constituting less than half of the total (National Oceanic and Atmospheric Administration, 2006). Precipitation amounts at Rainier Mesa exhibit large interannual variability, with a maximum of 682.5 mm $yr^{-1}$ recorded in 1983, a minimum of 85.9 mm $yr^{-1}$ recorded in 2002, and a standard deviation of 129.3 mm $yr^{-1}$. The Rainier Mesa vegetation (table 3) is an elevation-dependent mix of trees [pinyon pine (Pinus edulis) and juniper (Juniperus sp.)], rabbitbrush (Chrysothamnus sp.), and perennial grasses (Beatley, 1976; DeMeo and others, 2006; Russell, 1987). Annual evapotranspiration at Rainier Mesa was measured from 2002 to 2004 by DeMeo and others (2006) using the eddy covariance method and ranged from 244 to 348 mm $yr^{-1}$.

#### Shoshone Mountain Climate and Vegetation

The climate and vegetation of Shoshone Mountain in the higher elevation locations is similar to Rainier Mesa. Unfortunately, no site-specific information is available for Shoshone Mountain. The approximate average annual precipitation at Shoshone Mountain is 200 mm (Winograd and Thordarson, 1975). Evapotranspiration amounts are likely similar to those measured at Rainier Mesa by DeMeo and others (2006).

## Conceptual Flow Model for Rainier Mesa and Shoshone Mountain

### Groundwater Setting

The Rainier Mesa–Shoshone Mountain CAU is located within the Death Valley groundwater flow system; this large groundwater flow system transmits an estimated 70,000 ac-ft $yr^{-1}$ of water, which discharges at Ash Meadows, Oasis Valley, Alkali Flat, and Death Valley (Laczniak and others, 1996; Winograd and Thordarson, 1975). The Death Valley groundwater flow system provides water (from wells) for agricultural, livestock, industrial, and domestic use, and springs support wildlife (Laczniak and others, 1996). Rainier Mesa may supply recharge to both the Oasis Valley subbasin (Fenelon and others, 2008) and the Alkali Flat–Furnace Creek Ranch subbasin (Laczniak and others, 1996). Fenelon and others (Fenelon and others, 2008) suggest that the Eleana confining unit prevents significant groundwater discharge from Rainier Mesa to the Yucca Flat region of the NTS. Shoshone Mountain is within the Ash Meadows groundwater subbasin.

### Potentially Active Unsaturated Flow Processes at Rainier Mesa and Shoshone Mountain

Flow through the variably saturated subsurface at Rainier Mesa and Shoshone Mountain is considered here as either stable matrix or preferential flow. As mentioned previously, the flow that occurs preferentially can exist as macropore, finger, or funnel flow. Stable matrix flow will dominate when paths for macropore flow are absent and factors that favor finger and funnel flow are minimal. The presence of fractures in rock at Rainier Mesa and Shoshone Mountain

promotes macropore flow in some of the simplified lithologic units shown in figures 7 and 8. Finger flow has not been documented at Rainier Mesa or Shoshone Mountain, but some factors that promote finger flow are present. In laboratory studies, Sililo and Tellam (2000) and Scanlon and Goldsmith (1997) noted that (1) stratification enhances the development of fingering, (2) surface depressions concentrate fingers below them, (3) fingers can persist in the same location for long periods of time, and (4) preferential flow in an overlying layer can focus finger flow underneath the preferential flow path. Baker and Hillel (1990) noted that a contrast between lithologies, with a less hydrologically conductive porous medium overlying a more hydrologically conductive porous medium, can cause finger flow initiation at the lithologic boundary. The volcanic rocks at Rainier Mesa and Shoshone Mountain have approximately horizontal stratification, areas of surface topography that concentrate infiltration, lithologies that have macropore preferential flow paths, and lithologic transitions from a less conductive to a more conductive matrix, all of which tend to promote finger flow. At the same time, for finger flow to be a dominant flow process the matrix must have sufficient hydraulic conductivity to transmit significant quantities of water relative to the flux of water from competing processes.

A capillary barrier is an additional flow process that may affect unsaturated flow at Rainier Mesa and Shoshone Mountain. The concept of a capillary barrier relies on a contrast in pore sizes between two layers of porous media, with the uppermost layer having smaller pores. At the pore scale, each pore has a threshold pressure that allows water to enter; a collection of pores form a porous medium. A given porous medium may be considered to have a similar threshold pressure determined by the smallest of all the pores that form a continuous network within it (Hillel and Baker, 1988). Flow from the overlying layer into the underlying layer can be impeded if the pressure in the overlying layer does not exceed the threshold pressure of the underlying layer, termed the *breakthrough head* (Stormont and Anderson, 1999) when expressed as pressure head. The breakthrough head has also been called the *water-entry pressure* or *water-entry suction* to denote the minimum pressure at which water can enter an initially dry porous media (Hillel and Baker, 1988). As noted by Stormont and Anderson (1999), the breakthrough head that facilitates filling the smallest class of connected pores demarcates an increase in saturation and a corresponding increase in unsaturated hydraulic conductivity for the porous media. If the layer interface slopes in a direction that facilitates drainage, then the capillary barrier can be maintained, but if the interface is flat lying or slopes in a manner that allows flow along the capillary barrier to accumulate in a trough or syncline, then the pressure will increase in the overlying layer until the breakthrough head is reached and flow will occur across the interface into the underlying layer, breaking the capillary barrier. The effectiveness of the capillary barrier process is proportional to the pore size and uniformity of the pore-size distribution (Stormont and Anderson, 1999). If heterogeneity in the pore size distribution is present within a given porous medium at a lithologic boundary, then heterogeneity in the breakthrough head can exist, which will promote preferential finger flow.

An additional process that can as a barrier to flow at lithologic contacts is a permeability barrier. The concept of a permeability barrier relies on a contrast in saturated hydraulic conductivity between overlying rock layers where the underlying layer is less permeable and causes a perched saturated zone, as flow is impeded at the interface. The hydraulic conductivity contrast can be either in terms of effective hydraulic conductivity (including preferential paths) or in terms of matrix hydraulic conductivity alone, depending on the preferential path spacing relative to the scale of interest for flow.

The damping of temporal variations in infiltration flux with depth in the unsaturated zone is an important flow process relative to the SRPF model, given the model's dependence on temporal characteristics of supply to preferential flow paths. When stable matrix flow dominates

in the unsaturated zone, temporal variations are quickly damped (within several meters of the surface) with depth into a steady, time-averaged flux (Gardner, 1964). This process is analogous to the damping of surface temperature with depth in the subsurface into a quasi-steady state temperature (Koorevaar and others, 1983). Little is known about the damping of infiltration or recharge flux and its effects on flow through preferential paths, especially over long distances, and this process may be of critical importance for the pulsed preferential contaminant transport concept embodied in the SRPF model. Understanding of the role of preferential flow in short circuiting the damping process in thick unsaturated zones is beyond the scope of this report.

It is difficult to quantitatively estimate the fraction of water flux conveyed by each type of the aforementioned flow processes at Rainier Mesa and Shoshone Mountain, given the limited characterization of the unsaturated zone. Qualitative assessments of the predominant unsaturated flow processes will be given for the different lithologies at Rainier Mesa and Shoshone Mountain in the following sections.

## Rainier Mesa Conceptual Flow Model

This section presents a conceptual model of groundwater flow at Rainier Mesa as it originates at land surface and moves down into the saturated zone in the carbonate rock. Figure 9 illustrates the unsaturated flow processes most pertinent to the conceptualization.

### Recharge to Rainier Mesa

Rainier Mesa is estimated to have some of the highest recharge rates within the arid to semiarid NTS. Figure 10 shows a simplified map of spatially variable recharge estimates from Russell and Minor (2002), who use the approach of Dettinger (1989). Their map indicates recharge rates from 10 to 50 mm $yr^{-1}$ for Rainier Mesa and Shoshone Mountain. Russell (1987) estimated that 7 to 8 percent of precipitation becomes recharge at Rainier Mesa (which equates to recharge rates of about 22 to 25 mm $yr^{-1}$). In addition to natural recharge through precipitation, Thordarson (1965) noted that artificial recharge to Rainier Mesa has occurred from lost drilling fluid. Between the beginning of drilling in 1961 and 1964, Thordarson (1965) cited approximately 38,000 $m^3$ of lost drilling fluid. Russell and others (2001) stated that approximately 380,000 $m^3$ of drilling fluid have been added to Rainier Mesa over 30 years. Their estimate is a simple extrapolation of Thordarson's 3-year estimate over a period of 30 years. Averaged over a yearly basis, this artificial recharge is less than 10 percent of the estimated annual recharge from natural sources. Based on the tunnel discharges from table 2 in Russell and others (2001), the approximate annual discharge from Rainier Mesa tunnels is 58,700 $m^3\ yr^{-1}$ (19 $m^3\ yr^{-1}$ from U12g, 10,000 $m^3\ yr^{-1}$ from U12e, 34,800 $m^3\ yr^{-1}$ from U12n, and 13,900 $m^3\ yr^{-1}$ from U12t). The U12n annual discharge from Russell and others (2001) includes evaporative losses through the tunnel ventilation systems, which are about 20 percent of the total discharge. Because the U12e, U12g, and U12t tunnel discharge estimates do not include evaporative losses, the actual total annual amount of tunnel discharge may be larger than the estimate stated above. Using the Russell (1987) recharge estimate for the Rainier Mesa caprock (which does not include contributions from the mesa slope), annual tunnel discharge is approximately 20 percent of the annual recharge. This percentage is exclusive of any drilling fluid recharge.

The recharge at Rainier Mesa may occur both as distributed (that is, diffuse) recharge as well as focused recharge into ephemeral channels or surface depressions. Isotopic analyses and temporal variability in fracture discharge in tunnels suggests that the water comes from recharge of present-day precipitation (Russell, 1987; Russell and others, 1988; Russell and others, 2001).

These isotopic analyses also suggest that some of the tunnel seeps may be recharged by summer precipitation events and others by winter precipitation events (Russell and others, 2001). High potential evapotranspiration rates in the summer may preclude much diffuse recharge from summer storms at Rainier Mesa, but it is possible that summer recharge may be focused below ephemerally flowing channels such as those present at Aqueduct Mesa (see fig. 3). Previous investigations at other sites at the NTS have shown that ephemeral washes and collapse craters from underground nuclear detonations can focus recharge (Hokett and French, 2000; Hokett and others, 2000; Savard, 1998; Tyler and others, 1996; Tyler and others, 1992).

### Flow Through the Welded Tuff

Once water has passed beneath the zone of evaporation and transpiration, it enters the Rainier Mesa welded tuff. The saturated hydraulic conductivity of the matrix is relatively low in the Rainier Mesa welded tuff (table 2). The welded tuff is also heavily fractured, which in combination with the low matrix saturated hydraulic conductivity favors macropore preferential flow through fractures as the dominant flow process in the welded tuff (Thordarson, 1965). As water moves vertically downward through the welded tuff, it encounters the lithologic transition to the vitric tuff.

### Flow Into and Through the Vitric Tuff

The vitric tuff has a matrix with a much larger saturated hydraulic conductivity and porosity than the overlying welded tuff (table 2). Thordarson (1965) suggested that this lithologic boundary marks a transition from preferential flow in fractures through the welded tuff to matrix-dominated flow through the vitric tuff, where fractures may not be well preserved. It is possible that the transition from the fine grained, low hydraulic conductivity matrix of the welded tuff to the coarser grained, higher hydraulic conductivity matrix of the vitric tuff could serve as a capillary barrier. However, the likely prevalence of macropore preferential flow through fractures in the welded tuff at Rainier Mesa would short-circuit the capillary barrier process at the lithologic transition. Additionally, the analytical solutions of Ross (1990) and Steenhuis and others (1991) suggest that the capillary-barrier mechanism is most effective at relatively low fluxes, which is supported by laboratory experiments (Walter and others, 2000). Investigators at nearby Yucca Mountain, which has similar geology to Rainier Mesa, have suggested the capillary-barrier process is most effective at low fluxes but is minimal at high fluxes (greater than 10 mm $yr^{-1}$) (Altman and others, 1996; Montazer and Wilson, 1984; Moyer and others, 1996; Rulon and others, 1986; Scott and others, 1983; Wu and others, 2002). The estimates of recharge fluxes at Rainier Mesa (20-50 mm $yr^{-1}$) are sufficiently high to suggest that the capillary-barrier mechanism may be limited at the lithologic contact between the welded tuff and the vitric tuff. Additionally, the welded tuff and vitric tuff contact at Rainier Mesa forms a structural (depositional) syncline. If a capillary barrier is active at this contact, water perched at the interface would be diverted into the synclinal axis, where increased saturation would short-circuit the capillary barrier. Gauthier (1998) noted that seeps into the U12n tunnel in Rainier Mesa are concentrated below the syncline axis.

After flow crosses the lithologic transition between the welded and vitric tuff, the dominant unsaturated flow process through the vitric tuff at Rainier Mesa is unclear. Thordarson (1965) and Russell (1987) suggest that flow through the vitric tuff occurs as stable, matrix-dominated flow rather than preferential flow. Alternatively, the dominant flow process in the vitric tuff may be preferential flow through the matrix occurring as either finger flow beneath points of focused discharge below fractures in the welded tuff or as funnel flow at topographic

irregularities at the contact between the welded tuff and vitric tuff. It is also unclear how well finger flow can be sustained over 100 meters of unsaturated porous material; it may be the case that the fingers are adsorbed by capillary processes into the surrounding matrix to form steady, diffuse unsaturated flow through the collective pore space. If this is the case, then the flow through the vitric tuff may be nonpreferential and therefore slower than preferential flow. Wang and others (1993) and Gauthier (1998) suggest that water moves through the vitric tuff as macropore preferential flow via fractures. The conceptual model shown in figure 9 shows both fracture and finger preferential flow as possibilities at Rainier Mesa in the vitric tuff.

### Flow Into and Through the Zeolitic Tuff

Table 2 shows the large saturated hydraulic conductivity contrast between the zeolitic tuff matrix and the overlying vitric tuff matrix, with the zeolitic tuff potentially acting as a permeability barrier to vertical unsaturated matrix flow. Russell (1987) suggested that groundwater percolating through the vitric tuff perches on the zeolitic tuff and then drains slowly through fractures in the zeolitic tuff and potentially into the tunnel system. The lithologic transition between the zeolitic and vitric tuff is the approximate upper extent of the hummocky perched saturated zone at Rainier Mesa and occurs at 1,830±60 m (Russell and others, written commun., 2003). This irregular perched saturated zone, located within the zeolitic tuff, tends to coincide with the base of the vitric tuff (Thordarson, 1965).

Previous investigations have assumed that the dominant pathway for downward movement of water in the zeolitic tuff is as macropore preferential flow through fractures (Gauthier, 1998; Russell, 1987; Thordarson, 1965). Several lines of evidence from tunnel construction indicate that the fracture system within the zeolitic tuff is poorly connected. Thordarson, (1965) observed that (i) discharge from fractures breached by tunneling decreased rapidly with time after breaching, (ii) breaching another fracture further into the tunnel had a negligible influence on the discharge from previously breached fractures, (iii) discharging fracture water had temperature anomalies of up to 3.9° C, and (iv) the water content of fractures was variable, with only 2 percent of the joints and 50-60 percent of the fractures bearing measurable quantities of water. It is possible that the dry fractures may drain to the saturated zone in the carbonate rock or may be poorly connected to recharging fractures (Thordarson, (1965). Limited evidence suggests that there is some lateral hydrologic connectivity between the fractures in the zeolitic tuff. For example, Thordarson (1965) noted that breaching a fracture in a drift in the U12e tunnel flooded the drift and caused the nearby Hagestad 1 well (see fig. 2), which is 30 m from the drift, to drop 37 m in 1962. The Hagestad 1 well is screened in the zeolitic tuff from 580 to 490 m below land surface.

Differences in the ages of water in the matrix and fractures of the zeolitic tuff elucidate the degree of hydrologic connection between the saturated matrix of the zeolitic tuff and the fractures. Table 4 lists some of the age estimates of water in the fractures and matrix based on a variety of age-estimation techniques, including bacterial ecology, stable isotopes, artificial tracers, isotopes from atmospheric nuclear testing, major ion chemistry, and temporal patterns in fracture discharge. As noted by Russell and others (2001), an important distinction exists between actual traveltimes for water infiltrating at the surface and reaching the tunnel versus the timing of the hydrologic response, which drives discharge of water stored in fractures into the tunnels. Actual traveltimes for tracers to travel from land surface to the tunnels are 1-6 years, whereas observed increases in tunnel discharge as a response to infiltrating surface water are on time scales of 1-6 months. Table 4 shows that the matrix water is much older than the fracture water in the zeolitic tuff. Amy and others (1992) demonstrated that the bacterial ecology of the

matrix water indicated very old matrix water ages, which are consistent with the water in the matrix being emplaced in a previous pluvial period. The matrix water emplacement may be coupled with the zeolitization process, making the matrix water's age late Pliocene or early Pleistocene (Russell, 1987; Thordarson, 1965). This is consistent with previous conceptual models of the zeolitization process that act by leaching of vitric volcanic rocks in the unsaturated zone during a pluvial period (Bowers and Burns, 1990; Hay and Sheppard, 1977; Hoover, 1968; Vaniman and others, 2001). Matrix water in the zeolitic tuff has elevated sulfate concentrations, which also may indicate that water stored in the matrix is relict pluvial water (Russell, 1987; White and others, 1980). Keller (1960; 1962) noted that specific conductance, which is a proxy for salinity, of the matrix water was a factor of 25-30 times greater than the specific conductance of the fracture water. Diment and others (1959) analyzed fracture and matrix water samples from the U12b tunnel and found that the fracture seep water showed low concentrations of dissolved solids, which may indicate that the fracture water has not moved far from the recharge zone, has moved rapidly through the rock, or that the matrix does not contain highly soluble constituents. The aforementioned lines of evidence suggest that (i) the residence time of water in the zeolitic tuff matrix is on millennial time scales, (ii) the fracture water has a much shorter residence time and appears to be recharged by modern waters, and (iii) there may be little water exchange between the matrix and fractures.

Nuclear testing has most likely altered flow in the zeolitic tuff and other lithologies in which testing occurred at Rainier Mesa by enhancing fractures, which could enable water flowing through the rock where testing occurred to drain into a tunnel. One possible line of evidence for this local alteration is the observation of high sulfate concentrations in impounded water behind the U12t tunnel seal (Russell and others, written commun., 2003). These elevated sulfate concentrations could indicate a release of relict water from the matrix into the fractures that feed the tunnel. It is conceivable that matrix-water exchange has been enhanced by underground nuclear testing. This enhanced exchange, coupled with water-filled tunnels, may enable the rerouting of water across large distances through hydrologically connected fractures (Russell, 1987). Ongoing modeling efforts that simulate fracture flow in the U12t tunnel by Reeves and others (2007) will likely shed light on this topic.

### Flow Into and Through the Carbonate Rock

Groundwater is likely transmitted through macropore preferential flow in fractures through the zeolitic tuff to the base of the perched saturated zone. This base is approximately located at the lithologic contact between the zeolitic rock and the carbonate rock. The presence of argillic paleocolluvium above the carbonate rock may affect how groundwater discharging from the zeolitic tuff moves into the underlying carbonate rock. The effect of the paleocolluvium on flow into carbonate rock is uncertain because no information is available regarding the hydraulic properties of the argillic paleocolluvium. If the argillic paleocolluvium is fractured, then water is likely transferred primarily by macropore preferential flow in fractures between the zeolitic rock and the uppermost carbonate rock. The low saturated hydraulic conductivity of the matrix of the carbonate rock (table 2) indicates that water flows primarily through fractures downward to the saturated zone in the carbonate rock under the portions of Rainier Mesa where the majority of testing occurred (Russell and others, 2001; Thordarson, 1965).

### Summary of the Rainier Mesa Conceptual Model for Flow Through the Unsaturated Zone to the Saturated Zone in the Carbonate Rock

Within each lithologic unit, one or two modes of flow are likely to have the strongest influence on contaminant traveltimes and therefore to have overriding importance in determining the minimum possible traveltime through that unit. Based on the available site-specific hydrogeologic information and basic understanding of unsaturated-zone flow as described above, the following are the likeliest flow modes to dominate each major lithologic unit:

1. Preferential flow in fractures through the welded tuff.
2. Matrix and preferential (unstable finger) flow through the vitric tuff. Finger flow likely occurs below areas where fractures discharge water from the overlying welded tuff. The possibility of macropore preferential flow through fractures exists.
3. Preferential flow in fractures through the zeolitic tuff into tunnels and into underlying unsaturated carbonate rock.
4. Preferential flow in fractures through unsaturated carbonate rock to the saturated zone.
5. Fracture flow through the saturated zone in the upper carbonate aquifer.

## Shoshone Mountain Conceptual Flow Model

This section presents a conceptual model of the flow of water from the land surface to the lower carbonate aquifer below Shoshone Mountain, which is illustrated in figure 11. The conceptual flow model for Shoshone Mountain is similar to the Rainier Mesa conceptual model owing to the similar geology, although the upper carbonate aquifer is absent at Shoshone Mountain. Little hydraulic-property information is available for the lithologic units at Shoshone Mountain, but the properties can be approximated from the similar lithologic units at Rainier Mesa shown in table 2.

### Recharge to Shoshone Mountain

Examination of the recharge map in figure 10 shows that the Shoshone Mountain recharge rates are on the order of 2-10 mm $yr^{-1}$. However, if 7-8 percent of the estimated 200 mm of precipitation on Shoshone Mountain (Winograd and Thordarson, 1975) becomes recharge, as was applied by Russell (1987) for Rainier Mesa, the approximate recharge would be 14-16 mm $yr^{-1}$. Previous investigations (Department of Energy, 1997; Russell and Minor, 2002) have noted that recharge rates are low at the portion of Shoshone Mountain above the U16a tunnel relative to Rainier Mesa, which may lead to less percolation through the unsaturated zone at Shoshone Mountain.

### Flow Through the Welded Tuff

Percolation through the welded tuff at Shoshone Mountain likely occurs as preferential flow though fractures (Stoller-Navarro Joint Venture, 2006b), similar to the welded tuff at Rainier Mesa.

### Flow Into and Through the Vitric Tuff

The lithologic boundary between the welded and vitric tuff at Shoshone Mountain is likely similar to the same lithologic boundary at Rainier Mesa, and therefore the same unsaturated flow processes would be prevalent. The transition from the fine grained, low

hydraulic conductivity matrix of the welded tuff to the coarser grained, higher hydraulic conductivity matrix of the vitric tuff could serve as a capillary barrier if flow in both media is matrix dominated. The smaller recharge fluxes at Shoshone Mountain, relative to Rainier Mesa, may cause the capillary barrier mechanism to be more effective (see Ross, 1990; Steenhuis and others, 1991; Walter and others, 2000; Wu and others, 2002). However, it is likely that flow occurs predominantly in fractures in the welded tuff, suggesting that the capillary barrier mechanism would be ineffective for inhibiting flow across the transition between the fractured welded tuff into the vitric tuff.

Flow through the vitric tuff may be matrix-dominated, but as unstable finger flow, particularly below discharging fractures from the welded tuff into the vitric tuff. The potential for flow to be dominated by steady, diffuse flow through the collective pore space (matrix-flow) is also possible. Sweetkind and Drake (2007) observed that faults are more numerous and have larger displacements at Shoshone Mountain relative to Rainier Mesa. The more intensive faulting at Shoshone Mountain may form fault and fracture flow paths within the vitric tuff, which may facilitate macropore preferential flow through fractures, as proposed for the vitric tuff at Rainier Mesa by Wang and others (1993) and Gauthier (1998). The conceptual flow model shown in figure 11 considers preferential flow through fractures or fingers at Shoshone Mountain to be possible.

### Flow Into and Through the Zeolitic Tuff

The lithologic transition from the vitric tuff to the zeolitic tuff at Shoshone Mountain may have less of a permeability contrast than the same interface at Rainier Mesa, owing to the more intense fracturing of the zeolitic tuff at Shoshone Mountain (Sweetkind and Drake, 2007). The increase in fracturing may increase the effective permeability of the zeolitic tuffs, causing the permeability contrast between the vitric and zeolitic tuff to be less at Shoshone Mountain compared to Rainier Mesa. The possible decrease in the effective permeability contrast at the vitric and zeolitic tuff interface at Shoshone Mountain may explain why no perched saturated zone is evident in the zeolitic tuff at Shoshone Mountain near the U16a tunnel. The flow through the zeolitic tuff is likely to be macropore preferential flow in fractures, similar to Rainier Mesa, owing to the presence of fractures and the low saturated hydraulic conductivity of the tuff matrix. The U16a tunnel is driven into the zeolitic tuff, but there is no significant water flow into the tunnel.

### Flow Into and Through the Siliceous Rock

Groundwater percolates through the zeolitic tuff at Shoshone Mountain and reaches the interface defined by the contact with the siliceous rock. A relatively thin section of argillic paleocolluvium is present at the base of the zeolitic tuff that may impede vertical flow between the zeolitic tuff and siliceous rock. The fine grained siliceous rock, consisting primarily of shale, has low effective porosity and minimal open fracturing (Laczniak and others, 1996; Winograd and Thordarson, 1975) and was originally thought to act as a permeability barrier to vertical flow, possibly forming a perched saturated zone at the top of the shale (Stoller-Navarro Joint Venture, 2006b), but the ER-16-1 well at Shoshone Mountain demonstrated the absence of any perched water at this interface below the U16a tunnel.

It is not clear whether flow is preferential through fractures or matrix-dominated through the siliceous rock. Although fracturing in the siliceous rock is not prevalent (Winograd and Thordarson, 1975), the bedding planes in the upper 30 m of the siliceous rock dip 43° to the northwest (Leavitt, 2005; Stoller-Navarro Joint Venture, 2006b) and preferential flow may occur

along these bedding planes. The possibility of finger flow spanning the entire thickness of the siliceous rock is unlikely, because of the low recharge flux and several hundred meters of unsaturated conditions. The conceptual model in figure 11 favors stable, matrix-dominated flow as the most likely flow mechanism through the shale, although fracture or fault flow may be a possibility. As water moves through the siliceous rock, it ultimately reaches the lithologic contact with the carbonate rock.

### Flow Into and Through the Carbonate Rock

If, as expected, unsaturated flow through the siliceous rock is stable and matrix dominated, then the lithologic transition to the fractured carbonate has several potential active processes. If the permeability of the carbonate rock matrix is less than the permeability of the siliceous rock matrix, then a permeability barrier will exist at the lithologic interface and flow will enter the fractures in the carbonate rock and become macropore preferential flow. If the opposite is true and the permeability of the carbonate rock matrix is greater than the permeability of the siliceous rock matrix, then it is possible that preferential finger flow could initiate in the carbonate rock, depending on the water flux through the siliceous rock relative to the permeability of the carbonate rock. If the flow in the siliceous rock is dominated by preferential flow as fingers or macropore fracture flow, macropore preferential flow through fractures will likely occur through the carbonate rock. Given that the carbonate rock below the siliceous rock is heavily fractured (Laczniak and others, 1996; Winograd and Thordarson, 1975), it is likely that at least some macropore preferential flow occurs through fractures, percolating downward to the saturated zone in the carbonate rock.

### Summary of the Shoshone Mountain Conceptual Model for Flow Through the Vadose Zone to the Saturated Zone in the Carbonate Rock

The following are the likeliest flow modes to dominate each major lithologic unit at Shoshone Mountain.

1. Fracture flow through the welded tuff.
2. Matrix flow through the vitric tuff, with possible preferential finger flow beneath where fractures from the welded tuff discharge. Macropore preferential flow in fractures is a possibility.
3. Fracture flow through the zeolitic tuff.
4. Stable matrix flow through the siliceous rock.
5. Fracture flow through the carbonate rock to the saturated zone in the carbonate rock.

## Conceptual Differences in Unsaturated Flow Between Rainier Mesa and Shoshone Mountain

There are several differences between Rainier Mesa and Shoshone Mountain, and unsaturated flow could be dissimilar at the two locations. Differences include:

- Recharge is likely greater at Rainier Mesa.
- Shoshone Mountain lacks a synclinal structure that may focus recharge.
- Shoshone Mountain, in the vicinity of the U16a tunnel, has fewer large-scale surface topographic features that focus recharge.

- Faults are more numerous and have larger displacements at Shoshone Mountain relative to Rainier Mesa.
- Tunnel systems at Shoshone Mountain are not as extensive as those at Rainier Mesa.
- The volcanic rocks at Shoshone Mountain are underlain by the low permeability siliceous rock.
- Fewer nuclear tests were conducted at Shoshone Mountain compared to Rainier Mesa.
- Shoshone Mountain has no known perched water in the volcanic section near the U16a tunnel.
- The depth to the saturated zone in the carbonate rock is much greater at Shoshone Mountain.

## Potential Sources for Ground-Water Contamination by Radionuclides at Rainier Mesa and Shoshone Mountain

The issue of groundwater contamination from radionuclides at the NTS was recognized as early as 1959 (Batzel, 1959), and the first studies of the potential for groundwater contamination beneath Rainier Mesa were conducted in 1959-1960 (Clebsch, 1960). It should be noted that the radiologic source term for the Rainier Mesa and Shoshone Mountain is small relative to other areas on the NTS. However, the potential for active recharge to occur at Rainier Mesa and Shoshone Mountain (Russell and Minor, 2002; Thordarson, 1965) makes the loading of radionuclides to the saturated zone in the carbonate rock a concern. Potential sources for radionuclide contamination of groundwater in Rainier Mesa and Shoshone Mountain are:

- Working points in tunnels
- Working points in boreholes
- Tunnel inverts (floors) with continuous or intermittent flow
- Tunnel effluent ponds

The presence and the permeability of any nonnative materials used to construct tunnel inverts (floors), including concrete, are not well documented at Rainier Mesa and Shoshone Mountain. Emplacement of invert materials may affect the potential for radionuclide contamination by infiltration in the tunnels. Haldeman and others (1996) noted that the invert material in the U12n tunnel was unconsolidated and was higher in moisture content than the intact zeolitic tuff of the tunnel walls. The extent to which invert materials plug fractures in the tunnels is not characterized. The tunnel effluent ponds are another potential radionuclide source, despite the large potential evaporation rates at the NTS, because the presence of ponded water can enhance recharge (Tyler and others, 1986). Although the infiltration of the pond water may be a minor recharge source to the regional groundwater flow system, it may introduce a localized flux of radionuclide-contaminated water (Laczniak and others, 1996). The tunnel effluent is conveyed by pipes from the tunnel portals to the tunnel effluent ponds, and it is assumed that no effluent infiltration results from any pipe leakage. Potential radionuclide sources for Rainier Mesa and Shoshone Mountain differ because of differences in geology, hydrology, and the number of tests detonated, and thus are presented separately.

The potential sources for radionuclides that may contaminate groundwater at Rainier Mesa and Shoshone Mountain include: working points in tunnels, working points in boreholes, tunnel inverts with continuous or intermittent water flow, and tunnel effluent ponds. Table 5

summarizes the working points at Rainier Mesa, including the distance from the working point to the saturated zone in the carbonate rock. The table also includes a cavity-adjusted distance to account for the detonation cavity radius. Table 6 summarizes the tunnel effluent ponds at Rainier Mesa. Table 7 provides the working-point elevations and the distance and cavity-adjusted distance to the saturated zone in the carbonate rock for the six tests at Shoshone Mountain. Tunnel-source discussions in the following sections are separated into tunnels with and without continuous discharge of water.

## Rainier Mesa Tunnels With Continuous Water Discharge

### U12e Tunnel

The U12e tunnel currently produces water at rates from 30.3 to 56.8 L $m^{-1}$ and has been flowing continuously since construction began (National Security Technologies, 2007). The water discharges principally from fractures and small (less than 3 m) displacement faults trending northwest to southeast (Thordarson, 1965). Past attempts to stop the flow of water from the U12e tunnel using engineered barriers failed. Water currently flows from the portal (National Nuclear Security Administration, 2004) at 1,865 m elevation into a sequence of tunnel effluent ponds (fig. 4 and table 6) at 1,818-1,802 m elevation, where it infiltrates or evaporates. The continuous nature of the discharge from the U12e tunnel suggests the potential for radionuclide contamination from (i) percolation through working points in the U12e tunnel, (ii) infiltration of water as it drains along inverts within the tunnel, and (iii) infiltration from the ponds in which the tunnel drainage collects. The water draining through and from the U12e tunnel has been observed to be contaminated with radionuclides. Russell and others (1993) found tritium concentrations in the U12e tunnel effluent of 2.0 x $10^6$ pCi $L^{-1}$ from June 17, 1991, to May 12, 1992. The U12e tunnel ponds have also been observed to be radionuclide contaminated for periods of time; the U12e tunnel ponds had gross beta activities ranging from 8.1 to 161 pCi $L^{-1}$ between 1990 and 1996 (National Nuclear Security Administration, 2004). The U12e tunnel ponds were sampled for tritium in 2005 and had an average concentration of 6.0 x $10^5$ pCi $L^{-1}$ (Wills, 2006); U12e tunnel ponds 4 and 5 had tritium concentrations of 6.1 x $10^5$ pCi $L^{-1}$ and 6.0 x $10^5$ pCi $L^{-1}$ in 2007 (National Security Technologies, 2008).

### U12n Tunnel

The U12n tunnel intersects many fractures, some of which produced large amounts of water in the past. For example, the U12n.03 drift discharged up to 220 L $min^{-1}$ of water initially and 150 L $min^{-1}$ for months after excavation (Thordarson, 1965). Water drained continuously from the U12n tunnel since its construction and continued at approximately 47 L $min^{-1}$ until the tunnel was sealed with concrete in 1994 (Russell and others, written commun., 2003). The two ventilation shafts from the U12n tunnel were welded shut (Russell and others, 2001) and the tunnel has slowly filled with water. Because the U12n tunnel was sealed and consequently has filled with water, potential radionuclide sources are evaluated both under pre- and post-tunnel sealing conditions.

In the presealing case (before 1994), potential sources of radionuclide contamination are derived from (1) working points in the U12n tunnel, (2) infiltration of water as it drains along tunnel inverts, and (3) infiltration from the tunnel ponds (fig. 5) in which the tunnel drainage collects. The drainage from the U12n tunnel flows through pipes from the portal at 1,840 m down to the ponds at 1,767-1,735 m elevation (table 6). The uppermost tunnel ponds were frequently filled with tunnel effluent before portal sealing (Russell and others, written commun.,

2003). The gross beta activity in the U12n pond during the period from 1976 to 1993 ranged from 6,700 pCi $L^{-1}$ (in 1985) to 5.3 pCi $L^{-1}$ (in 1993), with a mean value of 602 pCi $L^{-1}$ (Russell and others, written commun., 2003). The tritium activity in the U12n ponds during the same period ranged from 1.1 x $10^7$ pCi $L^{-1}$ (in 1987) to 2.2 x $10^5$ pCi $L^{-1}$ (in 1983), with a mean value of 2.04 x $10^6$ pCi $L^{-1}$ (Russell and others, written commun., 2003).

For the postsealing case (1994 to present), the U12n tunnel has slowly filled with water. Water sampling from a pipe that extends behind the U12n tunnel seal has provided evidence from chloride and tritium data that there is some limited circulation of water within the flooded tunnel (Russell and others, written commun., 2003). The estimated average inflow rate into the sealed tunnels between closure and nearly complete inundation was 82.3 L $min^{-1}$, which is 42 percent less than the 117 L $min^{-1}$ discharge measured at the tunnel portal before closure (Russell and others, written commun., 2003). The decrease in inflow rate indicates either a decrease of flow into the tunnel from the surrounding rock or an increase of water flux percolating downward to the saturated zone in the carbonate rock, which could increase the potential for radionuclide contamination of the aquifer in the carbonate rock by the contaminated tunnel water. Reeves and others (2007) raised the possibility that the flooded tunnels may enhance the connectivity of previously noncommunicative fractures. Because of sealing, the working points and rubble chimneys are likely flooded, which may cause percolation of radionuclide-contaminated water downward towards the saturated zone in the carbonate rock. The consequent water-filling of the tunnel after sealing requires that the potential for radionuclide transport be evaluated before and after the sealing of the tunnel portal. Because water no longer flows from the portal, the ponds are no longer continuous sources of radionuclides. However, these dry ponds may intermittently supply radionuclide contaminated recharge if the pond-bed sediments contain radionuclides and surface fluxes move these radionuclides beyond the zone of evaporative and transpirative removal.

### U12t Tunnel

Extensive fracturing and faulting was noted during the U12t tunnel construction and in exploratory cores (National Security Technologies, 2007). Significant water flow occurred from fractures in the U12t tunnel, principally from two locations: one 610 m from the portal and another in the U12t.03 tunnel section (National Security Technologies, 2007). The U12t tunnel has produced drainage since construction and was actively draining at approximately 38 L $min^{-1}$ when the tunnel was sealed in 1993 (Russell and others, written commun., 2003). As is the case with the U12n tunnel, the consequent water-filling of the tunnel after sealing requires that the potential for radionuclide transport be evaluated before and after the sealing of the tunnel portal.

In the presealing case (before 1993), potential radionuclide contamination may occur from working points in the U12t tunnel, infiltration of water as it drains along tunnel inverts, and infiltration from the drainage ponds in which the tunnel effluent collects. The drainage from the U12t tunnel flows through pipes from the portal at 1,707 m down to the ponds at 1,678-1,649 m elevation (fig. 6 and table 6). The uppermost tunnel ponds were frequently filled with effluent before portal closure. The gross beta activity in the U12t ponds during the period from 1970 to 1993 ranged from 1.1 x $10^6$ pCi $L^{-1}$ (in 1986) to 10 pCi $L^{-1}$ (in 1976), with a mean value of 9.13 x $10^4$ pCi $L^{-1}$ (Russell and others, written commun., 2003). The tritium activity in the U12t ponds during the same period ranged from 3.0 x $10^8$ pCi $L^{-1}$ (in 1986) to 5.0 x $10^4$ pCi $L^{-1}$ (in 1977), with a mean value of 3.96 x $10^7$ pCi $L^{-1}$(Russell and others, written commun., 2003).

For the postsealing case (1993 to the present), chloride measurements and reducing conditions observed behind the U12t tunnel seals indicate that there is minimal circulation of

water within the tunnel (Russell and others, written commun., 2003). As was the case with the U12n tunnel, the potential exists for flooded tunnels to enhance the connectivity between previously noncommunicative fractures. Within the flooded U12t tunnels, the working points, the rubble chimneys, and the tunnels themselves may cause continuous percolation of radionuclide-contaminated water to the saturated zone in the carbonate rock. The estimated average inflow rate into the sealed U12t tunnels between closure and nearly complete inundation is 44.8 L $min^{-1}$, which is close to the 37.8 L $min^{-1}$ discharge measured at the tunnel portal before closure (Russell and others, written commun., 2003). The similarity in inflow rates suggests minimal changes in the flux downward to the saturated zone in the carbonate rock (Russell and others, written commun., 2003), although there is temporal variability in the U12t tunnel discharge. Because water has ceased to flow from the portal since 1993, the ponds are no longer continuous sources of radionuclides. However, these dry ponds may intermittently supply radionuclide-contaminated recharge if the pond-bed sediments contain radionuclides and infiltration exceeds evaporative and transpirative losses.

### Rainier Mesa Tunnels Without Continuous Water Discharge

The tunnels without continuous discharge of water (U12a, U12b, U12c, U12d, U12f, U12g, U12i, U12j, U12k, and U12p) have little or no drainage outside the portal and therefore no tunnel effluent ponds. Water infiltrating into the tunnel inverts is likely intermittent and discontinuous in space, but could still be a source of radionuclide contamination. The working points in the tunnel are potential sources of radionuclide contamination. The U12a and U12i tunnels have no nuclear test working points, and therefore, are not considered potential sources of radionuclide contamination. Information regarding the number of tests in each tunnel and the distances to the saturated zone for each working point is given in tables 1 and 5. The U12b tunnel is notable because, although the main tunnel itself had little flowing water (Diment and others, 1959; Thordarson, 1965), a vertical shaft bored downward 151 m from the tunnel invert was abandoned because of overwhelming water influx from fracture and fault flow (National Security Technologies, 2007). The difference in water flow between the U12b tunnel and the vertical shaft likely occurs because the tunnel is emplaced in the vitric tuff while the shaft is bored into the zeolitic tuff.

### Rainier Mesa Working Points in Boreholes

Two underground nuclear tests at Rainier Mesa were detonated in boreholes drilled vertically into the mesa from land surface (see fig. 2). One test was detonated in the U-12q borehole (CLEARWATER) and the other test was detonated in the U-12r borehole (WINESKIN). The U-12q borehole began filling on September 9, 1962, with drainage of perched water from the surrounding tuff immediately after construction (Fenelon, 2006). The working point elevation of the CLEARWATER test was 1,701 m, with an approximate cavity radius of 72 m (National Nuclear Security Administration, 2004). The distance from the CLEARWATER working point to the saturated zone in the carbonate rock is 212 m and the distance from the cavity bottom to the saturated zone is 140 m (table 5). No water elevations are available for the U-12r borehole, but the working point elevation for the WINESKIN test was 1,772 m with a cavity radius of 72.8 m. The distance from the WINESKIN working point to the saturated zone, which is emplaced in a quartz monzonite confining unit, is 251.2 m and the distance from the cavity bottom to the saturated zone is 178.3 m (table 5). The quartz monzonite is not underlain by the upper carbonate aquifer, and the low hydraulic conductivity of the monzonite may result in an elevated perched saturated zone (Laczniak, oral commun., 2008) that

could be poorly connected to the regional flow system. With the exception of the DES MOINES and PLATTE tests (table 5), both of these working points, which may be continuous water sources for preferential flow, are closer to the saturated zone than any of the other surface or tunnel sources at Rainier Mesa.

### Shoshone Mountain Tunnels Without Continuous Water Discharge

The U16a tunnel is summarized in table 1. Numerous fractures are present in the U16a tunnel, some with displacements of as much as 30 m (National Security Technologies, 2007). The structural geology surrounding the U16a tunnel lacks a depositional syncline like that present at Rainier Mesa. The tuff at the U16a tunnel is approximately planar bedded with low-to-moderate westward dips of 8 to 18° (National Security Technologies, 2007). The U16a tunnel has no recorded drainage in tunnel inverts, and any tunnel discharge that may have occurred is assumed to be intermittent in space and time. Groundwater recharge at Shoshone Mountain into perched or semiperched zones, not necessarily from the vicinity of the U16a tunnel, is assumed to be the source of the discharge at Tippipah and Topopah Springs (Johannesson and others, 1997; Johannesson and others, 2000; Stetzenbach and others, 2001; Winograd and Thordarson, 1975), which currently have no observed radionuclide contamination (National Nuclear Security Administration, 2004). Tippipah Spring is at 1,585 m elevation, approximately 70 m below the working points in U16a, and Topopah Spring is at 1,737 m elevation, approximately 80 m above the working points in U16a. The lack of perched water at the level of the working points in the vicinity of the U16a tunnel at Shoshone Mountain, coupled with low recharge rates and the presence of the low permeability siliceous rock, may decrease groundwater susceptibility to radionuclide contamination at Shoshone Mountain relative to Rainier Mesa.

## Traveltime Estimation Method

Radionuclide traveltimes are estimated using the SRPF model developed by Nimmo (2007). This model's output is an estimate of fastest estimated traveltime $t_t$ [T] (that is, from the maximum solute transport velocity, $V_{max}$ [L $T^{-1}$]) and is calculated as:

$$t_t = \frac{D_{transport}}{V_{\max}}, \tag{1}$$

where $D_{transport}$ is the distance of solute transport. The SRPF model estimates only maximum solute transport velocities or fastest traveltimes and not water fluxes or solute concentrations.

The SRPF model is based on data from 64 diverse field tests in the unsaturated zone with measured fastest solute transport rates (that is, the first arrival of a tracer) where solute transport by preferential flow was recognized to be dominant. Sites of the 64 tracer tests considered by Nimmo (2007) have climates ranging from arid to humid and a full spectrum of porous media from fractured rocks to soils. The solute transport distances represented range over nearly four orders of magnitude to a maximum of 1,300 m. An important observation from the study by Nimmo (2007) is the relatively small variability in fastest tracer velocity, compared to the approximately eight-order-of-magnitude range that could be expected based on porous media hydraulic properties. The analysis presented by Nimmo (2007) found no significant trends relating fastest tracer velocity to transport distance, porous medium, or tracer sampling technique; instead, the temporal distribution of water input to preferential paths was the most important factor correlating with the fastest tracer velocity. When applied to the 64 cases used for model development, the SRPF formulas estimated fastest solute transport times with

approximately order-of-magnitude accuracy; 85 percent of the SRPF model simulated traveltimes fell within a factor of 10 of the measurements.

In applying the SRPF model to Rainier Mesa, two separate formulas were developed for estimating fastest contaminant transport velocities, one for use when the water supply is continuous in time and one for when it is intermittent.

## Continuous Water Supply

For the case of continuous water supply to preferential flow paths, typically as infiltration of ponded water, the fastest contaminant transport velocity, $V_{max}$, is estimated simply as:

$$V_{\max} = V_0 , \tag{2}$$

where $V_0$ [L $T^{-1}$] is the geometric mean of the observed $V_{max}$ for the 34 continuous-supply cases examined by Nimmo (2007), which is 13 m $d^{-1}$. Given a transport distance from a source of contaminated water that is supplying a preferential path to a point of interest such as an aquifer, equation (1) can be used with $V_0$ as $V_{max}$, based on equation (2). For example, if 400 m of transport distance separates a contaminated surface pond from an aquifer below it, the fastest traveltime based on the SRPF model would be 400 m /13 m $d^{-1}$, or 31 days (0.08 years).

## Intermittent Water Supply

The $V_{max}$ for intermittent water supply is estimated in the SRPF model by assuming that the preferential solute transport is pulsed in an *on-off* mode. The tracer velocity is constant at $V_0$ when *on* and zero when *off*. $V_0$ takes the same value as for the continuous supply case, that is, the geometric mean of the continuous-case $V_{max}$ values (13 m $d^{-1}$). For the case of noncontrolled, intermittent water supply to preferential paths, for example from natural precipitation, estimating the duration of preferential solute transport (the total elapsed time when preferential flow is *on*) is a significant challenge. Comprehensive observations of preferential flow in space and time, of the type needed to precisely estimate active periods and extents of preferential flow and solute transport, are almost never collected at field sites. However, information is typically available on the total amount of water supplied over time, for example total annual precipitation. To apply the model to an intermittent case where what is known is an overall average rate of water supply, such as measured annual precipitation, a universal effective rate, $i_0$ [L $T^{-1}$], is hypothesized. This parameter represents a universal effective rate corresponding to the water supply rate associated with the generation of preferential flow. Given a value for this rate, the total volume (or "depth") of water supply can be apportioned into time periods when preferential flow is active or not. Considering that natural precipitation is supplied at various irregular rates, if one considered the total amount of *on* time to be the time during which the precipitation rate was measurably nonzero, it would cause an overestimate, because much of that time the precipitation rate would be too low to initiate preferential flow. Apportioning the total amount of precipitation into effective *on* pulses at rate $i_0$ gives a shorter and more realistic estimate of *on* time. The duration $t_p$ [T] of effective pulsed solute transport can be expressed, if the total water input, $I_{total}$ [L], is known and the total duration of the transport process is $t_f$ [T], as

$$t_p = \frac{I_{total}}{i_0} . \tag{3}$$

The intermittent $V_{max}$ for a known $I_{total}$ is estimated as:

$$V_{\max} = V_0 \frac{t_p}{t_f} = V_0 \frac{i_{avg}}{i_0} \ , \qquad (4)$$

where $i_{avg}$ [L $T^{-1}$] is the average input rate equal to $I_{total} / t_f$.

Nimmo (2007) estimated $i_0$ by using observed $V_{max}$ values from intermittent supply cases scaled by $i_0 / i_{avg}$ such that the geometric mean of the estimated velocity equals $V_0$. The estimated $i_0$ is 30 mm $hr^{-1}$ based on the 23 cases examined by Nimmo (2007) where $I_{total}$ is known. In the Nimmo (2007) model, if $I_{total}$ is not known but the total duration of water input, $t_{in}$ [T], is known, then $V_{max}$ can be estimated as:

$$V_{\max} = V_0 \frac{t_{in}}{t_f} \ . \qquad (5)$$

For example, if the annual rainfall at a location is known to be 300 mm $yr^{-1}$ (8.2 x $10^{-4}$ m $d^{-1}$) and using 30 mm $hr^{-1}$ (0.73 m $d^{-1}$) for $i_0$ and 13 m $d^{-1}$ for $V_0$, the $V_{max}$ value using equation (4) would be 1.5 x $10^{-2}$ m $d^{-1}$. Using the previous example of 400 m of transport distance between an aquifer and a contaminant source that is intermittently supplied by the 300 mm $yr^{-1}$ of precipitation, the SRPF model fastest traveltime would be 73 years. Comparing SRPF intermittent- and continuous-supply estimates for a case of natural precipitation versus continuous ponding, it is clear that the estimated fastest traveltimes may differ by orders of magnitude.

## Important Features of the SRPF Model

The SRPF model uses precipitation rate in a role for which recharge-rate estimates might be considered to be more directly appropriate. Some fraction of the incident precipitation must be assumed to become runoff or evapotranspiration and therefore would not be active in driving preferential flow to the deep unsaturated zone. Even so, for the SRPF model Nimmo (2007) used the precipitation rate to correlate with preferential solute transport speed because, for the great majority of $V_{max}$ measurements for intermittent water input, the infiltration or recharge rates were not known. In general, mean precipitation rate is much more commonly known than mean recharge rate. Therefore precipitation rate was used as $i_{avg}$ in SRPF model development, and it must consequently also be used when the model is applied to new situations. If, in the future, enough cases of measured $V_{max}$ exist for reliably estimated infiltration or recharge rates, it would be possible to reformulate the SRPF model for use with one of those parameters instead. Using either estimated infiltration or recharge rates in place of annual precipitation would lead to a different (smaller) $i_o$ value for use in predicting traveltimes for these situations. The 30 mm $hr^{-1}$ $i_o$ value must be applied when using annual precipitation $i_{avg}$. The fact that only a fraction of annual precipitation moves deep in the unsaturated zone as recharge is already accounted for by the relatively large $i_o$ value of Nimmo (2007).

A result of the empirical nature of the SRPF model is that rate-affecting quantities such as gravitational force and the viscosity of water are contained implicitly in its formulation, and specific properties of the media at the site of interest do not enter explicitly into the fastest-speed calculation. Those properties are instead taken into account earlier in the traveltime estimating process, in the evaluation of preferential and diffuse flow possibilities at a given site. Deemphasizing the porous media properties in the actual calculation of traveltimes is particularly advantageous in unsaturated zones like those of Rainier Mesa and Shoshone Mountain, where the basic character of the rock formations is known but there are no measurements of unsaturated hydraulic properties. In the present state of the SRPF model, the effects of tortuosity of

preferential flow paths are not explicitly accounted for and instead are represented in a lumped parameter sense into the relatively high $i_o$ value. For the fastest arrival of a tracer, the shortest preferential path may not be appreciably different than the straight line distance, used in equation (1), depending on the preferential path connectivity.

### Previous Investigations of Rainier Mesa Radionuclide Transport

#### Stoller-Navarro Joint Venture (2004)

In the work reported by Stoller-Navarro Joint Venture (2004), the movement of radionuclides by advective transport is estimated using a one-dimensional (vertical) flow approximation that depends primarily on infiltration rate, transport distance, and fracture porosity (Baetsle, 1969; Domenico and Schwartz, 1990). The infiltration rate used by Stoller-Navarro Joint Venture (2004) was 20 mm $yr^{-1}$. The transport distance was approximated using a 400-m average distance between the working points and the saturated zone (Stoller-Navarro Joint Venture, 2004). Uniform fracture porosity, with a range from 0.01 to 1 percent, was used (Stoller-Navarro Joint Venture, 2004). The aforementioned parameters provided a range of traveltime estimates from the working points vertically through Rainier Mesa to the saturated zone in the carbonate rock of 2 to 200 years (Stoller-Navarro Joint Venture, 2004).

#### Wang and others (1993)

The investigation by Wang and others (1993) considered the movement of water by fracture flow with imbibition of water by the fracture walls at Rainier Mesa. The fracture flow was estimated using the approach of Nitao and others (1992) and Martinez (1988). Only flow through the vitric tuff was considered; flow to the saturated zone in the carbonate rock was not considered. Using a nonpreferential flow estimation under a unit gradient, Wang and others (1993) estimated that for a recharge flux of 23.7 mm $yr^{-1}$, a matrix porosity of 0.4 $m^3$ $m^{-3}$, and a matrix saturation of 0.64 $m^3$ $m^{-3}$, that it would take 1,025 yr to flush one pore volume of the vitric tuff; although this estimate is clearly not a traveltime, it indicates a relatively long residence time and concomitant long traveltime for nonpreferential flow through the vitric tuff.

#### Gauthier (1998)

Gauthier (1998) used the *weeps* model (Gauthier, 1994; Gauthier and others, 1992) to examine fracture/fault flow through Rainier Mesa. The *weeps* model assumes that fracture flow occurs as fast-moving, isolated, episodic pulses through fully saturated fractures (Gauthier, 1998). The episodicity of flow at Rainier Mesa was assumed to have a log-uniform distribution between constant flow and flow for only a few days per year (Gauthier, 1998). The recharge was assumed to be spatially variable at Rainier Mesa, with a value of 23 mm $yr^{-1}$ at the U12n tunnel and 7 mm $yr^{-1}$ at U12e tunnel. Gauthier (1998) applied the *weeps* model to examine fracture-flow contributions to the U12e and U12n tunnels, but did not consider water fluxes or traveltimes below the tunnel level.

## Preferential Flow Traveltime Estimates

Traveltime estimates for both continuous [equation (2)] and intermittent [equation (4)] water supply are calculated for all identified sources of radionuclide contamination at Rainier Mesa and Shoshone Mountain. The intermittent calculations are based on the assumption that

natural rainfall is the only source of water, that it is not supplemented by streamflow or runoff. Therefore the continuous and intermittent calculations represent alternative scenarios that may correspond to end members of a range of plausible values for the fastest traveltime. Each particular contaminant source (working points, tunnels, ponds, etc.) has characteristics that make one end of the range a likelier indication of actual traveltime than the other. The estimated traveltimes are referred to as *fastest traveltime* to denote that this is the first detectable tracer arrival, but does not indicate a flux or specific concentration threshold. The SRPF model travel times use the detonation cavity-adjusted distances to the saturated zone given in tables 5 and 7. In each section below that pertains to the sources at Rainier Mesa and Shoshone Mountain, the most likely temporal nature of the infiltration is identified. The traveltime estimates for Rainier Mesa and Shoshone Mountain determined from the SRPF model are given for each working point in tables A1 and A2 in the appendix and are summarized in tables 8 (working points) and 9 (tunnel inverts and tunnel effluent ponds) and in figure 12. The $i_{avg}$ value used in equation (4) for intermittent infiltration is the average annual precipitation, which is 319 mm $yr^{-1}$ at Rainier Mesa (National Oceanic and Atmospheric Administration, 2006) and 200 mm $yr^{-1}$ at Shoshone Mountain (Winograd and Thordarson, 1975). All model calculations use the $V_0$ value of 13 m $d^{-1}$ from Nimmo (2007). The $i_0$ value used for the intermittent estimates is 0.73 m $d^{-1}$ as estimated by Nimmo (2007).

### Fastest Traveltime Estimates for Working Points and Tunnel Inverts for Rainier Mesa Tunnels With Continuous Water Discharge

The U12e tunnel currently has continuous water discharge, and the U12n and U12t tunnels had continuous discharge until sealed. The presence of continuous tunnel discharge suggests that traveltimes are best approximated using equation (2), which assumes a continuous source for preferential flow. The fastest traveltimes to the saturated zone in the carbonate rock from individual working points for the U12e, U12n, and U12t tunnels are shown in table A1 for both continuous and intermittent water supply, and the continuous estimates are in italics to denote these estimates as more appropriate based on the conceptual model. Table 8 is a summary for each tunnel or borehole based on the working points in that specific tunnel or borehole and includes the U12e, U12n, and U12t tunnels. For example, the U12e tunnel summary in table 8 presents the statistics for simulated traveltimes from the SRPF model based on the nine working points in the U12e tunnel shown in table A1. The statistics in table 8 include the mean, median, furthest to the saturated zone, and closest to the saturated zone traveltimes for the group of working points in each tunnel. Table 9 contains the simulated fastest traveltimes, based on the SRPF model, to the saturated zone in the carbonate rock from the tunnel inverts and includes the U12e, U12n, and U12t tunnels. The transport distance for the tunnel inverts is based on the elevation at the tunnel portal. As a result of the upward slope of the tunnels, the mean invert location is higher than the portal, which results in a shorter (that is, conservative or worst case) transport distance and SRPF model traveltime.

The working point traveltimes and summary statistics of traveltimes from the SRPF model suggest rapid radionuclide transmission to the saturated zone in the carbonate rock, on the order of one month (0.08 years) for the U12e, U12n, and U12t tunnel working points, if the preferential paths are continuously supplied. The estimated fastest traveltimes to the saturated zone shown in table 9 from the Rainier Mesa U12e, U12n, and U12t tunnel inverts suggest that the fastest traveling water reached the saturated zone in the carbonate rock approximately one month after the tunnel portal was sealed and the preferential paths became continuously supplied. Inspection of tables A1, 8, and 9 suggest much longer traveltimes to the saturated zone in the

carbonate rock if the preferential flow paths from the U12e, U12n, and U12t tunnel working points and inverts are intermittently supplied. For example, intermittently supplied traveltime estimates for the U12e, U12n, and U12t tunnel working points and inverts are approximately between 60 and 80 years.

### Fastest Traveltime Estimates for Working Points and Tunnel Inverts for Rainier Mesa Tunnels Without Continuous Water Discharge

The U12b, U12c, U12d, U12f, U12g, U12j, U12k, and U12p tunnels have intermittent water discharge, and therefore the intermittent supply equation from the SRPF model (equation 4) would most likely apply. The fastest traveltimes to the saturated zone in the carbonate rock from individual working points for the U12b, U12c, U12d, U12f, U12g, U12j, U12k, and U12p tunnels are shown in table A1 for both continuous and intermittent water supply, and the intermittent estimates are in italics to denote these estimates as more appropriate based on the conceptual model. Table 8 contains the statistical summary for the U12b, U12c, U12d, U12f, U12g, U12j, U12k, and U12p tunnels. Table 9 contains the simulated fastest traveltimes, based on the SRPF model, to the saturated zone in the carbonate rock in the carbonate rock from the tunnel inverts and includes the U12b, U12c, U12d, U12f, U12g, U12j, U12k, and U12p tunnels.

The working point traveltimes and summary statistics of traveltimes from the SRPF model for intermittent water supply suggest radionuclide transport to the saturated zone in the carbonate rock at time scales on the order of 35 to 155 years for the U12b, U12c, U12d, U12f, U12g, U12j, U12k, and U12p tunnel working points. The traveltimes for the DES MOINES (35 years) and PLATTE (39 years) test working points seem unusually short, and the validity of the distances to the saturated zone for these tests are suspect because the working point elevations are more than 100 m below the tunnel portal elevations and no vertical shaft construction within the tunnel was noted for these tests. The upward slope of the tunnels should cause most working point elevations to be higher than the tunnel portals. If the working points for the DES MOINES and PLATTE tests are taken to be the same as the tunnel portal elevation, then the estimated intermittent supply traveltimes are closer to the other working point traveltimes; DES MOINES is 69 years and PLATTE is 72 years. Correcting the DES MOINES and PLATTE traveltime estimates suggests radionuclide transport to the saturated zone in the carbonate rock at time scales on the order of 49 to 155 years for the U12b, U12c, U12d, U12f, U12g, U12j, U12k, and U12p tunnel working points. The estimated fastest traveltimes to the saturated zone shown in table 9 from the Rainier Mesa U12b, U12c, U12d, U12f, U12g, U12j, U12k, and U12p tunnels inverts are similar to those from the working points, ranging from 70 to 120 years. Although the estimated traveltimes for the working points and tunnel inverts are given for the U12b, U12c, U12d, U12f, U12g, U12j, U12k, and U12p tunnels in tables A1, 8, and 9, the conceptual model in this report indicates that continuous supply of preferential flow paths from the aforementioned tunnels is unlikely.

### Fastest Traveltime Estimates for Rainier Mesa Boreholes

The traveltimes for the working points within the U-12q and U-12r boreholes are provided in tables A1 and 8. The U-12q test traveltimes are 11 days for continuous water supply or 25 years for intermittent water supply; the U-12r test traveltimes are 14 days for continuous water supply or 31 years for intermittent water supply. Fenelon (2006) noted that the U-12q borehole filled with water immediately after construction, but that the current water level in the

U-12q borehole is unknown because the test destroyed the borehole. The water-level history and current water level at the location of the U-12r borehole are unknown. Based on the knowledge that the U-12q borehole filled with water after construction, it is likely that preferential flow paths supplied by this borehole are continuously supplied. The temporal nature of water supply U-12r borehole is probably similar to the U-12q borehole and potentially filled with drainage of perched water in fractures after test detonation. However, the U-12r borehole is emplaced in a quartz monzonite confining unit that may significantly impede advective solute transport owing to the low hydraulic conductivity of the monzonite. The upper carbonate aquifer is absent below the monzonite, and it is possible that the U-12r borehole is poorly connected to the regional flow system in the lower carbonate aquifer.

### Fastest Traveltime Estimates for Rainier Mesa Tunnel Ponds

Table 9 shows the SRPF model estimated traveltimes to the saturated zone in the carbonate rock for the U12e, U12n, and U12t tunnel ponds (see fig. 4-6). The tunnel ponds serve as a continuous source of water to preferential flow paths when filled and an intermittent source when empty. It is unknown whether all the ponds contain water simultaneously, but the tunnel discharge history suggests that at least some of the U12n and U12t ponds contained effluent until tunnel sealing, while at least some the U12e tunnel ponds consistently contain water at the present time. After sealing, the intermittent traveltimes would apply for the U12n and U12t tunnel ponds. The estimated traveltimes for continuous supply from U12e, U12n, and U12t tunnel ponds are rapid, on the order of 0.09 years (approximately one month) and for intermittent supply are considerably longer, on the order of 60 to 90 years (see table 9).

### Fastest Traveltime Estimates for the Working Points and Tunnel Invert for the Shoshone Mountain Tunnel

The U16a working points and tunnel invert at Shoshone Mountain most likely have intermittent water discharge, and therefore the intermittent supply equation from the SRPF model (equation 4) would most likely apply. Table A2 shows the fastest traveltimes to the saturated zone in the carbonate rock from the individual working points in the U16a tunnel for both continuous and intermittent water supply, and the intermittent estimates are in italics to denote these estimates as more appropriate based on the conceptual model. Table 8 contains the statistical summary for the working points in the U16a tunnel and table 9 contains the simulated fastest traveltimes, based on the SRPF model, to the saturated zone in the carbonate rock from the U16a tunnel invert.

The working point traveltimes in table A2 and summary statistics of working point traveltimes in table 8 from the SRPF model for intermittent water supply suggest radionuclide transport to the saturated zone in the carbonate rock at time scales on the order of 240 years for the U16a tunnel working points. The estimated fastest traveltime to the saturated zone shown in table 9 from the U16a tunnel invert at Shoshone Mountain is approximately 250 years, which is slightly longer than those from the working points owing to the inclusion of the detonation cavity radius in the working point distances to the saturated zone in the carbonate rock . Although the estimated traveltimes for the working points and tunnel inverts are given for the U16a tunnel in tables A1, 8, and 9, the conceptual model in this report indicates that continuous supply of preferential flow paths from the U16a tunnel is unlikely.

## Possibility of Nonpreferential flow at Rainier Mesa and Shoshone Mountain

For the SRPF model to be appropriate for estimating unsaturated traveltimes at Rainier Mesa and Shoshone Mountain, flow in the unsaturated zone must be preferential. Flow through Shoshone Mountain is considered to be preferential throughout all the lithologies shown in figures 8 and 11, with the possible exception of the vitric tuff and the siliceous rock (Stoller-Navarro Joint Venture, 2006b). At Rainier Mesa, flow is thought to be preferential through all of the lithologic layers shown in figures 7 and 9, with the possible exception of the vitric tuff (Russell and others, 2001; Thordarson, 1965). If flow is nonpreferential in some of the lithologies beneath the contaminant sources, then the estimated fastest traveltimes presented here will be too fast. An estimate of the tracer velocity $v$ for steady, matrix-dominated flow can be approximated using the expression from Warrick and others (1971):

$$v = \frac{i}{\theta_s} , \tag{6}$$

where $i$ is the infiltration rate [L $T^{-1}$] and $\theta_s$ is the soil-water content [$L^3$ $L^{-3}$] at the top boundary condition.

Most of the underground testing at Rainier Mesa and Shoshone Mountain was conducted in the zeolitic tuff, which is stratigraphically below the vitric tuff. Therefore, the downward transport of radionuclides from the working points, tunnels, and tunnel effluent ponds at Rainier Mesa occurs in lithologies that are likely to have preferential flow through fractures (Thordarson, 1965). The argument can be made that if the recharge flux must pass through the vitric tuffs, which may be dominated by stable matrix flow that would be expected to dampen the temporal variability in flux, that this damping process may impede preferential flow below the vitric tuffs and affect the SRPF estimates of traveltimes. However, the traveltimes of 1-6 years from the surface to tunnel level (approximately 500 m of transport) at Rainier Mesa (Clebsch and Barker, 1960), despite traveling through the vitric tuffs, suggest that preferential flow is active from the surface to the tunnel level. Additionally, the tunnel discharge shows temporal variability (Russell, 1987; Thordarson, 1965) that would be unlikely if flow though the vitric tuffs was stable, matrix-dominated flow because of the damping process.

At Shoshone Mountain, the clastic confining unit of the siliceous rock may be dominated by matrix flow. The presence of the low-permeability, relatively unfractured siliceous rock (Stoller-Navarro Joint Venture, 2006b) between the Shoshone Mountain working points and the carbonate rock likely inhibits preferential flow through fractures. However, geophysical logs from ER-16-1 note (1) increased uranium concentrations in some shale sections, which may indicate fracture flow and (2) bedding planes that dip 43°, which may serve as preferential paths (Stoller-Navarro Joint Venture, 2006b).

Based on the ER-16-1 borehole at Shoshone Mountain (Stoller-Navarro Joint Venture, 2006b), the approximate thickness of the siliceous rock is 450 m. The flux and water content at the top of the siliceous rock are unknown, although the estimated recharge rate (2 to 16 mm $yr^{-1}$) can be used as a flux estimate if steady flow is assumed. If the flow through the shale is stable, matrix-dominated flow, then any temporal variations in flux would likely be damped into steady flow. Siliceous rock porosity estimates, taken from measurements at oil and gas exploration wells in Southern Nevada, ranged up to 0.06 $m^3$ $m^{-3}$ (Plume, 1996; Sweetkind and others, 2007). A simple estimate of contaminant velocity uses equation (6) with a water content of 0.03 $m^3$ $m^{-3}$, which is a saturation of 0.5 based on the 0.06 $m^3$ $m^{-3}$ porosity, and a flux estimate of 9 mm $yr^{-1}$, which is the mean of the recharge estimates from Shoshone Mountain (2 to 16 mm $yr^{-1}$) and provides a contaminant velocity estimate of 0.3 m $yr^{-1}$. The traveltime through the shale can be

calculated using equation (1) as 450 m divided by 0.3 m $yr^{-1}$ to give 1,500 years. Using the mean distance from the Shoshone Mountain working points to the saturated zone in the carbonate rock, the preferential flow through the 400 m of rock that is not siliceous rock takes approximately 113 years, based on the intermittent supply fastest traveltime estimates from the SRPF model, giving a total average traveltime from the working points of 1,613 years. Clearly having matrix-dominated flow instead of entirely preferential flow makes a large difference in traveltime estimates for Shoshone Mountain, comparing the 1,613-year traveltime estimate with matrix-dominated flow to the 240-year mean traveltime for the U16a tunnel working points shown in table 8.

### Traveltime Summary

Figure 12 presents a summary of the continuous-supply and intermittent-supply traveltimes to the saturated zone in the carbonate rock based on the SRPF model. The several-orders-of-magnitude range in traveltimes between the continuous- and intermittent-supply traveltimes shown in figure 12 suggests, as expected, that the dominant factor in controlling solute transport time in the SRPF model is the temporal nature of the water supply. Figure 12 suggests that intermittent-supply traveltime estimates range from tens to hundreds of years while continuous-supply traveltimes are one to two months for travel from contaminant sources to the saturated zone in the carbonate rock at Rainier Mesa. Shoshone Mountain likely has intermittent water supply, implying that traveltime estimates probably fall in the upper portions of the calculated range, hundreds of years. The overall SRPF-based evaluation suggests that contaminant sources most strongly associated with a continuous water supply are most likely to lead to short-term (less than a few years) transport through the unsaturated zone to the carbonate-rock saturated zone at Rainier Mesa. The U12e, U12n, and U12t tunnel ponds and inverts and the U12-q and U12-r boreholes probably have the briefest traveltimes, if the SRPF model applies at Rainier Mesa and preferential paths are indeed continuously supplied. The U12b, U12c, U12d, U12f, U12g, U12j, U12k, and U12p tunnel working points and inverts at Rainier Mesa and the U16a tunnel working points and invert at Shoshone Mountain likely have intermittent water supply to preferential paths, and therefore much longer traveltimes based on the SRPF model, but the estimated fastest traveltimes to the saturated zone in the carbonate rock are still all less than 250 years, given that preferential flow and contaminant transport occurs.

## Discussion

### Appropriateness of Applying the SRPF Model at Rainier Mesa and Shoshone Mountain

#### Comparison to Preferential Solute Transport at Field Sites With Tuff Lithology

The SRPF model was developed on the basis of data from highly diverse porous media. One test of the model is its ability to estimate the fastest tracer traveltimes in tuff lithology for both continuous and intermittent supply tracer experiments. The field sites considered by Nimmo (2007) that possess tuff lithologies are Apache Leap, Arizona, and Yucca Mountain, Nevada. The observed $V_{max}$ values taken from Nimmo (2007) for continuous supply from tuffs can be compared to the $V_0$ value (that is, the geometric mean) from the 34 continuous supply tracer tests shown in table 1 from Nimmo (2007). The geometric mean of the observed $V_{max}$ values from the six continuous supply tracer tests in tuffs (see Glass and others, 2002; Hu and others, 2001; Salve, 2005; Salve and Oldenburg, 2001; Salve and others, 2003) presented by Nimmo (2007) is 12.3 m $d^{-1}$, which is close to the 13 m $d^{-1}$ $V_0$ reported for all 34 continuous supply cases. It should

be noted that the geometric mean of the transport distances for the six continuous-supply cases of preferential paths in tuff lithology is 6.1 m, which is considerably less than the hundreds of meters of transport at Rainier Mesa. The observed $V_{max}$ values from the four cases of intermittent supply with solute transport through tuff lithology considered by Nimmo (2007) can be compared with $V_{max}$ estimates calculated from equation (4) using the average annual precipitation values given in table 1 from Nimmo (2007). The $i_{avg}$ at Yucca Mountain is 170 mm $yr^{-1}$ and the $i_{avg}$ at Apache Leap is 370 mm $yr^{-1}$, which gives intermittent supply $V_{max}$ estimates, using the 13 m $d^{-1}$ value for $V_0$ from Nimmo (2007), of 8.3 x $10^{-3}$ m $d^{-1}$ and 1.8 x $10^{-2}$ m $d^{-1}$, respectively. The observed $V_{max}$ values are 3.0 x $10^{-2}$ m $d^{-1}$ (Fabryka-Martin and others, 1997), 1.0 x $10^{-2}$ m $d^{-1}$ (Davidson and others, 1998), 6.0 x $10^{-3}$ m $d^{-1}$ (Yang, 1992), and 4.0 x $10^{-3}$ m $d^{-1}$(Yang, 1992). These four intermittent supply cases all use radionuclides deposited from atmospheric nuclear tests as the tracer [see table 1 in Nimmo (2007)] and have a geometric mean transport distance of 88 m and an arithmetic mean transport distance of 127 m. The six aforementioned continuous supply cases and four intermittent supply cases in tuff lithologies were used in the development of the SRPF model by Nimmo (2007) and are not outliers in terms of $V_{max}$ values, suggesting the applicability of the SRPF model in its present form in unsaturated tuffs at Rainier Mesa and Shoshone Mountain.

## Evidence for Preferential Solute Transport at Rainier Mesa and Shoshone Mountain

The few existing measurements of unsaturated traveltimes at Rainier Mesa support the potential for preferential solute transport. For example, Clebsch (1960) reported transport of the tritium concentration peak from atmospheric nuclear testing taking 1-6 years from the surface to tunnel level (approximately 500 m) at Rainier Mesa. Preferential solute transport from the surface to tunnel level seems probable in this case, despite the tritium transport occurring through the vitric tuff lithologic unit, within which stable matrix flow has been suggested to be dominant. Additional tracer observations in table 4 suggest relatively rapid hydrologic response and tracer traveltimes at Rainier Mesa, considering the presence of a thick unsaturated zone. It is possible that the ability of the unsaturated rock at Rainier Mesa to rapidly convey hydrologic pressure response and tracer pulses is a result of the near-saturated conditions that exist in some of the lithologic units. For example, National Nuclear Security Administration (2004) noted matrix saturations of 0.9, 0.86, and 0.96 $m^3$ $m^{-3}$ of the pore space in the Rainier Mesa welded tuff, vitric tuff, and zeolitic tuff, respectively. These nearly saturated conditions suggest there is little adsorption of water into the matrix by capillarity as water moves through preferential paths. For Shoshone Mountain, there are no data regarding preferential solute transport from the surface to tunnel level.

There is sparse instrumentation to provide confirmation data of preferential solute transport from tunnel level or working point level to the saturated zone in the carbonate rock at Rainier Mesa and Shoshone Mountain. Intermittent (annual to multiannual) monitoring at the Rainier Mesa wells ER-12-1, ER-12-3, and ER-12-4, which all sample the upper carbonate aquifer, has not detected radionuclides above NTS background levels (Bechtel Nevada, 2006; Stoller-Navarro Joint Venture, 2006a). At Shoshone Mountain, neither well ER-16-1 nor the springs at Tippipah Spring and Topopah Spring has radionuclide concentrations above background NTS levels (Stoller-Navarro Joint Venture, 2006b).

## Potential for Radionuclide Contamination of the Regional Flow System at Rainier Mesa and Shoshone Mountain

The SRPF model traveltimes, even for intermittent supply, are faster than one might expect in a semiarid climate with a thick unsaturated zone. As noted previously, the SRPF model only estimates the fastest traveltime, which necessarily is faster than the traveltime of the main bulk of transported material. It does not give a flux value for the transport of either water or contaminant. Therefore this model cannot directly indicate the time when the amount of transported contaminant has reached any particular amount, or the time to reach any particular threshold of contaminant concentration. Viewed in a particle-tracking framework, it would indicate the estimated arrival time of the first particle. If there is a broad spread of traveltimes for the other particles, the average traveltime of those particles would be much slower and substantially more time would have to elapse before enough contaminant has been transported to raise concentrations to a given level of significance.

Furthermore, at Rainier Mesa, the degree of continuity within the upper carbonate aquifer, which may consist of multiple sections separated by younger siliceous rocks that hydrologically isolate the carbonate blocks, reduces hydrologic connectivity. Fenelon and others (2008) noted large differences in water levels in wells and the hummocky nature of the saturated zone as evidence that that the upper carbonate aquifer consists of hydrologically isolated blocks of carbonate rock. If the upper carbonate aquifer is hydrologically discontinuous, transport of radionuclides would be significantly impeded. If this is the case, water may move from the upper carbonate aquifer beneath Rainier Mesa southward and then westward into the Pahute Mesa–Timber Mountain volcanic aquifer (Fenelon and others, 2008). Even if the upper carbonate aquifer is continuous, the lower carbonate aquifer beneath Rainier Mesa is separated from the overlying upper carbonate aquifer by 300 to 1200 m of siliceous rock with low permeability that restricts flow between the upper and lower carbonate aquifer and would increase traveltimes by at least 1,000 years (Fenelon and others, 2008), likely reducing the potential for radionuclide contamination of the lower carbonate aquifer. At Shoshone Mountain, the SRPF model estimated traveltimes are to the lower carbonate aquifer in the carbonate rock, which is within the regional flow system.

## Benefits of Further Testing and Development of the SRPF model

There is not yet a published test of the SRPF model for data other than the dataset used in its development. Nimmo (2007) did not develop the model with a split-sample approach [partitioning available data into distinct sets for empirical development versus model testing (Klemes, 1986)] because of the small size of the available dataset and the need to consider it in separate categories such as continuous supply and intermittent supply. Further testing of the SRPF model with additional first-arrival tracer data would increase confidence in its reliability. Ideally, results from the SRPF model used in this report will supplement and complement the understanding gained from more complex modeling efforts, based on more traditional types of unsaturated flow models, that are currently underway for Rainier Mesa (Reeves and others, 2007; Sun and others, 2008).

The SRPF model may benefit from incorporating more physics into its formulation. One possible avenue for making the SRPF model more physically based is to use film flow formulations with Stokes flow in the preferential paths and a Richards' equation approach in the porous media. Extending the SRPF model could allow increased understanding of preferential flow and conceptual development by enabling simulation of (1) water and solute fluxes between

the porous media and preferential paths, (2) intermittent, pulsed solute transport at the time scale of single storms, and (3) tortuous preferential flow paths with varying connectivity.

## Summary

The work presented here develops a conceptual model of flow and conservative radionuclide transport from the land surface to the shallowest saturated zone within the carbonate rock at Rainier Mesa and Shoshone Mountain. An inventory of potential radionuclide sources is provided, including working points, tunnel inverts, and tunnel effluent ponds. An SRPF model is employed to estimate fastest unsaturated traveltimes for conservatively transported radionuclides to the saturated zone from the potential radionuclide sources. The fastest traveltimes from the contaminant sources for intermittent-supply sources to preferential flow paths that reach the saturated zone in the carbonate rock at Rainier Mesa range from tens to hundreds of years. Traveltimes for continuous-supply sources at Rainier Mesa are on the order of one month, assuming continuous preferential radionuclide transport. The fastest traveltimes at Shoshone Mountain for both the continuous and intermittent supply cases are approximately twice the Rainier Mesa estimates owing to the longer transport distance and smaller intermittent supply flux. At Shoshone Mountain the intermittent case is more likely than the continuous case, judged from the lack of known perched water within the unsaturated zone. The presence of the siliceous rock (considered to be minimally fractured) at Shoshone Mountain may provide a barrier to preferential flow from the possible radionuclide sources above to the upper carbonate saturated zone below. If the siliceous rock effectively inhibits preferential flow, it would increase the total estimated unsaturated-zone radionuclide transport times by an order of magnitude, to more than a thousand years.

Our analysis of the possibilities for unsaturated transport of radionuclides using a relatively simple SRPF model suggests (1) that contaminated locations associated with continuous water sources, such as tunnel ponds and water-filled tunnels, may be likely to have significantly shorter radionuclide traveltimes than locations not associated with such sources but (2) substantially longer traveltimes if conditions are such that some portions of the unsaturated zone permit only matrix-dominated rather than preferential flow.

## Acknowledgements

This report benefitted from insightful comments by Joe Fenelon, Randy Laczniak, and Rich Niswonger. Prepared in cooperation with the U.S. Department of Energy, National Nuclear Security Administration, Nevada Site Office under Interagency Agreement DE-AI52-07NV28100

Table 1. Summary of tunnel characteristics at Rainier Mesa and Shoshone Mountain (see fig. 3).

[(TB) Tunnel Bed; (GC) Grouse Canyon; (R/GC) pre Rainier / post Grouse Canyon; (TS) Tub Spring; (C) Paleozoic Carbonate; ? denotes unknown or unmeasured; m, meters; yrs, years. Information from (Davis, written commun., 1962; Dickey and others, 1962; Diment and others, 1959; Emerick, written commun., 1963; Fernandez and Freshley, 1984; National Nuclear Security Administration, 2004; National Security Technologies, 2007; Russell and others, written commun., 2003; Russell and others, 2001; Thordarson, 1965)]

| Tunnel | Dates of Construction | Total Length [m] | Portal elevation [m] | Lithologic unit | Presence of water | Number of nuclear tests |
|---|---|---|---|---|---|---|
| Rainier Mesa | | | | | | |
| U12a (USGS) | 1956 | 187 | 1,702 | Zeolitic tuff (TB3-4) | None | 0 |
| U12b | 1956-1963 | 4,903 | 2,016 | Vitric tuff (Upper GC) | Little | 6 |
| U12c | 1957-1958 | 91 | 2,046 | Vitric tuff (Lower GC; R/GC) | ? | 3 |
| U12d | pre-1958 | 61 | 2,050 | Vitric tuff (Lower GC; R/GC) | ? | 1 |
| U12e | 1957-1977 | 15,149 | 1,865 | Zeolitic tuff (TB1-4; TS; C) | Yes | 9 |
| U12f | pre-1958 | 351 | 2,046 | Vitric tuff (Lower GC; R/GC) | ? | 2 |
| U12g | 1961-1989 | 11,667 | 1,864 | Vitric tuff (TB2-4; GC) | Little | 5 |
| U12i | 1959 | 760 | 1,718 | Vitric tuff (R/GC) | None | 0 |
| U12j | 1959 | 760 | 1,718 | Vitric tuff (R/GC) | None | 1 |
| U12k | 1959 | 760 | 1,718 | Vitric tuff (R/GC) | None | 1 |
| U12n | 1964-1993 | 25,000 | 1,840 | Zeolitic tuff (TB1-2; GC; TS) | Yes | 22 |
| U12p | 1962-1984 | 7,192 | 1,677 | Vitric tuff (R/GC) | None | 4 |
| U12t | 1968-1988 | 10,642 | 1,707 | Zeolitic tuff (TB2-4; TS) | Yes | 6 |
| Shoshone Mountain | | | | | | |
| U16a | 1961-1971 | 1,105 | 1,649 | Zeolitic tuff (TB) | None | 6 |

Table 2. Hydraulic properties of lithologic units at Rainier Mesa (after (Russell, 1987); data from (Thordarson, 1965).

[- denotes unknown or unmeasured; m, meters; s, seconds; <, less than; >, greater than]

| Lithologic unit | Dominant flow path | Matrix property | | |
|---|---|---|---|---|
| | | Saturated hydraulic conductivity[1] [m $s^{-1}$] | Porosity [$m^3$ $m^{-3}$] | Saturation [$m^3$ $m^{-3}$] |
| Welded tuff [2] | Fracture | $4.72 \times 10^{-9}$ | 0.14 | - |
| Vitric tuff [3] | Matrix | $1.75 \times 10^{-6}$ | 0.40 | 0.64 |
| Vitric tuff [4] | Fracture | $2.80 \times 10^{-10}$ | 0.19 | - |
| Zeolitic tuff [5] | Fracture | $9.44 \times 10^{-9}$ | 0.38 | ~1.0 |
| Zeolitic tuff [6] | Fracture | $1.40 \times 10^{-9}$ | 0.35 | ~1.0 |
| Zeolitic tuff [7] | Fracture | - | 0.32 | ~1.0 |
| Zeolitic tuff [8] | Fracture | - | 0.25 | ~1.0 |
| Carbonate rock | Fracture | $3.30 – 9.43 \times 10^{-11}$ | 0.04 | - |

[1] Saturated hydraulic conductivity based on permeameter measurements of core samples (Thordarson, 1965).

[2] Rainier Mesa Tuff.

[3] Paintbrush Group.

[4] Grouse Canyon Tuff Member.

[5] Tunnel Bed 4, Tunnel Formation.

[6] Tunnel Bed 3, Tunnel Formation.

[7] Tunnel Bed 2, Tunnel Formation.

[8] Tunnel Bed 1, Tunnel Formation.

Table 3. Vegetation at Rainier Mesa.

[Based on information from (Beatley, 1976; Russell, 1987). - denotes unknown or unmeasured; m, meters; <, less than; >, greater than]

| Elevation range [m] | Community | Genus-species | Common name | Preferred habitat |
|---|---|---|---|---|
| <1,500 m | Shrub-grassland | *Atriplex confertifolia* | Shadscale | - |
| <1,500 m | Shrub-grassland | *Coleogyne* spp. | Black brush | - |
| >1,500 m | Artemisia-Pinus-Juniperus | *Artemisia tridentate* | Big sagebrush | Deep, sandy soils |
| >1,500 m | Artemisia-Pinus-Juniperus | *Artemisia nova* | Black sagebrush | Shallow soils |
| >1,750 m | Artemisia-Pinus-Juniperus | *Pinus minophylla* | Pinyon pine | - |
| >1,750 m | Artemisia-Pinus-Juniperus | *Juniperus osteosperma* | Utah juniper | - |
| >1,750 m | Artemisia-Pinus-Juniperus | *Quercus gabellia* | Scrub oak | - |
| >1,750 m | Artemisia-Pinus-Juniperus | *Rhus* spp. | Snowberry | - |
| >1,750 m | Artemisia-Pinus-Juniperus | *Cowania* spp. | Cliff rose | - |
| >1,750 m | Artemisia-Pinus-Juniperus | *Castilleja* spp. | Indian paintbrush | - |
| >1,750 m | Artemisia-Pinus-Juniperus | *Grayia spinosa* | Hopsage | - |
| >1,750 m | Artemisia-Pinus-Juniperus | *Chrysothamnus* spp. | Rabbit brush | - |
| >1,750 m | Artemisia-Pinus-Juniperus | *Ephedra torreyana* | Mormon tea | - |
| >1,750 m | Artemisia-Pinus-Juniperus | *Purshia tridentate* | Bitter bush | - |
| >1,750 m | Artemisia-Pinus-Juniperus | *Stipa comata* | Sewing needlegrass | - |
| >1,750 m | Artemisia-Pinus-Juniperus | *Stipa pinetorum* | Pineforest needlegrass | - |
| >1,750 m | Artemisia-Pinus-Juniperus | *Stipa thurberiana* | Thurber’s needlegrass | - |

Table 4. Groundwater age observations from the Rainier Mesa tunnels.

[- denotes unknown or unmeasured; m, meters; yrs, years; <, less than; >, greater than]

| Lithologic unit | Tunnel | Depth below surface [m] | Distance from portal [m] | Fracture-water age [yrs] | Matrix-water age [yrs] | Age determination method | Reference |
|---|---|---|---|---|---|---|---|
| Vitric tuff | U12n | 400 | 1,800 | - | Several million | Bacterial ecology | (Haldeman and others, 1993) |
| Zeolitic tuff | U12n.21 | 400 | - | - | >250,000 | Bacterial ecology | (Amy and others, 1992) |
| Zeolitic tuff | U12n.05 | 400 | - | - | >250,000 | Bacterial ecology | (Amy and others, 1992) |
| Zeolitic tuff | U12n.ND | 400 | - | - | >250,000 | Bacterial ecology | (Amy and others, 1992) |
| Zeolitic tuff | U12n.SD | 400 | - | 6 to 30 | - | Bacterial ecology | (Amy and others, 1992) |
| Zeolitic tuff | U12n.05 | 400 | - | 1 to 6 | - | Stable isotopes, tracers[2] | (Russell and others, 2001) |
| Zeolitic tuff | U12e.05 | 500[1] | | 0.8 to 6 | >50 | Tritium (pre-testing) | (Clebsch and Barker, 1960) |
| Zeolitic tuff | U12g | - | - | <37 | - | $^{36}$Chlorine | (Norris, 1989) |
| - | - | - | - | 0.12-0.25 | - | Cation to silica ratios | (Jacobson and others, 1986) |
| - | - | - | - | 0.25-0.5 | - | Tunnel-discharge delay | (Jacobson and others, 1986) |
| Vitric tuff | U12b | - | - | <0.5 | - | Tunnel-discharge delay | (Diment and others, 1959) |

[1] Distance below eastern slope of Rainier Mesa, not from caprock surface.

[2] Tracers included fluorocene, direct yellow, lithium bromide, and optical brightener (Tinopal 5BM).

Table 5. Working-point elevations, water-table elevations in the carbonate rock, and distances to the saturated zone in the carbonate rock for underground nuclear tests at Rainier Mesa.

[All elevations and distances reported in the table are rounded to the nearest meter but are calculated to 0.1 meters. Information from (Department of Energy, 1997; National Nuclear Security Administration, 2004). - denotes unknown or unmeasured; m, meters. Note that two traveltime estimates are provided from both the continuous and intermittent traveltimes for the DES MOINES and PLATTE working points and analysis of the working point and tunnel portal elevations suggests that the longer traveltimes are more appropriate.]

| Tunnel or borehole location of working point | Detonation name | Detonation date [mo/d/yr] | Working point elevation [m] | Elevation of the saturated zone in the carbonate rock [m] | Distance from the working point to the saturated zone [m] | Cavity radius[1] [m] | Distance from the bottom of the cavity to the saturated zone [m] |
|---|---|---|---|---|---|---|---|
| U12b | RAINIER | 9/19/1957 | 2,017 | 1,392 | 624 | 17 | 607 |
| U12b.02 | TAMALPAIS | 10/8/1958 | 2,039 | 1,381 | 658 | 8 | 650 |
| U12b.04 | EVANS | 10/29/1958 | 2,021 | 1,398 | 623 | 6 | 617 |
| U12b.08 | FEATHER | 12/22/1961 | 2,021 | 1,412 | 609 | 8 | 601 |
| U12b.09 | CHENA | 10/10/1961 | 2,022 | 1,407 | 615 | 40 | 575 |
| U12b.10 | YUBA | 6/5/1963 | 2,025 | 1,417 | 607 | 22 | 585 |
| U12c.02 | SATURN | 8/10/1957 | 2,113 | 1,377 | 736 | 0 | 736 |
| U12c.03 | NEPTUNE | 10/14/1958 | 2,265 | 1,375 | 890 | 12 | 878 |
| U12d.01 | VENUS | 2/22/1958 | 2,157 | 1,389 | 768 | 2 | 765 |
| U12c.01 | URANUS | 3/14/1958 | 2,023 | 1,373 | 650 | 2 | 648 |
| U12e.02 | LOGAN | 10/16/1958 | 1,872 | 1,377 | 494 | 25 | 470 |
| U12e.03a | ANTLER | 9/15/1961 | 1,879 | 1,403 | 476 | 18 | 457 |
| U12e.05 | BLANCA | 10/30/1958 | 1,871 | 1,381 | 490 | 40 | 450 |
| U12e.10 | DORSAL FIN | 2/29/1968 | 1,878 | 1,411 | 466 | 36 | 430 |
| U12e.11 | DIESEL TRAIN | 12/5/1969 | 1,879 | 1,406 | 472 | 36 | 437 |
| U12e.12 | HUDSON MOON | 5/26/1970 | 1,879 | 1,415 | 463 | 36 | 427 |
| U12e.14 | DIDO QUEEN | 6/5/1973 | 1,883 | 1,422 | 461 | 36 | 424 |
| U12e.18 | DINING CAR | 4/5/1975 | 1,882 | 1,423 | 458 | 36 | 422 |
| U12f.01 | MERCURY | 9/23/1958 | 1,990 | 1,374 | 616 | 59 | 557 |
| U12f.02 | MARS | 9/28/1958 | 2,012 | 1,378 | 633 | 5 | 628 |
| U12g.01 | MADISON | 12/12/1962 | 1,877 | 1,378 | 498 | 36 | 462 |
| U12g.06 | RED HOT | 3/5/1966 | 1,921 | 1,396 | 524 | 36 | 488 |
| U12g.07 | DOOR MIST | 8/31/1967 | 1,876 | 1,400 | 476 | 35 | 441 |
| U12g.09 | CYPRESS | 2/12/1969 | 1,880 | 1,403 | 477 | 36 | 442 |
| U12g.10 | CAMPHOR | 6/29/1971 | 1,893 | 1,406 | 487 | 35 | 451 |
| U12j.01 | DES MOINES | 6/13/1962 | 1,522 | 1,301 | 221, 415 | 23 | 198, 392 |
| U12k.01 | PLATTE | 4/14/1962 | 1,530 | 1,288 | 248, 429 | 20 | 222, 410 |
| U12n.02 | MIDI MIST | 6/26/1967 | 1,850 | 1,417 | 433 | 37 | 397 |
| U12n.04 | HUDSON SEAL | 9/24/1968 | 1,850 | 1,415 | 436 | 37 | 398 |
| U12n.05 | MISTY NORTH | 5/2/1972 | 1,850 | 1,425 | 425 | 37 | 388 |

| Tunnel or borehole location of working point | Detonation name | Detonation date [mo/d/yr] | Working point elevation [m] | Elevation of the saturated zone in the carbonate rock [m] | Distance from the working point to the saturated zone [m] | Cavity radius[1] [m] | Distance from the bottom of the cavity to the saturated zone [m] |
|---|---|---|---|---|---|---|---|
| U12n.06 | DIANA MIST | 2/11/1970 | 1,854 | 1,407 | 447 | 36 | 411 |
| U12n.07 | HUSKY ACE | 10/12/1973 | 1,849 | 1,397 | 452 | 36 | 416 |
| U12n.08 | MING BLADE | 6/19/1974 | 1,851 | 1,422 | 429 | 36 | 392 |
| U12n.09 | HYBLA FAIR | 10/28/1974 | 1,850 | 1,402 | 448 | 36 | 412 |
| U12e.20 | HYBLA GOLD | 11/1/1977 | 1,881 | 1,420 | 461 | 36 | 425 |
| U12n.10 | MIGHTY EPIC | 5/12/1976 | 1,853 | 1,445 | 408 | 36 | 372 |
| U12n.10a | DIABLO HAWK | 9/13/1978 | 1,851 | 1,435 | 416 | 36 | 380 |
| U12n.11 | MINERS IRON | 10/31/1980 | 1,850 | 1,416 | 434 | 36 | 398 |
| U12n.12 | MINI JADE | 5/26/1983 | 1,877 | 1,413 | 464 | 37 | 427 |
| U12n.15 | DIAMOND ACE | 9/23/1982 | 1,835 | 1,422 | 414 | 35 | 379 |
| U12n.15 | HURON LANDING | 9/23/1982 | 1,853 | 1,422 | 431 | 36 | 395 |
| U12n.17 | MISTY RAIN TOMME/ MIDNIGHT | 4/6/1985 | 1,850 | 1,413 | 437 | 36 | 401 |
| U12n.18 | ZEPHYR | 9/21/1983 | 1,851 | 1,429 | 423 | 36 | 387 |
| U12n.19 | DIAMOND BEECH | 10/9/1985 | 1,852 | 1,432 | 421 | 36 | 385 |
| U12n.20 | MILL YARD | 10/9/1985 | 1,859 | 1,413 | 446 | 37 | 410 |
| U12n.21 | MIDDLE NOTE MINERAL | 3/18/1987 | 1,852 | 1,427 | 425 | 36 | 389 |
| U12n.22 | QUARRY | 7/25/1990 | 1,854 | 1,452 | 402 | 36 | 366 |
| U12n.22 | RANDSBURG | 7/25/1990 | 1,854 | 1,452 | 402 | 36 | 366 |
| U12n.23 | MISTY ECHO | 12/10/1988 | 1,865 | 1,421 | 444 | 70 | 374 |
| U12n.24 | HUNTERS TROPHY | 9/18/1992 | 1,854 | 1,429 | 425 | 36 | 388 |
| U12p.02 | MISSION CYBER | 12/2/1987 | 1,682 | 1,288 | 394 | 40 | 355 |
| U12p.03 | DISKO ELM | 9/14/1989 | 1,683 | 1,358 | 324 | 40 | 284 |
| U12p.04 | DISTANT ZENITH DIAMOND | 9/19/1991 | 1,685 | 1,364 | 321 | 40 | 281 |
| U12p.05 | FORTUNE | 4/30/1992 | 1,687 | 1,347 | 340 | 41 | 298 |
| U-12q | CLEARWATER | 10/16/1963 | 1,715 | 1,503 | 212 | 72 | 140 |
| U-12r | WINESKIN | 1/15/1969 | 1,772 | 1,521 | 251 | 73 | 178 |
| U12t.01 | MINT LEAF | 5/5/1970 | 1,715 | 1,352 | 363 | 36 | 327 |
| U12t.02 | DIAMOND SCULLS | 7/20/1972 | 1,716 | 1,346 | 370 | 35 | 335 |
| U12t.03 | HUSKY PUP MIDAS | 10/24/1975 | 1,735 | 1,352 | 383 | 38 | 346 |
| U12t.04 | MYTH/MILAGRO | 2/15/1984 | 1,715 | 1,355 | 360 | 37 | 323 |
| U12t.08 | MIGHTY OAK | 4/10/1986 | 1,716 | 1,353 | 363 | 36 | 326 |
| U12t.09 | MISSION GHOST | 6/20/1987 | 1,723 | 1,342 | 380 | 38 | 342 |

[1]Cavity radius is calculated using the highest yield of the reported yield ranges (Department of Energy, 2000).

Table 6. Tunnel effluent pond elevations, water-table elevations in the carbonate rock, and distances from ponds to the saturated zone in the carbonate rock for Rainier Mesa.

[See figs. 4-6 for pond locations. m, meters]

| Tunnel supplying effluent | Tunnel effluent pond elevation[1] [m] | Elevation of the saturated zone in the carbonate rock [m] | Distance from tunnel effluent pond to saturated zone [m] |
|---|---|---|---|
| U12e | 1,802-1,818 | 1,303[2] | 499-515 |
| U12n | 1,735-1,767 | 1,303[2] | 432-464 |
| U12t | 1,649-1,678 | 1,294[3] | 355-384 |

[1] Pond elevation ranges are from Google Earth.

[2] Water-table elevation from the nearby ER-12-1 well in the shallowest portion of the upper carbonate aquifer (Fenelon and others, 2008).

[3] Average water-table elevation from the nearby PLATTE and DES MOINES working points.

Table 7. Working-point elevations, water-table elevations in the carbonate rock, and distances to the saturated zone in the carbonate rock for underground nuclear tests Shoshone Mountain.

[All elevations and distances reported in the table are rounded to the nearest meter but are calculated to 0.1 meters. Information from (Department of Energy, 1997; National Nuclear Security Administration, 2004). m, meters]

| Tunnel or borehole location of working point | Detonation name | Detonation date [mo/d/yr] | Working point elevation [m] | Elevation of the saturated zone in the carbonate rock [m] | Distance from the working point to the saturated zone [m] | Cavity radius[1] [m] | Distance from the bottom of the cavity to the saturated zone [m] |
|---|---|---|---|---|---|---|---|
| U16a | MARSHMALLOW | 6/28/1962 | 1,653 | 762 | 891 | 40 | 851 |
| U16a.02 | GUM DROP | 4/21/1965 | 1,656 | 762 | 892 | 41 | 851 |
| U16a.03 | DOUBLE PLAY | 6/15/1966 | 1,653 | 762 | 892 | 40 | 852 |
| U16a.04 | MING VASE | 11/20/1968 | 1,651 | 762 | 889 | 40 | 849 |
| U16a.05 | DIAMOND DUST | 5/12/1970 | 1,674 | 762 | 912 | 42 | 870 |
| U16a.06 | DIAMOND MINE | 7/1/1971 | 1,657 | 762 | 896 | 42 | 854 |

[1]Cavity radius is calculated using the highest yield of the reported yield ranges (Department of Energy, 2000).

Table 8. Summary of traveltime estimates for tunnel and borehole working points to the saturated zone in the carbonate rock at Rainier Mesa and Shoshone Mountain for continuous and intermittent supply using the SRPF model.

[Italics denote the most likely temporal nature of the preferential source based on the conceptual model presented in this report. The statistics represent all the working points conducted in a given tunnel or borehole. Individual working point traveltime estimates are provided in appendix tables A1 and A2. -, statistics cannot be calculated because there is only one working point; yrs, years. Note that two traveltime estimates are provided from both the continuous and intermittent traveltimes for the U12j (DES MOINES) and U12k (PLATTE) tunnels and analysis of the working point and tunnel portal elevations suggest that the longer traveltimes are more appropriate.]

| Tunnel or borehole location of working points | Continuous travel time [yrs] | | | | Intermittent travel time [yrs] | | | |
|---|---|---|---|---|---|---|---|---|
| | Mean | Median | Longest distance to saturated zone | Shortest distance to saturated zone | Mean | Median | Longest distance to saturated zone | Shortest distance to saturated zone |
| Rainier Mesa | | | | | | | | |
| U12b | 0.13 | 0.13 | 0.14 | 0.12 | *107* | *106* | *114* | *101* |
| U12c | 0.16 | 0.16 | 0.18 | 0.14 | *133* | *130* | *155* | *114* |
| U12d[1] | 0.16 | - | - | - | *135* | - | - | - |
| U12e | *0.09* | *0.09* | *0.10* | *0.09* | 77 | 76 | 83 | 74 |
| U12f | 0.12 | 0.12 | 0.13 | 0.12 | *104* | *104* | *110* | *98* |
| U12g | 0.1 | 0.10 | 0.10 | 0.09 | *80* | *79* | *86* | *78* |
| U12j[1] | 0.04, 0.08 | - | - | - | *35, 69* | - | - | - |
| U12k[1] | 0.05, 0.09 | - | - | - | *39, 72* | - | - | - |
| U12n | *0.08* | *0.08* | *0.09* | *0.08* | 69 | 69 | 75 | 64 |
| U12p | 0.06 | 0.06 | 0.07 | 0.06 | *54* | *51* | *62* | *49* |
| U12t | *0.07* | *0.07* | *0.07* | *0.07* | 59 | 58 | 61 | 57 |
| U-12q[1,2] | *0.03* | - | - | - | 25 | - | - | - |
| U-12r[1, 2] | *0.04* | - | - | - | 31 | - | - | - |
| Shoshone Mountain | | | | | | | | |
| U16a | 0.18 | 0.18 | 0.18 | 0.18 | *240* | *239* | *244* | *238* |

[1]One working point.

[2] Borehole working point.

Table 9. Summary of traveltime estimates for tunnel inverts and tunnel effluent ponds to the saturated zone in the carbonate rock at Rainier Mesa and Shoshone Mountain for continuous and intermittent supply using the SRPF model.

[Italics denote the most likely temporal nature of the preferential source based on the conceptual model presented in this report. -, statistics cannot be calculated because there is only one estimate; m, meters; yrs, years. Note that tunnel invert traveltimes are based on a transport distance from the tunnel portal and owing to the upward slope of the tunnels, the mean invert location is higher than the portal, which results in a conservative (that is, worst case) transport distance and traveltime.]

| Tunnel invert or ponds | Continuous travel time [yrs] | | | Intermittent travel time [yrs] | | |
|---|---|---|---|---|---|---|
| | Based on tunnel portal elevation | Longest distance to saturated zone | Shortest distance to saturated zone | Based on tunnel portal elevation | Longest distance to saturated zone | Shortest distance to saturated zone |
| Rainier Mesa | | | | | | |
| U12b | 0.13 | - | - | *108* | - | - |
| U12c | 0.14 | - | - | *118* | - | - |
| U12d | 0.14 | - | - | *116* | - | - |
| U12e | *0.10* | - | - | 81 | - | - |
| U12e ponds | - | *0.11* | *0.11* | - | 91 | 88 |
| U12f | 0.14 | - | - | *118* | - | - |
| U12g | 0.10 | - | - | *82* | - | - |
| U12j | 0.09 | - | - | *73* | - | - |
| U12k | 0.09 | - | - | *76* | - | - |
| U12n | *0.09* | - | - | 73 | - | - |
| U12n ponds | - | *0.10* | *0.09* | - | 82 | 76 |
| U12p | 0.07 | - | - | *59* | - | - |
| U12t | *0.07* | - | - | 63 | - | - |
| U12t ponds | - | *0.08* | *0.07* | - | 68 | 62 |
| Shoshone Mountain | | | | | | |
| U16a | 0.19 | - | - | *249* | - | - |

# Appendix A. Estimated Traveltimes for All Working Points at Rainier Mesa and Shoshone Mountain.

Table A1. Continuous and intermittent-source estimated traveltimes for the individual working points at Rainier Mesa to the saturated zone in the carbonate rock estimated using the SRPF model.

[Italics denote the most likely temporal nature of the preferential source based on the conceptual model presented in this report. All estimated traveltimes for the working points at Rainier Mesa are based on the transport distances given in table 5. Note that two traveltime estimates are provided from both the continuous and intermittent traveltimes for the DES MOINES and PLATTE working points and analysis of the working point and tunnel portal elevations suggests that the longer traveltimes are more appropriate. ]

| Tunnel or borehole location of working point | Detonation name | Detonation date [mo/d/yr] | Working point continuous-source traveltime [yrs] | Working point intermittent-source traveltime [yrs] |
|---|---|---|---|---|
| U12b | RAINIER | 9/19/1957 | 0.13 | *107* |
| U12b.02 | TAMALPAIS | 10/8/1958 | 0.14 | *114* |
| U12b.04 | EVANS | 10/29/1958 | 0.13 | *109* |
| U12b.08 | FEATHER | 12/22/1961 | 0.13 | *106* |
| U12b.09 | CHENA | 10/10/1961 | 0.12 | *101* |
| U12b.10 | YUBA | 6/5/1963 | 0.12 | *103* |
| U12c.02 | SATURN | 8/10/1957 | 0.16 | *130* |
| U12c.03 | NEPTUNE | 10/14/1958 | 0.18 | *155* |
| U12d.01 | VENUS | 2/22/1958 | 0.16 | *135* |
| U12c.01 | URANUS | 3/14/1958 | 0.14 | *114* |
| U12e.02 | LOGAN | 10/16/1958 | 0.10 | 83 |
| U12e.03a | ANTLER | 9/15/1961 | 0.10 | 80 |
| U12e.05 | BLANCA | 10/30/1958 | 0.09 | 79 |
| U12e.10 | DORSAL FIN | 2/29/1968 | 0.09 | 76 |
| U12e.11 | DIESEL TRAIN | 12/5/1969 | 0.09 | 77 |
| U12e.12 | HUDSON MOON | 5/26/1970 | 0.09 | 75 |
| U12e.14 | DIDO QUEEN | 6/5/1973 | 0.09 | 75 |
| U12e.18 | DINING CAR | 4/5/1975 | 0.09 | 74 |
| U12f.01 | MERCURY | 9/23/1958 | 0.12 | *98* |
| U12f.02 | MARS | 9/28/1958 | 0.13 | *110* |
| U12g.01 | MADISON | 12/12/1962 | 0.10 | *81* |
| U12g.06 | RED HOT | 3/5/1966 | 0.10 | *86* |
| U12g.07 | DOOR MIST | 8/31/1967 | 0.09 | *78* |
| U12g.09 | CYPRESS | 2/12/1969 | 0.09 | *78* |

| Tunnel location of working point | Detonation name | Detonation date [mo/d/yr] | Working point continuous-source traveltime [yrs] | Working point intermittent-source traveltime [yrs] |
|---|---|---|---|---|
| U12g.10 | CAMPHOR | 6/29/1971 | 0.10 | *79* |
| U12j.01 | DES MOINES | 6/13/1962 | 0.04, 0.08 | *35*, *69* |
| U12k.01 | PLATTE | 4/14/1962 | 0.05, 0.09 | *39*, *72* |
| U12n.02 | MIDI MIST | 6/26/1967 | *0.08* | 70 |
| U12n.04 | HUDSON SEAL | 9/24/1968 | *0.08* | 70 |
| U12n.05 | MISTY NORTH | 5/2/1972 | *0.08* | 68 |
| U12n.06 | DIANA MIST | 2/11/1970 | *0.09* | 72 |
| U12n.07 | HUSKY ACE | 10/12/1973 | *0.09* | 73 |
| U12n.08 | MING BLADE | 6/19/1974 | *0.08* | 69 |
| U12n.09 | HYBLA FAIR | 10/28/1974 | *0.09* | 72 |
| U12e.20 | HYBLA GOLD | 11/1/1977 | *0.09* | 75 |
| U12n.10 | MIGHTY EPIC | 5/12/1976 | *0.08* | 65 |
| U12n.10a | DIABLO HAWK | 9/13/1978 | *0.08* | 67 |
| U12n.11 | MINERS IRON | 10/31/1980 | *0.08* | 70 |
| U12n.12 | MINI JADE | 5/26/1983 | *0.09* | 75 |
| U12n.15 | DIAMOND ACE | 9/23/1982 | *0.08* | 67 |
| U12n.15 | HURON LANDING | 9/23/1982 | *0.08* | 70 |
| U12n.17 | MISTY RAIN | 4/6/1985 | *0.08* | 71 |
| U12n.18 | TOMME/ MIDNIGHT ZEPHYR | 9/21/1983 | *0.08* | 68 |
| U12n.19 | DIAMOND BEECH | 10/9/1985 | *0.08* | 68 |
| U12n.20 | MILL YARD | 10/9/1985 | *0.09* | 72 |
| U12n.21 | MIDDLE NOTE MINERAL | 3/18/1987 | *0.08* | 68 |
| U12n.22 | QUARRY | 7/25/1990 | *0.08* | 64 |
| U12n.22 | RANDSBURG | 7/25/1990 | *0.08* | 64 |
| U12n.23 | MISTY ECHO HUNTERS | 12/10/1988 | *0.08* | 66 |
| U12n.24 | TROPHY | 9/18/1992 | *0.08* | 68 |
| U12p.02 | MISSION CYBER | 12/2/1987 | 0.07 | *62* |
| U12p.03 | DISKO ELM | 9/14/1989 | 0.06 | *50* |
| U12p.04 | DISTANT ZENITH DIAMOND | 9/19/1991 | 0.06 | *49* |
| U12p.05 | FORTUNE | 4/30/1992 | 0.06 | *53* |
| U-12q | CLEARWATER | 10/16/1963 | *0.03* | 25 |
| U-12r | WINESKIN | 1/15/1969 | *0.04* | 31 |
| U12t.01 | MINT LEAF DIAMOND | 5/5/1970 | *0.07* | 58 |
| U12t.02 | SCULLS | 7/20/1972 | *0.07* | 59 |
| U12t.03 | HUSKY PUP | 10/24/1975 | *0.07* | 61 |
| U12t.04 | MIDAS MYTH/ MILAGRO | 2/15/1984 | *0.07* | 57 |
| U12t.08 | MIGHTY OAK | 4/10/1986 | *0.07* | 57 |
| U12t.09 | MISSION GHOST | 6/20/1987 | *0.07* | 60 |

Table A2. Continuous and intermittent-source traveltimes for the individual working points at Shoshone Mountain to the regional saturated zone estimated using the SRPF model.

[Italics denote the most likely temporal nature of the preferential source based on the conceptual model presented in this report. All estimated traveltimes for the working points at Rainier Mesa are based on the transport distances given in table 7.]

| Tunnel location of working point | Detonation name | Detonation date [mo/d/yr] | Working point continuous-source traveltime [yrs] | Working point intermittent-source traveltime [yrs] |
|---|---|---|---|---|
| U16a | MARSHMALLOW | 6/28/1962 | 0.18 | *239* |
| U16a.02 | GUM DROP | 4/21/1965 | 0.18 | *239* |
| U16a.03 | DOUBLE PLAY | 6/15/1966 | 0.18 | *239* |
| U16a.04 | MING VASE | 11/20/1968 | 0.18 | *238* |
| U16a.05 | DIAMOND DUST | 5/12/1970 | 0.18 | *244* |
| U16a.06 | DIAMOND MINE | 7/1/1971 | 0.18 | *240* |

## References Cited


Altman, S.J., Arnold, B.W., Barnard, R.W., Barr, G.E., Ho, C.K., McKenna, S.A., and Eaton, R.R., 1996, Flow calculations for Yucca Mountain groundwater travel time (GWTT-95): Sandia National Laboratories Report SAND96-0819, 214 p.

Amy, P.S., Haldeman, D.L., Ringelberg, D., Hall, D.H., and Russell, C.E., 1992, Comparison of identification systems for classification of bacteria isolated from water and endolithic habitats within the deep subsurface: Applied and Environmental Microbiology, v. 58, no. 10, p. 3367-3373.

Armstrong, R.L., 1968, Sevier orogenic belt in Nevada and Utah: Geological Society of America Bulletin, v. 79, p. 429-458.

Baetsle, L.H., 1969, Migration of radionuclides in porous media, *in* Duhamel, A.M.H., ed., Progress in nuclear energy series XII, Health physics, Pergamon Press, Elmsford, NY, p. 707-730.

Baker, R.S., and Hillel, D., 1990, Laboratory tests of a theory of fingering during infiltration into layered soils: Soil Science Society of America Journal, v. 54, p. 20-30.

Batzel, R.E., 1959, Radioactivity associated with underground nuclear explosions: Lawrence Radiation Laboratory Report UCRL-5623, 14 p.

Beatley, J.C., 1976, Vascular plants of the Nevada Test Site and Central-Southern Nevada: Technical Information Center, Energy Research and Development Administration Report 22161, 308 p.

Bechtel Nevada, 2006, Completion report for well ER-12-3, Corrective action unit 99; Rainier Mesa - Shoshone Mountain: U.S. Department of Energy Report DOE/NV/11718--1182, 115 p.

Borg, I.Y., Stone, R., Levy, H.B., and Ramspott, L.D., 1976, Information pertinent to the migration of radionuclides in groundwater at the Nevada Test Site: Lawrence Livermore Laboratory Report UCRL-52078, Part 1; review and analysis of existing information, 216 p.

Bourcier, W.L., 1993, Waste glass corrosion modeling; comparison with experimental results: Lawrence Livermore National Laboratory Report UCRL-CR--116354 UCRL-CR--116354, 16 p.

Bowen, S.M., Finnegan, D.L., Thompson, J.L., Miller, C.M., Baca, P.L., Olivas, L.F., Geoffrion, C.G., Smith, D.K., Goishi, W., Esser, B.K., Meadows, J.W., Namboodiri, N., and Wild, J.F., 2001, Nevada Test Site radionuclide inventory, 1951-1992: Los Alamos National Laboratory Report LA-13859-MS, 29 p.

Bowers, T.S., and Burns, R.G., 1990, Activity diagrams for clinoptilolite; susceptibility of this zeolite to further diagenetic reactions: American Mineralogist, v. 75, p. 601-619.

Byers, F.M.J., 1962, Porosity, density, and water content data on tuff of the Oak Spring Formation from U12e tunnel system, Nevada Test Site, Nye County, Nevada: U.S. Geological Survey Open-File Report 62-23, 28 p.

Clebsch, A.J., 1960, Ground water in the Oak Spring Formation and hydrologic effects of underground nuclear explosions at the Nevada Test Site: U.S. Geological Survey Open-File Report 60-27, 29 p.

Clebsch, A.J., and Barker, F.B., 1960, Analyses of ground water from Rainier Mesa, Nevada Test Site, Nye County, Nevada: U.S. Geological Survey Open File-Report 60-28, 23 p.

Cole, J.C., Harris, A.G., Lanphere, M.A., Barker, C.E., and Warren, R.G., 1993, The case for pre-middle Cretaceous extensional faulting in northern Yucca Flat, southwestern Nevada, Geological Society of America, Abstracts with Programs, Geological Society of America, v. 25, p. 22.

Davidson, G.R., Bassett, R.L., Hardin, E.L., and Thompson, D.L., 1998, Geochemical evidence of preferential flow of water through fractures in unsaturated tuff, Apache Leap: Applied Geochemistry, v. 13, p. 184-195.

Davis, P.K., and Bigelow, J.H., 2003, Motivated metamodels; synthesis of cause-effect reasoning and statistical metamodeling: RAND Corporation Report MR-1570, 78 p.

DeMeo, G.A., Flint, A.L., Laczniak, R.J., and Nylund, W.E., 2006, Micrometeorological and soil data for calculating evapotranspiration for Rainier Mesa, Nevada Test Site, Nevada, 2002–05: U.S. Geological Survey Open-File Report 2006-1312, 12 p.

Department of Energy, 1997, Regional groundwater flow and tritium transport modeling and risk assessment of the underground test area, Nevada Test Site, Nevada: U.S. Department of Energy Report DOE/NV--477, 396 p.

Department of Energy, 2000, United States nuclear tests July 1945 through September 1992: U.S. Department of Energy Report DOE/NV--209-REV 15, 185 p.

Dettinger, M.D., 1989, Reconnaissance estimates of natural recharge to desert basins in Nevada, U.S.A., by using chloride-balance calculations: Journal of Hydrology, v. 106, p. 55-78.

Dickey, D.D., Emerick, W.L., Bunker, C. M., 1962, Interim geological investigations in the U12b.09 and U12b.07 tunnels, Nevada Test Site, Nye County, Nevada, with a section on gamma-radioactivity: U.S. Geological Survey Open-File Report 62-37, 64 p.

Diment, W.H., Wilmarth, V.R., McKeown, F.A., Dickey, D.D., Hinrichs, E.N., Botinelly, T., Roach, C.H., Byers, F.M.J., Hawley, C.C., Izett, G.A., and Clebsch, A.J., 1959, Geological survey investigations in the U12b.03 and U12b.04 tunnels, Nevada Test Site: U.S. Geological Survey U.S. Geological Survey Open-File Report 59-36, 75 p.

Domenico, P.A., and Schwartz, F.W., 1990, Physical and chemical hydrogeology: New York, John Wiley, 506 p.

Ege, J.R., and Cunningham, M.J., 1976, Geology of the U12n.10 UG-1 horizontal drill hole, Rainier Mesa, Area 12, Nevada Test Site, Nevada: U.S. Geological Survey Open-File Report 474-218, 78 p.

Emerick, W.L., and Dickey, D.D., 1962, Interim geological investigations in the U12e.03a and U12e.03b tunnels, Nevada Test Site, Nye County, Nevada: U.S. Geological Survey Trace Elements Investigations Report 806, 29 p.

Evans, D.D., and Nicholson, T.J., 1987, Flow and transport through unsaturated fractured rock; an overview, *in* Evans, D.D., and Nicholson, T.J., eds., Flow and Transport Through Unsaturated Fractured Rock, Geophysical Monograph 42, American Geophysical Union, Washington, D.C., p. 1-10.

Fabryka-Martin, J.T., Flint, A.L., Sweetkind, D.S., Wolfsberg, A.V., Levy, S.S., Roemer, G.J.C., Roach, J.L., Wolfsberg, L.E., and Duff, M.C., 1997, Evaluation of flow and transport models of Yucca Mountain, based on chlorine-36 and chloride studies for FY97: Yucca Mountain Project Milestone Report SP2224M3.

Fenelon, J.M., 2006, Database of ground-water levels in the vicinity of Rainier Mesa, Nevada Test Site, Nye County, Nevada 1957-2005.: U.S. Geological Survey Data Series 190 USGS DS 190, 14 p.

Fenelon, J.M., Laczniak, R.J., and Halford, K.J., 2008, Predevelopment water-level contours for aquifers in the Rainier Mesa and Shoshone Mountain area of the Nevada Test Site, Nye County, Nevada: U.S. Geological Survey Scientific Investigations Report 2008-5044, 38 p.

Fernandez, J.A., and Freshley, M.D., 1984, Repository sealing concepts for the Nevada nuclear waste storage investigations project: Sandia National Laboratories Report SAND--83-1778 SAND--83-1778, 91 p.

Finnegan, D.L., and Thompson, J.L., 2001, Laboratory and field studies related to the radionuclide migration at the Nevada Test Site in support of the underground test area program and hydrologic resources management project: Los Alamos National Laboratory Report LA-13787-PR, 27 p.

Fishwick, P.A., 1995, Simulation model design and execution: Englewood Cliffs, New Jersey, Prentice-Hall, 432 p.

Frantz, F.K., 1995, A taxonomy of model abstraction techniques, Proceedings of the 27th conference on Winter Simulation, Arlington, Virginia, IEEE Computer Society, p. 1413 - 1420.

Frizzell, V.A.J., and Shulters, J., 1990, Geologic map of the Nevada Test Site, southern Nevada: U.S. Geological Survey Miscellaneous Investigations Map I-2046, scale 1:100,000.

Gardner, W.R., 1964, Water movement below the root zone, 8th International Congress of Soil Science, Bucharest, Romania, Rompresfilatelia, Bucharest, p. 63-68.

Gauthier, J.H., 1994, An updated fracture-flow model for total-system performance assessment of Yucca Mountain: Sandia National Laboratories Report Sand-94-0414C Conf-940553--68, 8 p.

Gauthier, J.H., 1998, Modeling unsaturated-zone flow at Rainier Mesa as a possible analog for a future Yucca Mountain: Sandia National Laboratories Report SAND97-2743C, 3 p.

Gauthier, J.H., Wilson, M.L., and Lauffer, F.C., 1992, Estimating the consequences of significant fracture flow at Yucca Mountain, Proceedings of the Third Annual International High-Level Radioactive Waste Management Conference, Las Vegas, Nevada, p. 891–989.

Gerke, H.H., 2006, Preferential flow descriptions for structured soils: Journal of Plant Nutrition and Soil Science, v. 169, no. 3, p. 382-400.

Ghodrati, M., and Jury, W.A., 1990, A field study using dyes to characterize preferential flow of water: Soil Science Society of America Journal, v. 54, p. 1558-1563.

Gjettermann, B., Hansen, H.C.B., Jensen, H.E., and Hansen, S., 2004, Transport of phosphate through artificial macropores during film and pulse flow: Journal of Environmental Quality, v. 33, p. 2263-2271.

Gjettermann, B., Nielsen, K.L., Petersen, C.T., Jensen, H.E., and Hansen, S., 1997, Preferential flow in sandy loam soils as affected by irrigation intensity: Soil Technology, v. 11, p. 139-152.

Glascoe, A., Olson, J., Lu, G., McGraw, M.A., Lichtner, P.C., and Wolfsberg, A.V., 2000, Radionuclide transport from an underground nuclear test in the presence of residual heat and colloids, *in* Bentley, H.W., Sykes, J., Brebbia, C., Gray, W., and Pinder, G., eds., Computational methods in water resources XIII, 1, AA Balkema, Rotterdam, p. 357-364.

Glass, R.J., Nicholl, M.J., Ramirez, A.L., and Daily, W.D., 2002, Liquid phase structure within an unsaturated fracture network beneath a surface infiltration event; field experiment: Water Resources Research, v. 38, no. 10, p. 1199, doi:10.1029/2000WR000167.

Glass, R.J., Parlange, J.Y., and Steenhuis, T.S., 1989a, Wetting front instability; 1. theoretical discussion and dimensional analysis: Water Resources Research, v. 25, no. 6, p. 1187-1194.

Glass, R.J., Parlange, J.Y., and Steenhuis, T.S., 1989b, Wetting front instability; 2. experimental determination of relationships between system parameters and two-dimensional unstable flow field behavior in initially dry porous media: Water Resources Research, v. 25, no. 6, p. 1195-1207.

Glass, R.J., Steenhuis, T.S., and Parlange, J.Y., 1988, Wetting front instability as a rapid and far-reaching hydrologic process in the vadose zone: Journal of Contaminant Hydrology, v. 3, p. 207-226.

Glass, R.J., Steenhuis, T.S., and Parlange, J.Y., 1989c, Mechanism of finger persistence in homogeneous, unsaturated porous media; theory and verification: Soil Science, v. 148, no. 1, p. 60-69.

Guell, M.A., 1997, Subsurface transport of radionuclides at the Nevada Test Site, Berkeley, University of California, Ph.D dissertation.

Guell, M.A., and Hunt, J.R., 2003, Groundwater transport of tritium and krypton-85 from a nuclear detonation cavity: Water Resources Research, v. 39, p. 1175.

Haldeman, D.L., Amy, P.S., Ringelberg, D., and White, D.C., 1993, Characterization of the microbiology within a 21 $m^3$ section of rock from the deep subsurface: Microbial Ecology, v. 26, p. 145-159.

Haldeman, D.L., Lagadinos, T., Hersman, L., Meike, L., and Amy, P.S., 1996, The effects of diesel exhaust on the microbiota within a tuffaceous tunnel system: Lawrence Livermore National Laboratory Report UCRL-ID-125176, 38 p.

Hamdi, M., Durnford, D., and Loftis, J., 1994, Bromide transport under sprinkler and ponded irrigation: Journal of Irrigation and Drainage Engineering, v. 120, p. 1086-1097.

Hansen, M.E., Terhune, R.W., and McKee, C.R., 1981, Explosion phenomenology and permeability enhancement in porous media: Lawrence Livermore National Laboratory Report UCRL-85811, 11 p.

Hansen, W.R., Lemke, R.W., Cattermole, J.M., and Gibbons, A.B., 1963, Stratigraphy and structure of the Rainier and USGS tunnel areas, Nevada Test Site: U.S. Geological Survey Professional Paper 382-A, 47 p.

Hay, R.L., and Sheppard, R.A., 1977, Geology of zeolites in sedimentary rocks, *in* Mumpton, F.A., ed., Mineralogy and geology of natural zeolites: Short Course Notes, 4, Mineralogical Society of America, p. 53-63.

Hendrickx, J.M.H., Dekker, L.W., and Boersma, O.H., 1993, Unstable wetting fronts in water-repellent soils: Journal of Environmental Quality, v. 22, p. 109-118.

Hendrickx, J.M.H., and Yao, T.-M., 1996, Prediction of wetting front instability in dry field soils using soil and precipitation data: Geoderma, v. 70, no. 2-4, p. 265-280.

Hillel, D., and Baker, R.S., 1988, A descriptive theory of fingering during infiltration into layered soils: Soil Science, v. 146, no. 1, p. 51-56.

Hodges, K.V., and Walker, J.D., 1992, Extension of the Cretaceous Sevier orogeny, North American cordillera: Geology, v. 104, p. 560-569.

Hoffman, D.C., Stone, R., and Dudley, W.W.J., 1977, Radioactivity in the underground environment of the Cambric nuclear explosion at the Nevada Test Site: Los Alamos Scientific Laboratory Report LA-6877-MS, 93 p.

Hokett, S.L., and French, R.H., 2000, Evaluation of recharge potential at subsidence crater U19b, central Pahute Mesa, Nevada Test Site: Desert Research Institute Publication #45161, 39 p.

Hokett, S.L., Gillespie, D.R., Wilson, G.V., and French, R.H., 2000, Evaluation of recharge potential at subsidence crater U10i, northern Yucca Flat, Nevada Test Site.: Desert Research Institute Publication #45174, 39 p.

Hoover, D.L., 1968, Genesis of zeolites, Nevada Test Site, *in* Eckel, E.B., ed., Nevada Test Site: Memoir 110; studies of geology and hydrology, Geological Society of America, Boulder, Colorado, p. 275-284.

Hoover, D.L., and Magner, J.E., 1990, Geology of the Rainier Mesa-Aqueduct Mesa tunnel areas-U12n tunnel: U.S. Geological Survey Open-File Report 90-623, 49 p.

Hu, Q., Salve, R., Stringfellow, W.T., and Wang, J.S.Y., 2001, Field tracer-transport tests in unsaturated fractured tuff: Journal of Contaminant Hydrology, v. 51, no. 1-2, p. 1-12.

Jacobson, R.L., Henne, M.S., and Hess, J.W., 1986, A reconnaissance investigation of hydrogeochemistry and hydrology of Rainier Mesa: Water Resources Center Publication No. 45046, DOE/NV/10384-05 DOE/NV/10384--05, 57 p.

Jarvis, N., 1998, Modeling the impact of preferential flow on nonpoint source pollution, *in* Selim, H.M., and Ma, L., eds., Physical non-equilibrium in soils; modeling and application, CRC Press, Boca Raton, Florida, p. 195-221.

Johannesson, K.H., Stetzenbach, K.J., Hodge, V.F., Kreamer, D.K., and Zhou, X., 1997, Delineation of groundwater flow systems in the southern Great Basin using aqueous rare earth element distributions.: Ground Water, v. 35, p. 807-819.

Johannesson, K.H., Zhou, X., Guo, C., Stetzenbach, K.J., and Hodge, V.F., 2000, Origin of rare earth element signatures in groundwaters of circumneutral pH from southern Nevada and eastern California, USA.: Chemical Geology, v. 164, p. 239-257.

Kasteel, R., 1997, Solute transport in an unsaturated field soil; describing heterogeneous flow fields using spatial distribution of hydraulic properties, Zurich, Switzerland, ETH Zurich, Ph.D. dissertation 12477, 108 p.

Keller, G.V., 1960, Physical properties of the Oak Spring Formation, Nevada: U.S. Geological Survey Professional Paper 400-B, p. B396-B400.

Keller, G.V., 1962, Electrical resistivity of rocks in the Area 12 tunnels, Nevada Test Site, Nye County, Nevada: Geophysics, v. 27, no. 2, p. 242-252.

Kersting, A.B., Efurd, D.W., Finnegan, D.L., Rokop, D.J., Smith, D.K., and Thompson, J.L., 1998, Migration of plutonium in groundwater at the Nevada Test Site, *in* Hydrologic resources management program and underground test area operable unit FY 1997 progress report: Lawrence Livermore National Laboratory Report UCRL-ID-130792, p. 76-92.

Kersting, A.B., Efurd, D.W., Finnegan, D.L., Rokop, D.J., Smith, D.K., and Thompson, J.L., 1999, Migration of plutonium in ground water at the Nevada Test Site: Nature, v. 397, p. 56-59.

Klemes, V., 1986, Operational testing of hydrologic simulation models: Hydrological Sciences Journal, v. 31, p. 13–23.

Koorevaar, P., Menelik, G., and Dirksen, C., 1983, Elements of soil physics: Amsterdam, Elsevier, 230 p.

Kung, K.-J.S., 1990a, Preferential flow in a sandy vadose zone, 1, Field observation: Geoderma, v. 46, p. 51-58.

Kung, K.-J.S., 1990b, Preferential flow in a sandy vadose zone, 2, Mechanism and implications: Geoderma, v. 46, p. 59-71.

Kung, K.-J.S., 1993, Laboratory observation of funnel flow mechanism and its influence on solute transport: Journal of Environmental Quality, v. 22, p. 91-102.

Laczniak, R.J., Cole, J.C., Sawyer, D.A., and Trudeau, D.A., 1996, Summary of hydrogeologic controls on ground-water flow at the Nevada Test Site, Nye County, Nevada: U.S. Geological Survey Water-Resources Investigations Report 96-4109, 59 p.

Laraway, W.H., and Houser, F.N., 1962, Outline of geology of the U12j and U12j.01 tunnels, Nevada Test Site: U.S. Geological Survey Open-File Report 62-76, 12 p.

Leavitt, A.J., 2005, Formation image interpretation report, Well-ER-16-1, Nevada Test Site, Nye County Nevada, Structure Interpretation in the Paleozoic Carbonate Rocks: Written communication prepared for Bechtel Nevada, Las Vegas, Nevada.

Martinez, M.J., 1988, Capillary-driven flow in a fracture located in a porous medium: Sandia National Laboratories Report SAND84-1697, 52 p.

Mazer, J.J., 1987, Kinetics of glass dissolution as a function of temperature, glass composition, and solution pH, Evanston, Illinois, Northwestern University, Ph.D. dissertation.

Maxwell, R.M., Tompson, A.F.B., Rambo, J.T., Carle, S.F., and Pawloski, G.A., 2000, Thermally induced groundwater flow resulting from an underground nuclear test, *in* Bentley, H.W., Sykes, J., Brebbia, C., Gray, W., and Pinder, G., eds., Computational methods in water resources XIII, 1, AA Balkema, Rotterdam, p. 45-50.

Miyakazi, T., 1993, Water flow in soils:New York, Marcel Dekker, 296 p.

Moncure, G.K., Surdam, R.C., and McKague, H.L., 1981, Zeolite diagenesis below Pahute Mesa, Nevada Test Site: Clays and Clay Minerals, v. 29, no. 5, p. 385-396.

Montazer, P., and Wilson, W.E., 1984, Conceptual hydrologic model of flow in the unsaturated zone, Yucca Mountain, Nevada: U.S. Geological Survey Water Resources Investigation Report 84-4345, 59 p.

Moyer, T.C., Geslin, J.K., and Flint, L.E., 1996, Stratigraphic relations and hydrologic properties of the Paintbrush Tuff nonwelded (PTn) hydrologic unit, Yucca Mountain, Nevada: U.S. Geological Survey Open-File Report 95-397, 157 p.

National Nuclear Security Administration, 2004, Corrective action investigation plan for corrective action unit 99; Rainier Mesa/Shoshone Mountain, Nevada Test Site, Nevada: U.S. Department of Energy Report DOE/NV--1031, revision no. 0, 320 p.

National Oceanic and Atmospheric Administration, 2006, Overview of the climate of the Nevada Test Site (NTS): National Oceanic and Atmospheric Administration, Air Resources Laboratory—Special Operation and Research Division.

National Security Technologies, 2007, A hydrostratigraphic model and alternatives for the groundwater flow and contaminant transport model of corrective action unit 99; Rainier

Mesa-Shoshone Mountain, Nye County, Nevada: U.S. Department of Energy Report DOE/NV/25946--146, 302 p.

National Security Technologies, 2008, Nevada Test Site environmental report 2007: U.S. Department of Energy Report DOE/NV/25946--543, 319 p.

Nimmo, J.R., 2007, Simple predictions of maximum transport rate in unsaturated soil and rock: Water Resources Research, v. 43, p. W05426.

Nitao, J.J., Buscheck, T.A., and Chestnut, D.A., 1992, The implications of episodic nonequilibrium fracture-matrix flow on site suitability and total system performance, International High Level Radioactive Waste Conference, Las Vegas, Nevada, p. 279-296.

Norris, A.E., 1989, The use of chlorine isotope measurements to trace water movements at Yucca Mountain, Nuclear waste isolation in the unsaturated zone: FOCUS`89, Las Vegas, Nevada, p. 7.

Olsen, C.W., 1993, Site selection and containment evaluation for LLNL nuclear events, Proceedings of the 7th Symposium on Containment of Underground Nuclear Explosions, Kent, WA, Lawrence Livermore National Laboratory, p. 33.

Pachepsky, Y.A., Guber, A.K., Van Genuchten, M.T., Nicholson, T.J., Cady, R.E., Simunek, J., and Schaap, M.G., 2006, Model abstraction techniques for soil water flow and transport: NUREG CR-6884, 175 p.

Pawloski, G.A., Tompson, A.F.B., Carle, S.F., Bourcier, W.L., Bruton, C.J., Daniels, J.I., Maxwell, R.M., Shumaker, D.E., Smith, D.K., and Zavarin, M., 2001, Evaluation of the hydrologic source term from underground nuclear tests on Pahute Mesa at the Nevada Test Site; the CHESHIRE test: Lawrence Livermore National Laboratory Report UCRL-ID-147023, 507 p.

Plume, R.W., 1996, Hydrogeologic framework of the Great Basin region of Nevada, Utah, and adjacent states: U.S. Geological Survey Professional Paper 1409-B, 64 p.

Poole, F.G., and Rooler, J.C., 1959, Summary of some physical data from five vertical drill holes over the U12b.04 (Evans) explosion chamber, Nevada Test Site, Nye County, Nevada: U.S. Geological Survey Trace Element Investigations Report TEI-762, 32 p.

Pruess, K., Faybishenko, B., and Bodvarsson, G.S., 1999, Alternative concepts and approaches for modeling flow and transport in thick unsaturated zones of fractured rocks: Journal of Contaminant Hydrology, v. 38, p. 281-322.

Ramsay, J.D.F., 1988, The role of colloids in the release of radionuclides from nuclear waste: Radiochemica Acta, v. 44/45, p. 165-170.

Reeves, D.M., Schultz, R., Bingham, C., Pohlmann, K., Russell, C.E., and Chapman, J., 2007, Characterization of preferential flowpaths at the T tunnel complex, Rainier Mesa, Nevada, Eos (American Geophysical Union Transactions), Fall Meeting Supplement, Abstract H33H-1721.

Rice, R.C., Jaynes, D.B., and Bowman, R.S., 1991, Preferential flow of solutes and herbicides under irrigated fields: Transactions of the American Society of Agricultural Engineers, v. 34, p. 914-918.

Ross, B., 1990, The diversion capacity of capillary barriers: Water Resources Research, v. 26, no. 10, p. 2625-2629.

Rozsa, R., Snoeberger, D.F., and Baker, J., 1975, Permeability of a nuclear chimney and surface alluvium: Lawrence Livermore National Laboratory Report UCID-16722, 13 p.

Rulon, J.J., Bodvarsson, G.S., and Montazer, P., 1986, Preliminary numerical simulations of groundwater flow in the unsaturated zone, Yucca Mountain, Nevada: Lawrence Berkeley National Laboratory Report LBL20553, 91 p.

Russell, C.E., 1987, Hydrogeologic investigations of flow in fractured tuffs, Rainier Mesa, Nevada Test Site, Las Vegas, Nevada, University of Nevada, M.S., 154 p.

Russell, C.E., Gillespie, L., and Gillespie, D., 1993, Geochemical and hydrologic characterization of the effluent draining from U12e, U12n, and U12t tunnels, area 12, Nevada Test Site: Desert Research Institute Report 45105, 193 p.

Russell, C.E., Hess, J.W., and Tyler, S.W., 1988, Hydrogeologic investigations of flow in fractured tuffs, Rainier Mesa, Nevada Test Site: U.S. Department of Energy Report DOE/NV/10384-21, 71 p.

Russell, C.E., Hess, J.W., and Tyler, S.W., 2001, Hydrogeologic investigations of flow in fractured tuffs, Rainier Mesa, Nevada Test Site, *in* Evans, D.D., Nicholson, T.J., and Rasmussen, T.C., eds., Flow and transport through unsaturated fractured rock, Geophysical Monograph 42, American Geophysical Union, Washington, D.C., p. 105-112.

Russell, C.E., and Minor, T., 2002, Reconnaissance estimates of recharge based on an elevation-dependent chloride mass-balance approach: Publication Number 45164, DOE/NV/11508-37, 66 p.

Salve, R., 2005, Observations of preferential flow during a liquid release experiment in fractured welded tuffs: Water Resources Research, v. 41, no. 9, p. W09427.

Salve, R., and Oldenburg, C.M., 2001, Water flow within a fault in altered nonwelded tuff: Water Resources Research, v. 37, no. 12, p. 3043-3056.

Salve, R., Oldenburg, C.M., and Wang, J.S.Y., 2003, Fault-matrix interactions in nonwelded tuff of the Paintbrush Group at Yucca Mountain: Journal of Contaminant Hydrology, v. 62–63, p. 269– 286.

Savard, C.S., 1998, Estimated ground-water recharge from streamflow in Fortymile Wash near Yucca Mountain, Nevada: U.S. Geological Survey Water-Resources Investigations Report 97-4273, 30 p.

Sawyer, D.A., Fleck, R.J., Lanphere, M.A., Warren, R.G., Broxton, D.E., and Hudson, M.R., 1994, Episodic caldera volcanism in the Miocene southwestern Nevada volcanic field; revised stratigraphic framework, Ar-40/Ar-39 geochronology, and implications for magmatism and extension: Geological Society of America Bulletin, v. 106, no. 10, p. 1304-1318.

Scanlon, B.R., and Goldsmith, R.S., 1997, Field study of spatial variability in unsaturated flow beneath and adjacent to playas: Water Resources Research, v. 33, p. 2239-2252.

Scott, R.B., Spengler, R.W., Diehl, S., Lappin, A.R., and Chornack, M.P., 1983, Geologic character of tuffs in the unsaturated zone of Yucca Mountain, southern Nevada, *in* Mercer, J.W., Rao, P.S.C., and Marine, I.W., eds., Role of the unsaturated zone in radioactive and hazardous waste disposal, Ann Arbor Sci., Ann Arbor, Michigan, p. 289-335.

Selker, J.S., Steenhuis, T.S., and Parlange, J.Y., 1992a, Fingered flow in two dimensions; 2. predicting finger moisture profile: Water Resources Research, v. 28, no. 9, p. 2523-2528.

Selker, J.S., Steenhuis, T.S., and Parlange, J.Y., 1992b, Wetting front instability in homogeneous sandy soils under continuous infiltration: Soil Science Society of America Journal, v. 56, p. 1346-1350.

Sililo, O.T.N., and Tellam, J.H., 2000, Fingering in unsaturated zone flow; a qualitative review with laboratory experiments on heterogeneous systems: Ground Water, v. 38, no. 6, p. 864-871.

Smith, D.K., 1998, A recent drilling program to investigate radionuclide migration at the Nevada Test Site: Journal of Radioanalytical and Nuclear Chemistry, v. 235, no. 1-2, p. 159-166.

Smith, D.K., Finnegan, D.L., and Bowen, S.M., 2003, An inventory of long-lived radionuclides residual from underground nuclear testing at the Nevada test site, 1951-1992: Journal of Environmental Radioactivity, v. 67, no. 1, p. 35-51.

Snoeberger, D.F., Baker, J., and Morris, C.J., 1973, Measurements and correlation analysis for nuclear chimney permeability: Lawrence Livermore National Laboratory Report UCID-16302, 30 p.

Steenhuis, T.S., Parlange, J.Y., and Kung, K.-J.S., 1991, Comment on "The diversion capacity of capillary barriers" by Benjamin Ross: Water Resources Research, v. 27, no. 8, p. 2155-2156.

Stetzenbach, K.J., Hodge, V.F., Guo, C., Farnham, I.M., and Johannesson, K.H., 2001, Geochemical and statistical evidence of deep carbonate groundwater within overlying volcanic rock aquifers/aquitards of southern Nevada, USA: Journal of Hydrology, v. 243, no. 3-4, p. 254-271.

Stoller-Navarro Joint Venture, 2004, Value of information analysis for corrective action unit 99; Rainier Mesa/ Shoshone Mountain, Nevada Test Site, Nevada: Stoller-Navarro Joint Venture Report S-N/99205--031, 215 p.

Stoller-Navarro Joint Venture, 2006a, Completion report for well ER-12-4, corrective action unit 99; Rainier Mesa - Shoshone Mountain: U.S. Department of Energy Report DOE/NV--1208, 111 p.

Stoller-Navarro Joint Venture, 2006b, Completion report for well ER-16-1, corrective action unit 99; Rainier Mesa - Shoshone Mountain: U.S. Department of Energy DOE/NV--1180, 117 p.

Stormont, J.C., and Anderson, C.E., 1999, Capillary barrier effect from underlying coarser soil layer: Journal of Geotechnical and Geoenvironmental Engineering, v. 125, no. 8, p. 641-648.

Sun, Y., Carle, S.F., Zavarin, M., and Pawloski, G.A., 2008, Modeling radionuclide transport with first-order chain reactions, Computational Methods in Water Resources, XVII International Conference, San Francisco, California, Lawrence Berkeley National Laboratory.

Sweetkind, D., and Drake, R.M.I., 2007, Characteristics of fault zones in volcanic rocks near Yucca Flat, Nevada Test Site, Nevada: U.S. Geological Survey Open-File Report 2007-1293, 52 p.

Sweetkind, D.S., Knochenmus, L.A., Ponce, D.A., Wallace, A.R., Scheirer, D.S., Watt, J.T., and Plume, R.W., 2007, Water resources of the Basin and Range carbonate- rock aquifer system, White Pine County, Nevada, and adjacent areas in Nevada and Utah: U.S. Geological Survey Scientific Investigations Report 2007–5261, p.

Thompson, T.L., and Misz, J.B., 1959, Geological studies of underground nuclear explosions Rainier and Neptune final report: University of California Lawrence Radiation Laboratory Report UCRL-5757, p.

Thordarson, W., 1965, Perched groundwater in zeolitized -bedded tuff, Rainier Mesa and vicinity, Nevada Test Site, Nevada: U.S. Geological Survey Open-File Report 66-130, 94 p.

Thordarson, W., 1987, Hydrogeology of the Faultless site, Nye County, Nevada: U.S. Geological Survey Water-Resources Investigations Report 86-4342 USGS/WRIR-86-4342, 40 p.

Tompson, A.F.B., Hudson, G.B., Smith, D.K., and Hunt, J.R., 2006, Analysis of radionuclide migration through a 200-m vadose zone following a 16-year infiltration event: Advances in Water Resources, v. 29, no. 2, p. 281-292.

Townsend, D.R., Townsend, M., and Ristvet, B.L., 2007, A geotechnical perspective on post-test data for underground nuclear tests conducted in Rainier Mesa: Defense Threat Reduction Agency Report DTRIAC-SR-07-002, U.S. Department of Energy Report DOE/NV/25946--269, 192 p.

Tyler, S.W., Chapman, J.B., Conrad, S.H., Hammermeister, D.P., Blout, D.O., Miller, J.J., Sully, M.J., and Ginanni, J.M., 1996, Soil-water flux in the southern Great Basin, United States; temporal and spatial variations over the last 120,000 years: Water Resources Research, v. 32, no. 6, p. 1481-1499.

Tyler, S.W., McKay, W.A., Hess, J.W., Jacobson, R.L., and Taylor, K., 1986, Effects of surface collapse structures in infiltration and moisture redistribution: Desert Research Institute Publication #45045, 48 p.

Tyler, S.W., McKay, W.A., and Mihevc, T.M., 1992, Assessment of soil moisture movement in nuclear subsidence craters: Journal of Hydrology, v. 139, p. 159-181.

U.S. Congress, 1989, The containment of nuclear explosions: OTA-ISC-414, p.

Vaniman, D.T., Chipera, S.J., Bish, D.L., Carey, J.W., and Levy, S.S., 2001, Quantification of unsaturated-zone alteration and cation exchange in zeolitized tuffs at Yucca Mountain, Nevada, USA: Geochimica et Cosmochmica Acta, v. 65, p. 3409-3433.

Wadman, R.E., and Richards, W.D., 1961, Postshot geologic studies of excavations below Rainier ground zero: Lawrence Livermore National Laboratory Report UCRL-6586, 27 p.

Walter, M.T., Kim, J.-S., Steenhuis, T.S., and Parlange, J.Y., 2000, Funnelled flow mechanisms in a sloping layered soil; laboratory investigation: Water Resources Research, v. 36, no. 4, p. 841-849.

Wang, J.S.Y., 1991, Flow and transport in fractured rocks: American Geophysical Union Reviews of Geophysics Supplement, 254-262 p.

Wang, J.S.Y., Cook, N.G.W., Wollenberg, H.A., Carnahan, C.L., Javandel, I., and Tsang, C.F., 1993, Geohydrologic data and models of Rainier Mesa and their implication to Yucca Mountain, Fourth Annual International High-Level Radioactive Waste Management, Las Vegas, Nevada, ASCE, Am. Nucl. Soc., p. 675-681.

Warrick, A.W., Biggar, J.W., and Nielsen, D.N., 1971, Simultaneous solute and water transfer for an unsaturated soil: Water Resources Research, v. 7, no. 5, p. 1216-1225.

White, A.F., Claasen, H.C., and Benson, L.V., 1980, The effect of dissolution of volcanic glass on the water chemistry in a tuffaceous aquifer, Rainier Mesa, Nevada: U.S. Geological Survey Water Supply Paper 1535-4, 34 p.

Wills, C.A., 2006, Nevada Test Site environmental report 2005: U. S. Department of Energy Report DOE/NV/11718--1214, 329 p.

Winograd, I.J., and Thordarson, W., 1975, Hydrogeologic and hydrochemical framework, South-Central Great Basin, Nevada-California, with special reference to the Nevada Test Site.: U.S. Geological Survey Professional Paper 712-C, 126 p.

Wu, Y.S., Zhang, K., Pan, L., Hinds, J., and Bodvarsson, G.S., 2002, Modeling capillary barriers in unsaturated fractured rock: Water Resources Research, v. 38, no. 11, p. 1253.

Yang, I.C., 1992, Flow and transport through unsaturated rock; data from two test holes, Yucca Mountain, Nevada, *in* Tulenko, J.S., Proceedings of the Third International Conference on High Level Radioactive Waste Management, Las Vegas, Nevada, American Nuclear Society, p. 732-737.

Yao, T.-M., and Hendrickx, J.M.H., 1996, Stability of wetting fronts in dry homogeneous soils under low infiltration rates: Soil Science Society of America Journal, v. 60, p. 20-28.

Figure 1

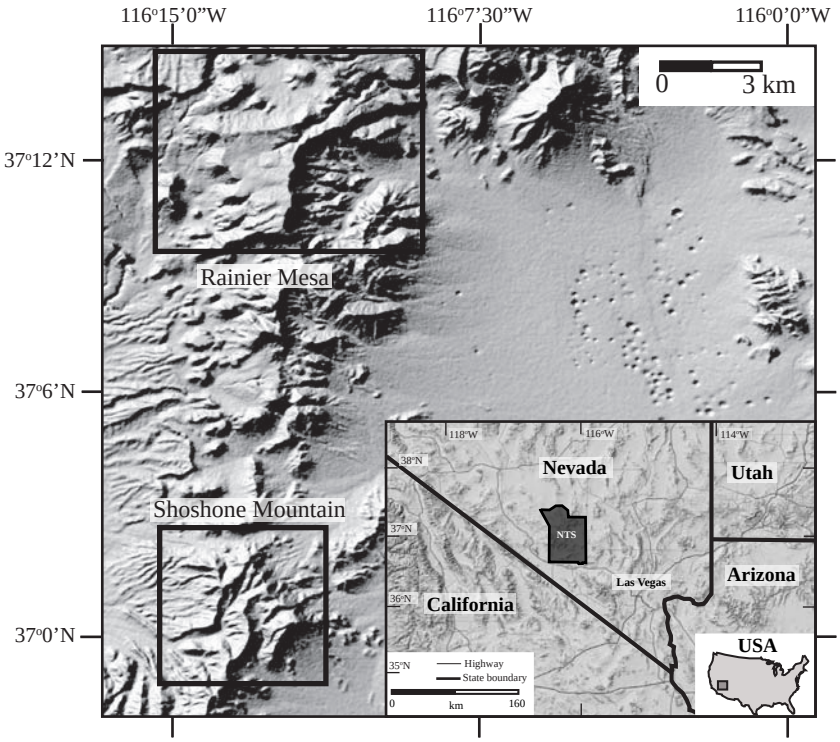


**Figure 1.** Shaded relief map showing the location of the Nevada Test Site (NTS) and the locations of Rainier Mesa and Shoshone Mountain within the NTS.

Figure 2

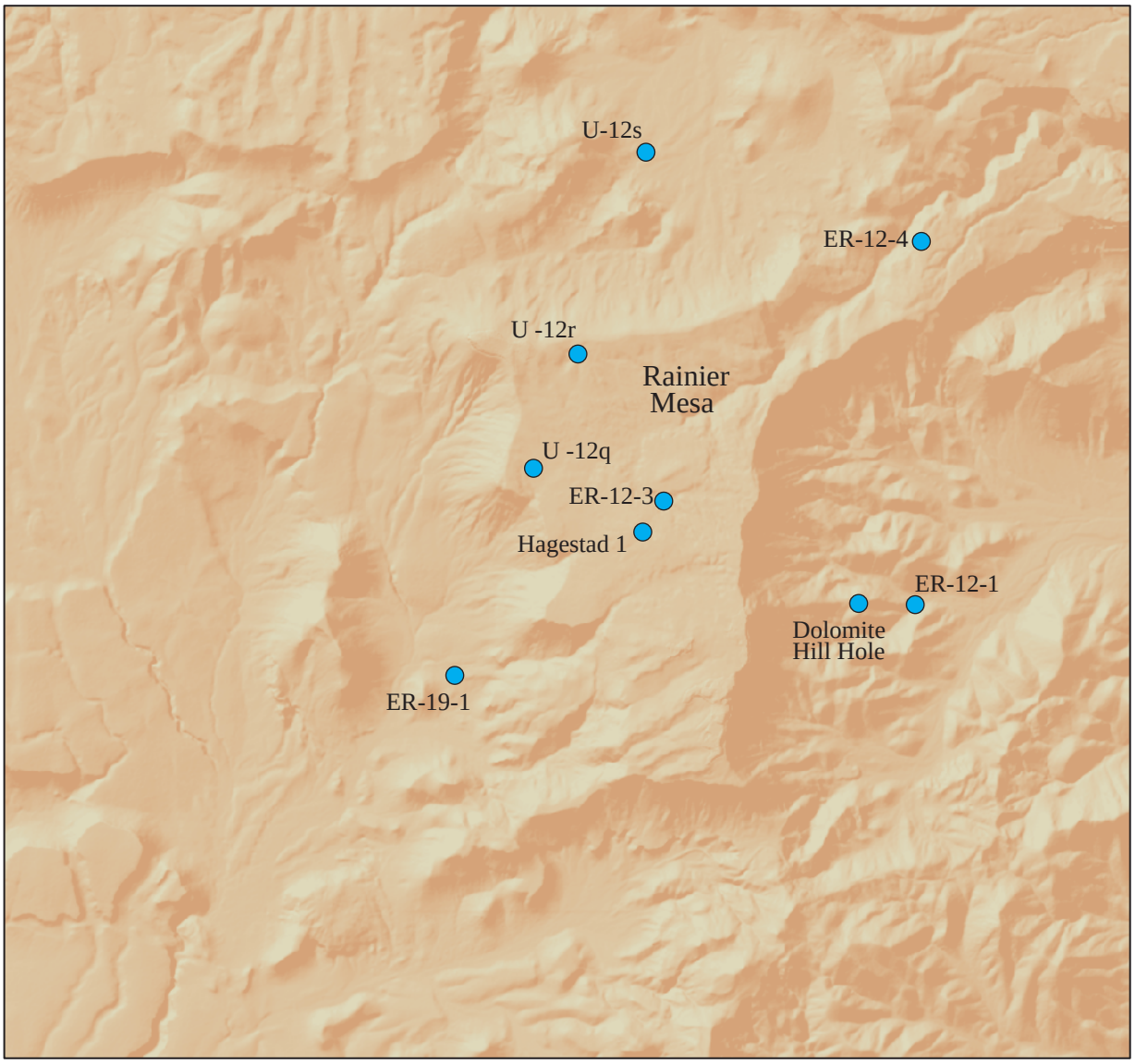


Shaded relief base map from U.S. Geological Survey
10 meter National Elevation Data

**Figure 2.** Map showing locations of selected boreholes at Rainier Mesa (after figure 1 from Fenelon, 2006). See Fenelon and others (2008) for a complete map of all boreholes at Rainier Mesa.

Figure 3

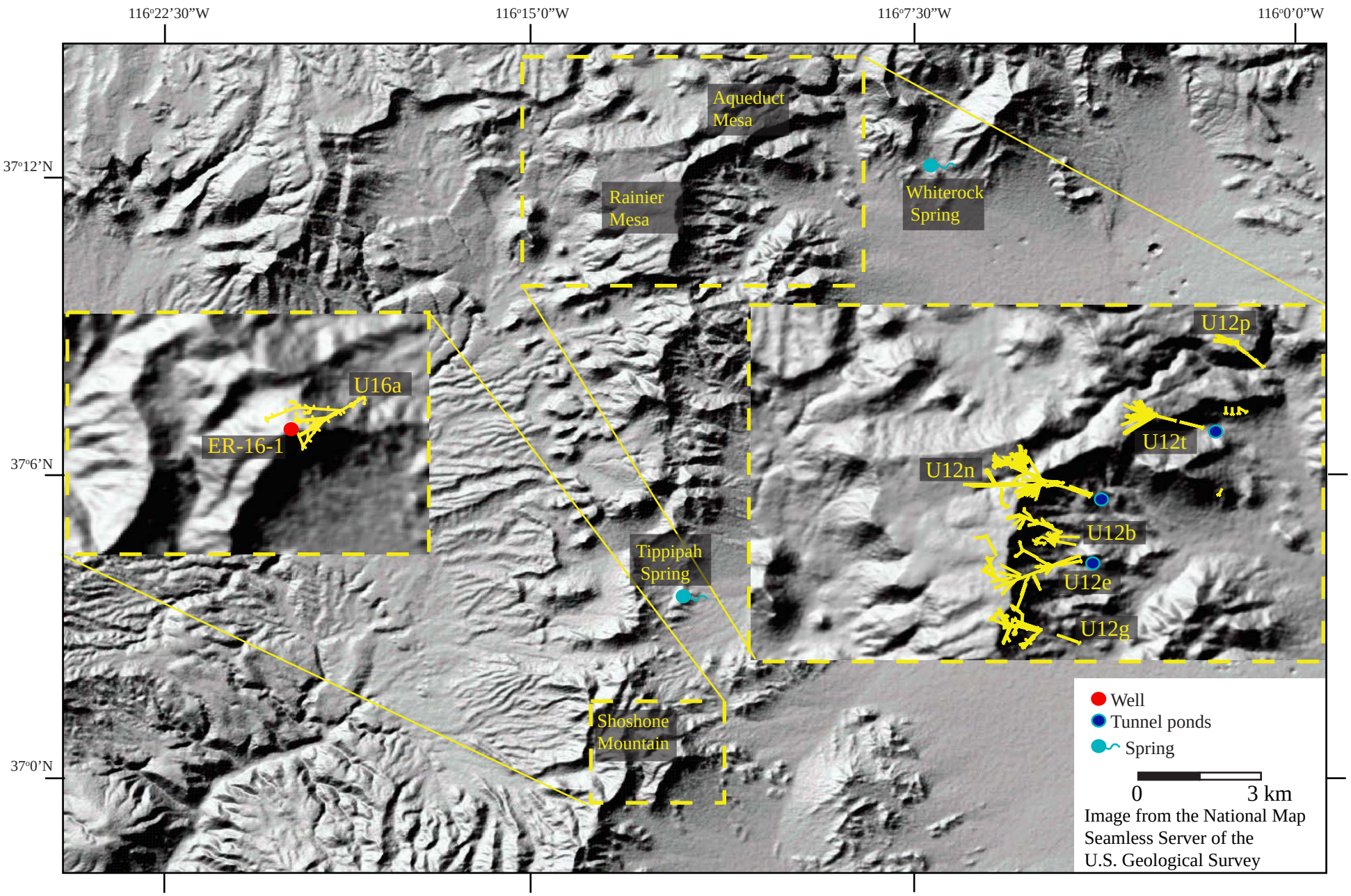


**Figure 3.** Locations of the major tunnel complexes at Rainier Mesa and Shoshone Mountain.

Figure 4

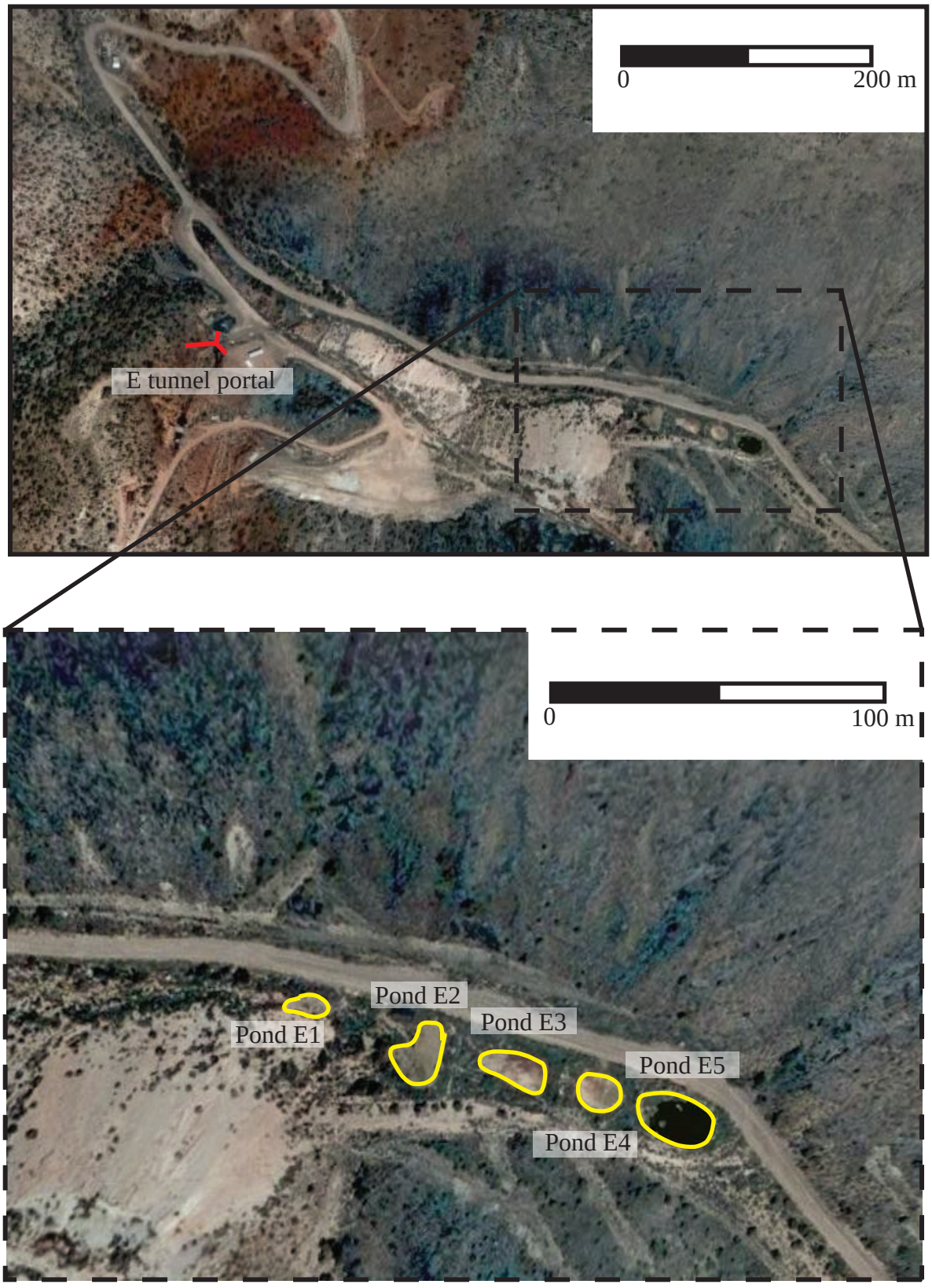


**Figure 4.** U12e tunnel portal area and tunnel ponds at Rainier Mesa.

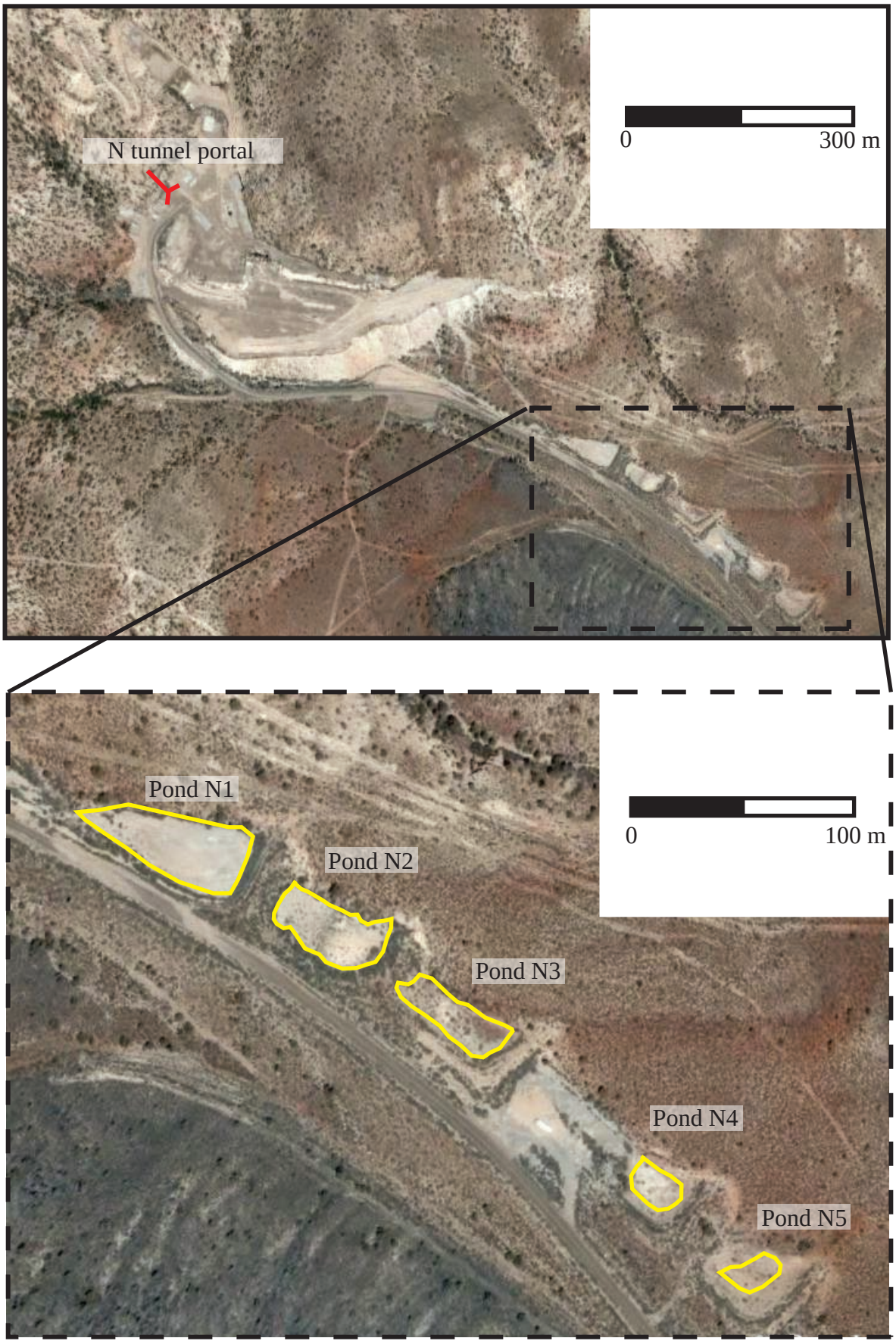


**Figure 5.** U12n tunnel portal area and tunnel ponds at Rainier Mesa.

Figure 6

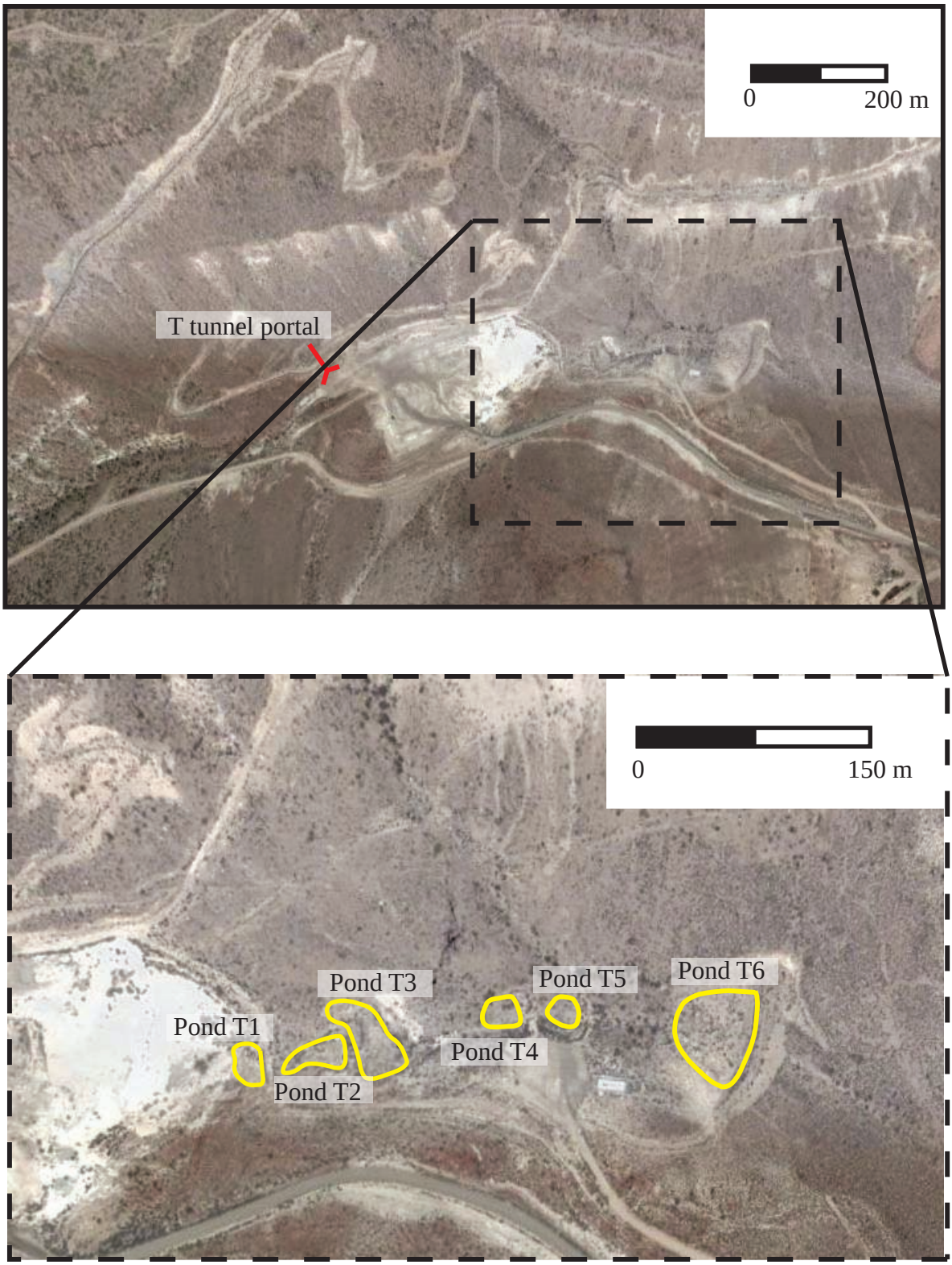


**Figure 6.** U12t tunnel portal area and tunnel ponds at Rainier Mesa.

Figure 7

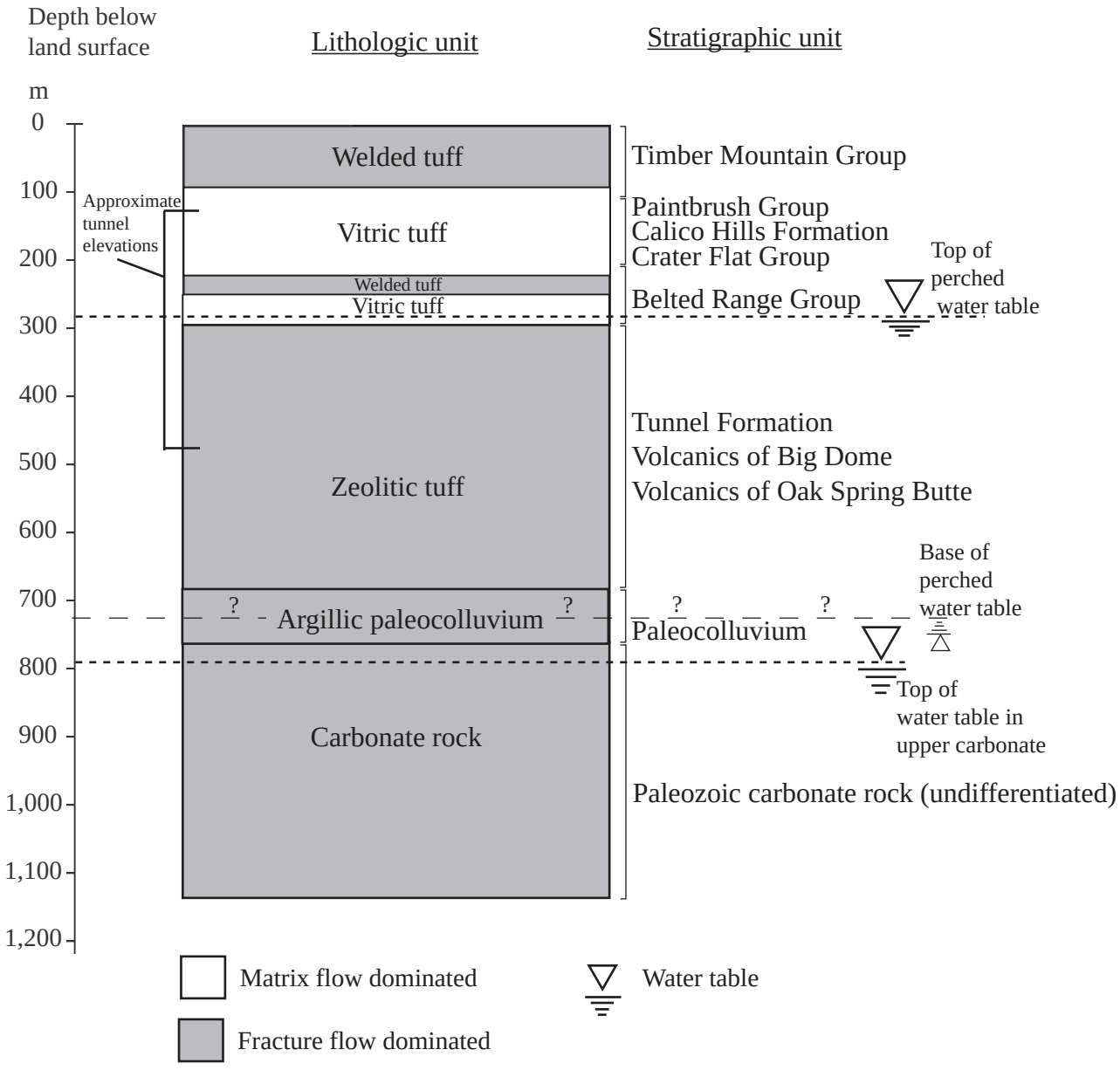


**Figure 7.** Generalized subsurface lithologic and stratigraphic section of Rainier Mesa based on the ER-12-4 borehole log (after Stoller-Navarro Joint Venture, 2006a).

Figure 8

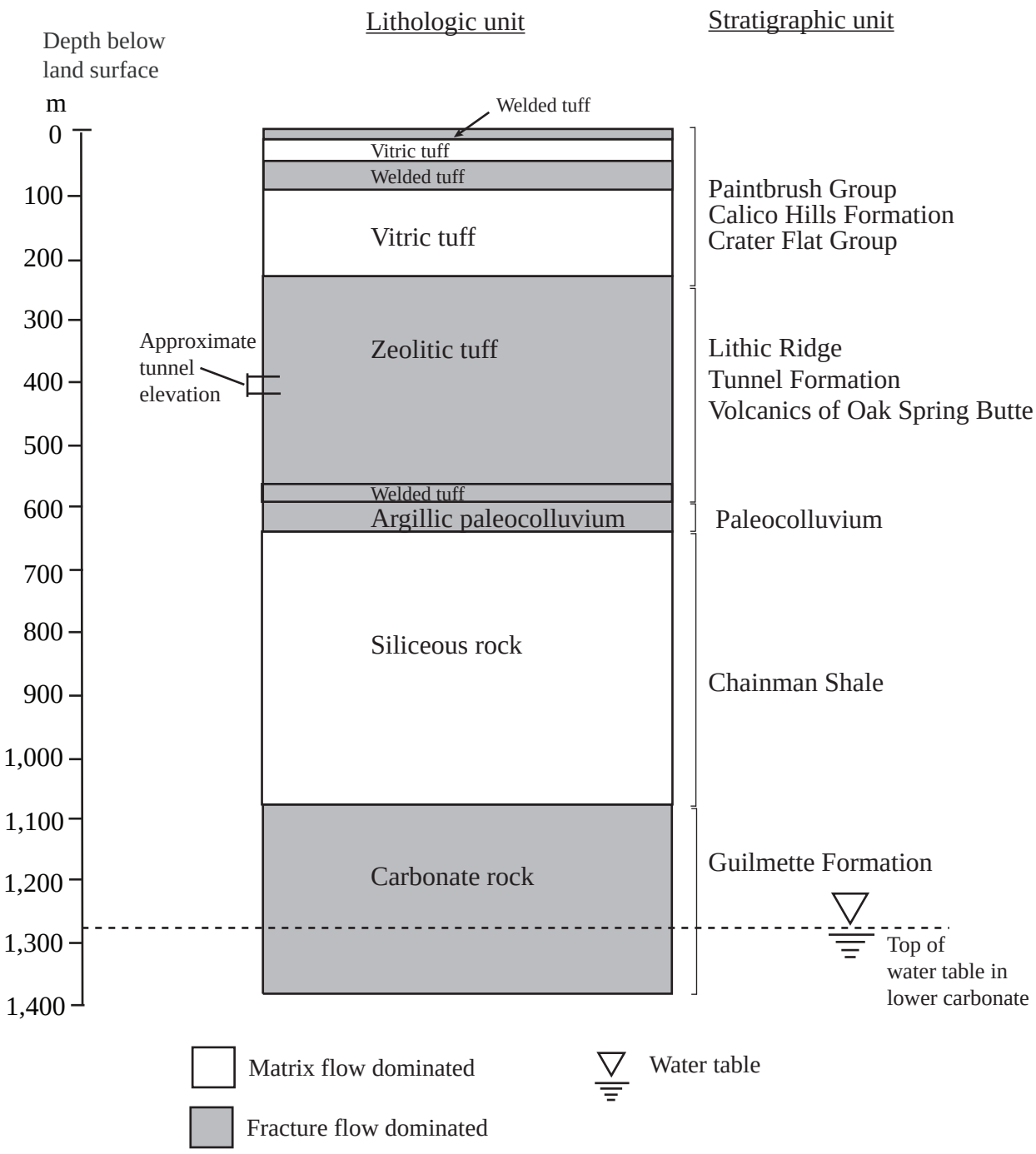


**Figure 8.** Generalized subsurface lithologic and stratigraphic section of Shoshone Mountain based on the ER-16-1 borehole log (after Stoller-Navarro Joint Venture, 2006b).

Figure 9

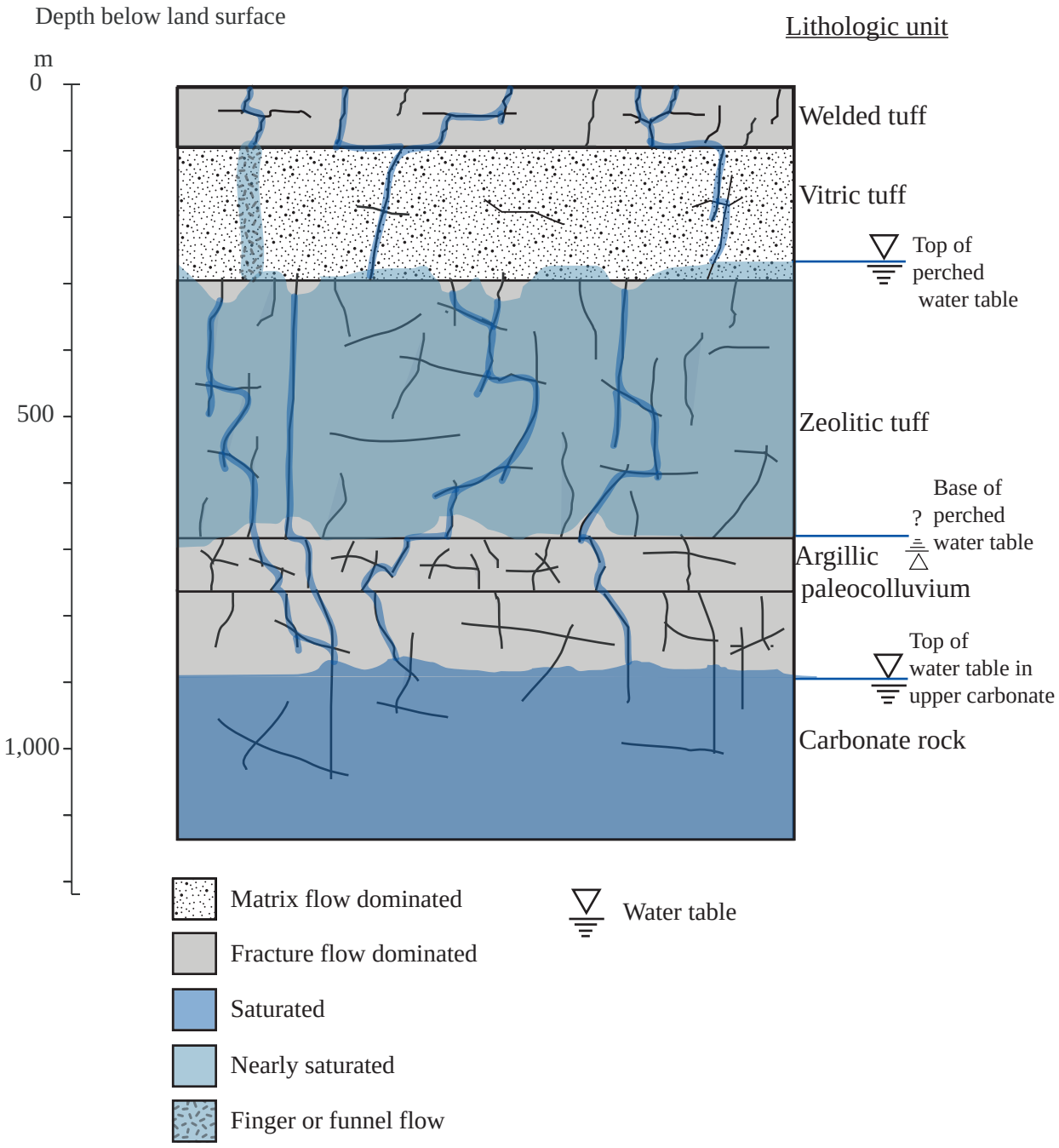


**Figure 9.** Conceptual flow model for Rainier Mesa.

Figure 10

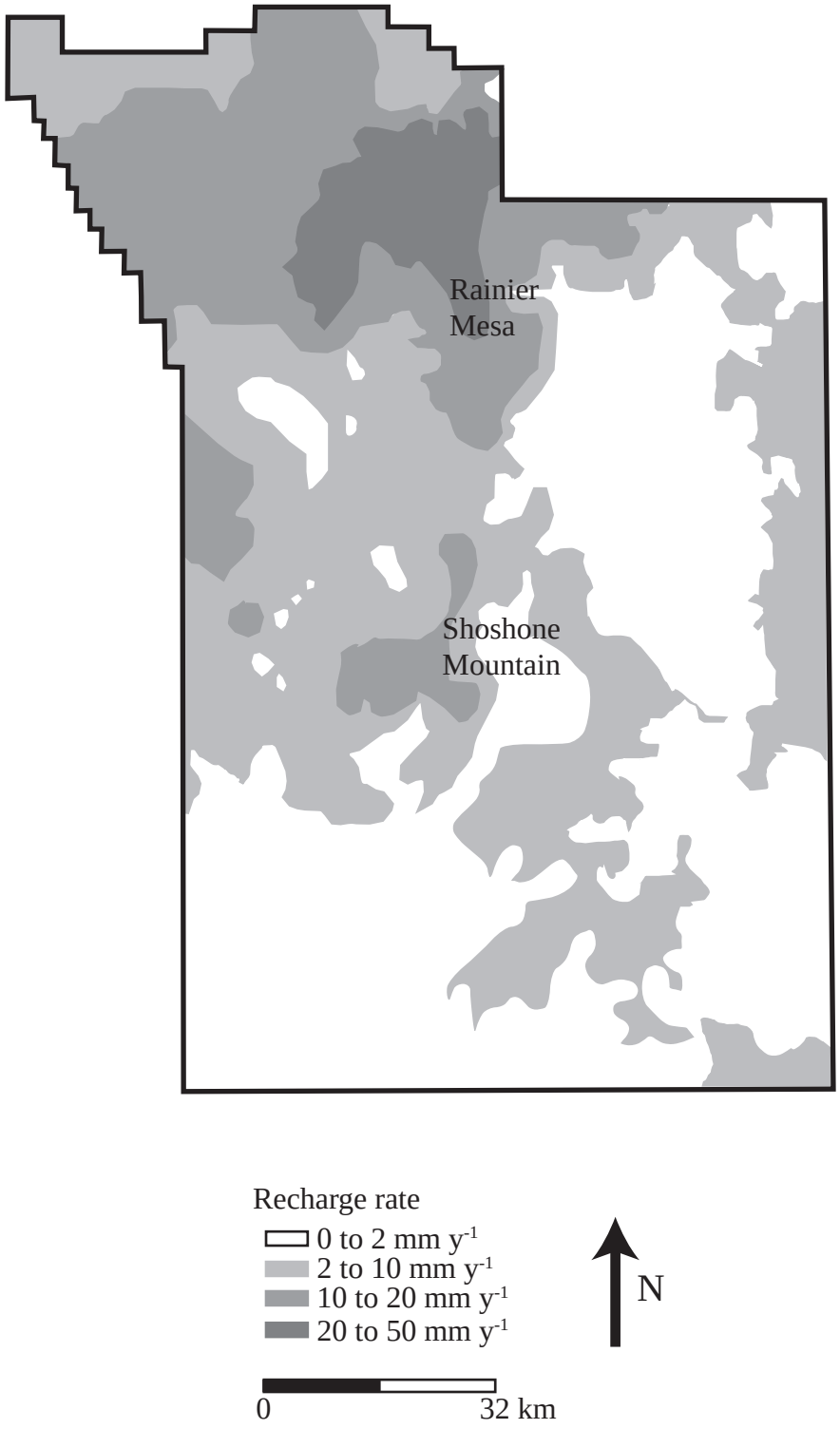


**Figure 10.** Spatially variable recharge estimates at the Nevada Test Site (NTS) (after Russell and Minor, 2002; Stoller-Navarro Joint Venture, 2004).

Figure 11

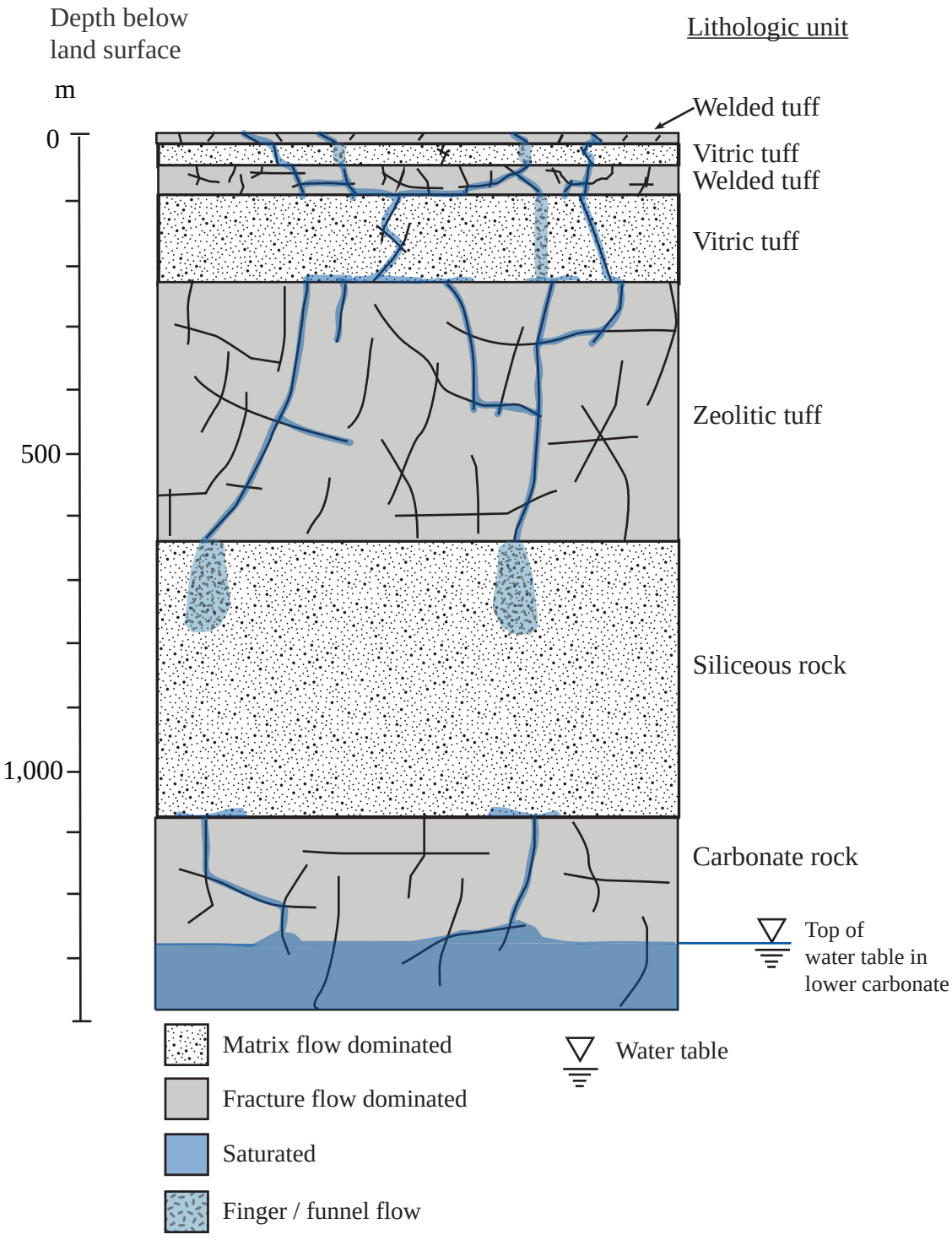


**Figure 11.** Conceptual flow model for Shoshone Mountain.

Figure 12

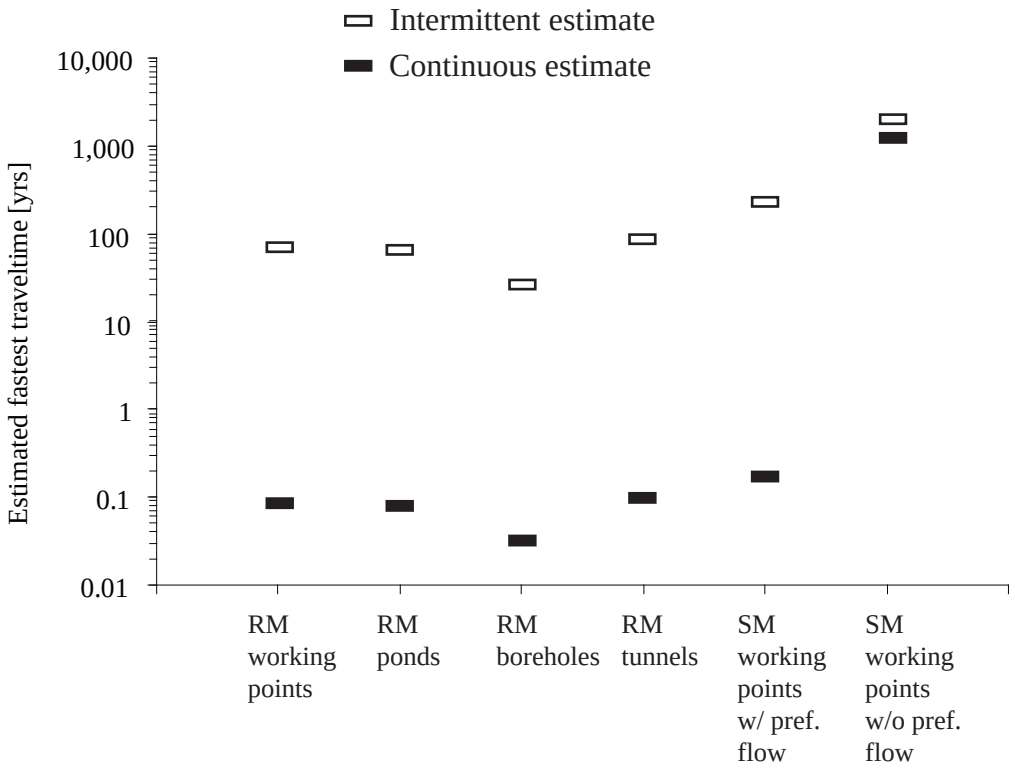


**Figure 12.** Range of unsaturated traveltime estimates for Rainier Mesa (RM) and Shoshone Mountain (SM) using an SRPF model (Nimmo, 2007) for continuous and intermittent water supply. The SM traveltime estimates are given for the cases with and without preferential flow in the siliceous rock.